



Study of Spin Fluctuation Induced High Temperature

Superconductivity:

The case of Cuprate ($\text{YBa}_2\text{Cu}_3\text{O}_{6.93}$) and Pnictide
(CaNdFeAsF)

by

Mequanint Assefa Tizazu

A dissertation submitted to the department of Physics
in partial fulfilment of the requirements for the degree of

DOCTOR OF PHILOSOPHY in PHYSICS

Addis Ababa University

Addis Ababa, Ethiopia

June 2016

Addis Ababa University

School of Graduate Studies

This is to certify that the thesis prepared by Mequanint Assefa, entitled Study of Spin fluctuation Induced High Temperature Superconductivity: The case of Cuprate ($\text{YBa}_2\text{Cu}_3\text{O}_{6.93}$) and Pnictide (CaNdFeAsF) and submitted in fulfillment of the requirements for the Degree of Doctor of Philosophy (Physics) complies with the regulations of the University and meets the accepted standards with respect to originality and quality.

Signed by the Examining Committee

1. Chairperson Dr. Teshome Senbeta Sign. _____ Date _____
2. Ext. Examiner Dr. Ajay Sign. _____ Date _____
3. Int. Examiner Dr. Tegessera Bedassa Sign. _____ Date _____
4. Advisor: Professor Pooran Singh Sign. _____ Date _____

Chair of Department or Graduate Program Coordinator

Addis Ababa University, 2016

Abstract

High temperature superconductivity is an interesting and fascinating phenomenon in which certain materials conduct electricity with zero electrical resistance and expulsion of interior magnetic field with superconducting transition temperature higher than 30 K. This was unexpectedly discovered in copper oxide materials by Bednorz and Muller. After this discovery, a search for new high temperature superconducting families began and still going on.

In this thesis, we study high temperature superconductivity involving cuprate and pnictides theoretically. In order to look for this, we consider a model Hamiltonian consisting of kinetic energy term, magnetic energy term and electron-spin fluctuation term. and we used Green function formalism to calculate superconducting transition temperature and obtain an expression for the superconducting order parameter for high temperature superconductors analytically. We get the superconducting transition temperatures for $\text{YBa}_2\text{Cu}_3\text{O}_{6.93}$ and CaNdFeAsF , 92.4 K and 56 K respectively as they being high T_c materials in their respective series. The spin fluctuation/magnon/ as a possible mechanism for high temperature superconductivity is also highlighted, as yet there is no consensus for the mechanism for high temperature superconductivity in these system.

Dedication

This work is Dedicated to my G/mother and Mother

Beyenech Adigh

Zewditu Rukie

Acknowledgements

It is a great pleasure and honor for me to express my deep regards and special gratitude to the following distinguished and honorable people:-

First, My special cordial gratitude goes to my research advisor Professor Pooran Singh who kindly accepted me and join his superconductivity research work as a PhD student. Also I thank him for introducing me to the great world of superconductivity research and giving me the opportunity of studying high temperature superconductivity. I really appreciate all this in addition to his kind treatment with a lot of patience, constant support, encouragement and valuable advice.

I appreciate endless and kind conversations, daily coffee breaks and get together with my colleagues, Kefeyalew Addis and Teklemariam Tessema, PhD student in Addis Ababa University.

Finally, my sincere thank go to Addis Ababa University and Debre Birhan University for their financial support.

Contents

1	INTRODUCTION	1
2	REVIEW OF LITERATURE	5
2.1	Superconductivity	5
2.2	The BCS Theory	14
2.3	High Temperature Superconductivity	20
2.3.1	Mechanisms of high temperature superconductivity	22
2.3.2	Pairing symmetry	25
2.4	Cuprates superconductivity	28
2.4.1	Phase diagram for cuprates superconductivity	29
2.4.2	Structure of cuprates superconductor	32
2.4.3	Layer of cuprates	34
2.4.4	Fermi surface of cuprates	34
2.5	Pnictides superconductivity	35
2.5.1	Discoveries of pnictides superconductors	35
2.5.2	Phase diagram for pnictides superconductivity	36
2.5.3	Structure of pnictides superconductor	37

2.5.4	Fermi surface of pnictides	40
2.5.5	Layer of pnictides	40
2.6	Electronic specific heat	44
2.7	Application of Superconductivity	46
2.7.1	Magnetic Levitation Train	46
2.7.2	Magnetic Resonance Imaging (MRI)	47
3	MATHEMATICAL TECHNIQUE	50
3.1	The Green Functions Method	50
3.2	Equation of motion for Heisenberg operators	57
4	FORMULATION OF THE PROBLEM	60
4.1	Cuprate superconductivity	60
4.2	Pnictides Superconductivity	79
4.3	Electronic specific heat	87
5	RESULTS AND DISCUSSION	88
5.1	The Superconducting Transition Temperature (T_C) for cuprate based superconductor	89
5.2	The Transition Temperature(T_C)for Pnictides Superconductor . .	92
5.3	Electronic specific heat	98
6	CONCLUSION	100

List of Figures

2.1	Resistance versus Temperature [14]	6
2.2	(a)magnetic flux distribution in the presence of a magnetic field (b) Expulsion of weak external magnetic field in the interior super- conducting material [15,100]	7
2.3	a)Type-I superconductor where the penetration depth is shorter than the coherence length. b)Type II superconductor where the coherence length is shorter than the penetration depth [16]	12
2.4	Electron-phonon interaction mediated by emission and absorp- tion of a Virtual Phonon [19]	19
2.5	Graph represents the highest temperature superconductors and the year of discovery [28].	21
2.6	Pairing symmetry [35]	27
2.7	Typical cuprates phase diagram [42]	30
2.8	Structure of cuprates: $\text{YBa}_2\text{Cu}_3\text{O}_{7-x}$ [46]	33
2.9	Structure of cuprates: LaCuO [46]	33
2.10	layer of cuprates [47]	34
2.11	Fermi surface cuprates [48]	34

2.12 phase diagrams of pnictides [60]	37
2.13 Structure of iron pnictides (1111), RFeAs, R= rare earth [63] . . .	38
2.14 Structure of iron pnictides (1111) ,(A,R)FeAsF, A= Alkaline [63] . .	38
2.15 Structure of iron- pnictides (111), AFeAs [64]	39
2.16 Structure of iron pnictide 122, BaFe ₂ As ₂ [65]	39
2.17 Structure of 11, Fe (S,Se,Te) [66]	39
2.18 Fermi surface of pnictides [67]	40
2.19 layer of pnictides [68].	40
2.20 Temperature versus resistivity for FeTe _{0.5} Se _{0.5} under pressure [76] .	42
2.21 Structure of iron chalcogenides [77,66,83]	43
2.22 The electronic specific heat versus Temperature [81]	45
2.23 The Yamanashi MLX01MagLev Train [83]	46
2.24 MRI (Magnetic Resonance Imaging) [85]	47
5.1 Superconducting order parameter (Δ) versus superconducting tran- sition temperature(T_c) for YBa ₂ Cu ₃ O _{6.93} [90]	90
5.2 Superconducting transition temperature (T_c) versus coupling strength (λ) YBa ₂ Cu ₃ O _{6.93} [90]	91
5.3 Superconducting order parameter (Δ) versus superconducting tran- sition temperature (T_c) for Ca _{1-x} Nd _x FeAsF	93
5.4 Superconducting transition temperature(T_c) versus coupling strength (λ) for Ca _{1-x} Nd _x FeAsF	94

5.5	Superconducting transition temperature(T_c) versus coupling strength (λ)	95
5.6	Superconducting transition temperature(T_c) versus coupling strength (λ)	95
5.7	Superconducting transition temperature (T_c) versus coupling strength (λ)	96
5.8	Superconducting transition temperature (T_c) versus coupling strength (λ)	96
5.9	Superconducting transition temperature (T_c) versus coupling strength (λ) [90]	97
5.10	Superconducting order parameter ($\frac{\Delta}{\Delta_0}$) versus ($t = \frac{T}{T_c}$)	97
5.11	The electronic specific heat versus Temperature for $\text{YBa}_2\text{Cu}_3\text{O}_{6.93}$.	98
5.12	The electronic specific heat versus Temperature for CaNdFeAsF .	99

List of Tables

- 5.1 Comparison between theoretical and experimental value of superconducting transition temperatures for cuprates 90
- 5.2 Comparison between theoretical and experimental value of superconducting transition temperatures for iron pnictides 93

1

INTRODUCTION

Superconductivity is the ability of certain materials to conduct electricity with zero electrical resistance below a certain temperature, referred to as the superconducting transition temperature T_c . This superconducting property was first discovered by Dutch Physicist Heike Kammerlingh Onnes in Leiden in 1911, while cooling elemental mercury with liquid helium to about 4.2 K [1]. He noticed that its resistance suddenly disappeared.

In 1933, Messiner and Orchsenfeld discovered that superconductors expelled applied magnetic fields, which has come to be known as the Messiner-Ochsenfeld effect [2].

Superconductivity remained an empirical science for several decades. After quantum mechanics was introduced in the late 1920s, theorists gradually began to suspect that superconductivity and superfluidity were quantum phenomena. In 1950 the phenomenological Ginzburg-Landau theory of superconductivity was devised by Landau and Ginzburg [3], this theory had great success in explaining the macroscopic properties of superconductors. In the same year, Maxwell and Reynolds et al found that the critical temperature of a superconductor depends on the isotopic mass of the constituent elements [4].

The first widely accepted theoretical understanding of superconductivity was advanced in 1957 by American physicists John Bardeen, Leon Cooper and John Schrieffer [5]. Their theory of superconductivity became known as the BCS theory derived from the first letter of each of man's last name. In 1971 Niobium Germanium (Nb_3Ge) with transition temperature $T_c=23$ K was discovered [6], this material held the record of high transition temperature from 1971-1986. In 1991, the fullerite K_3C_{60} become superconducting below $T_c=18$ K [7], It has pushed with $T_c=29$ K for Rb_3C_{60} under high pressure [8]. In 1986 Bednorz and Muller discovered superconductivity in a lanthanum based cuprate perovskite material, which had a transition temperature of 35 K (Nobel Prize in physics, in 1987) which is the high temperature superconductors [9]. In 2001, Nagamatsu, et al, reported superconductivity in MgB_2 with $T_c=39$ K [10].

In 1995, the highest temperature superconductor for mercury barium calcium copper oxide ($\text{HgBa}_2\text{Ca}_2\text{Cu}_3\text{O}_x$), with T_c 135 K at ambient pressure [11] and reaches 164 K under high pressure [12] discovered. Cuprates remained a high priority due to its high T_c until the discovery of superconductivity in iron-pnictides by Yoichi Kamihara who discovered that CuO plane is not a requirement for superconductivity.

In 2008, the highest T_c non cuprate superconductor was pnictide ($\text{Ca}_{1-x}\text{Nd}_x\text{FeAsF}$) with $T_c=57$ K [13]. The search for high temperature superconductors has been going on since the discovery of the first high temperature superconductor.

High temperature superconductivity could revolutionize technologies ranging from magnetically-levitated trains to electrical power transmission. However, the mechanism by which these cuprate materials become superconducting and the superconducting transition temperature had remained a mystery for the last 30 years. Many solid state researchers are still engaged with research on high temperature superconductors.

Research Objective

The main objective of this research is to:

1. determine the superconducting transition temperature of high temperature superconductives involving cuprate and iron pnictides theoretically.
2. look into the the possible mechanisms for cuprate and pnictide superconductors,
3. find the relationship between the superconducting order parameter and temperature

Statement of the problem

The discovery of high temperature superconductor is ongoing process, Theorists and experimentalists in condensed matter Physics have tried to look for new high temperature superconductor, here, we are going to study high temperature superconductivity entitled on Study of Spin fluctuations induced High Temperature Superconductivity: the case of cuprate ($\text{YBa}_2\text{Cu}_3\text{O}_{6.93}$) and pnictide (CaNdFeAsF) involving spin fluctuations as a possible mechanism for both the cuprates and pnictides.

Research Questions

1. What are the possible mechanisms for high temperature superconductives?
2. How can we compute the superconducting transition temperature theoretically?
3. What are the pairing symmetry of HTS?
4. How do we relate the superconducting order parameter with superconducting transition temperature?
5. What sort of mathematical technique and Hamiltonian model is convenient to study high temperature superconductivity?

Many theorists and experimentalists have still tried to seek solutions for the problems HTS and search new high temperature superconductivity as well as room temperature superconductivity.

Chapter one describes motivation of the thesis, In Chapter two summarized presentation of the discovery and theoretical understanding of superconductivity and high temperature superconductivity will be given. Chapter three further offers mathematical technique and derivation of equation of motions for Heisenberg operators so as to solve our problem.

In chapter four formulation of the problem, chapter five describes the result and discussion.

In chapter six conclusion of results is given.

REVIEW OF LITERATURE

2.1 Superconductivity

Superconductivity is a phenomena that the materials can conduct electricity without loss of electric energy. Superconducting materials have two fundamental properties, which are:-

(a) Zero resistivity ($\rho = 0$) for all $T < T_c$ i.e. infinite conductivity, is carried out in a superconductor at all temperatures below the superconducting transition temperature T_c as depicted in Fig2.1, However, if the passing current is higher than the critical current, superconductivity disappears. conduction electron of a given momentum and spin get weakly coupled with another electron of the opposite momentum and spin. These pairs are called Cooper pairs. The coupling energy is provided by lattice elastic waves, called phonons. The behavior of such a fluid of correlated Cooper pairs is different from the normal electron gas. They all move in a single coherent motion.

A local perturbation, like, an impurity, which in the normal state would scatter conduction electrons and cause resistivity, cannot do so in the superconducting state without immediately affecting the Cooper pairs that participate in the col-

lective superconducting state. Once this collective highly coordinated, state of coherent super-electrons (Cooper pairs) is set into motion, its flow is without any dissipation. There is no scattering of individual pairs of the coherent fluid, and therefore, no resistivity.

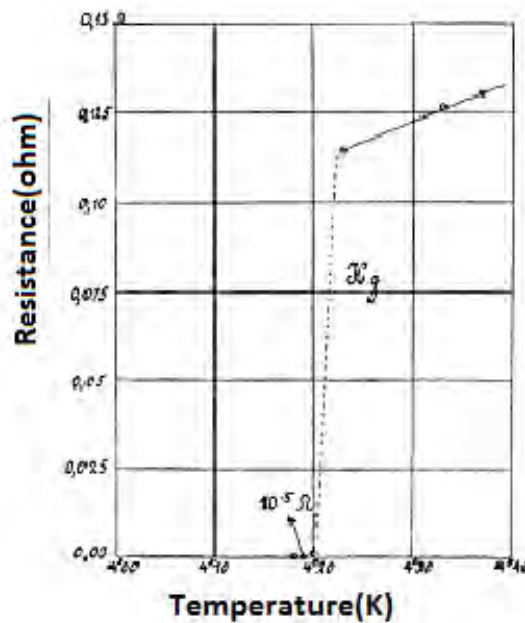


Figure 2.1: Resistance versus Temperature [14]

In fig2.1,we can observe that

- above critical temperature, the material behaves like a normal conductor with electrons scattering causing resistance
- Over a narrow range of temperatures, the resistance drops suddenly as the material enters the superconducting state.
- Below the critical temperature, the material becomes superconducting and the electrons are no longer scattered resulting in zero resistance.

(b) No magnetic fields ($B=0$) inside the superconductor:

When a superconductor is placed in external magnetic fields which is lower than the critical magnetic field B_c , the magnetic field becomes zero inside the superconductor when it is cooled below the superconducting transition temperature T_c . This effect is called the Meissner-Ochsenfeld effect(Fig2.2).

Above the critical magnetic flux,superconductivity can no longer be achieved.

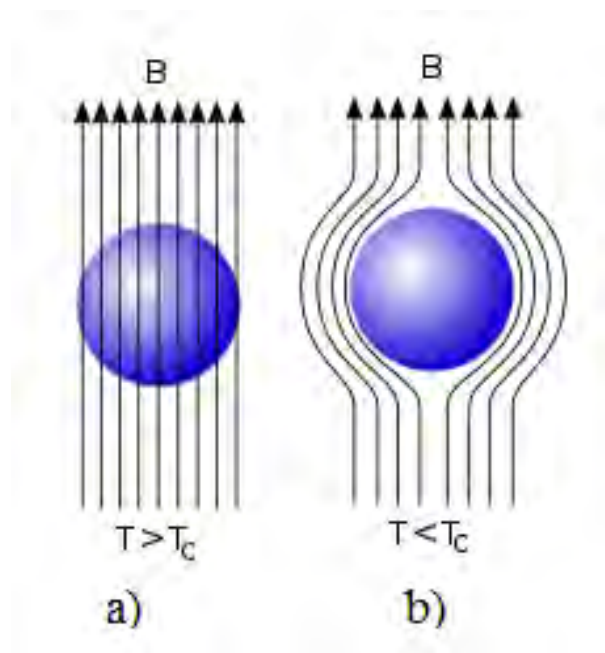


Figure 2.2: (a)magnetic flux distribution in the presence of a magnetic field (b) Expulsion of weak external magnetic field in the interior superconducting material [15,100]

If electrons flow in a circulating current around the surface of a superconductor, they will setup magnetic field which is equal in magnitude but opposite in direction to the external field applied.

For the case, when magnetic field is expelled from the specimen, we have

$$B = 0 = \mu_0(H + M) = \mu_0(H + \chi H) = \mu_0 H(1 + \chi) \quad (2.1)$$

Where M is magnetization and χ is magnetic susceptibility,

$$\chi = -1.$$

A superconductor in magnetic field will act as a perfect diamagnet.

The other property is that superconductivity can be destroyed not only by increasing the temperature but also by applying a sufficiently strong magnetic field.

The critical magnetic field in which superconductivity is destroyed decreases with increasing temperature. The dependence of magnetic field $H_c(T)$ is given by

$$H_c(T) = H_c(0)[1 - (T/T_c)^2] \quad (2.2)$$

where T_c -critical temperature, $H_c(0)$ -magnetic field at critical temperature (T_c)

London equation

In 1935, H. and F. London gave a phenomenological description of the basic facts of superconductivity by proposing a two fluid type concept with superfluid and normal fluid densities associated with velocities v_s and v_n .

London equation provided the first theoretical description of Meissner effect and correctly predicted magnetic penetration into the superconducting material, but cannot give a microscopic picture.

Let n_s and v_s be super-electron density and velocity of superconducting electrons respectively.

The equation of motion is

$$m \frac{d\vec{v}_s}{dt} = -e\vec{E} \quad (2.3)$$

The current density \vec{J}_s due to superconducting electrons is given by

$$\vec{J}_s = -n_s e \vec{v}_s \quad (2.4)$$

$$\frac{d\vec{J}_s}{dt} = -n_s e \frac{d\vec{v}_s}{dt} \quad (2.5)$$

This is the First London Equation

Combining eqn (2.4), and eqn(2.5), we get

$$\frac{d\vec{J}_s}{dt} = \frac{n_s e^2}{m} \vec{E} \quad (2.6)$$

Taking the curl of eqn(2.6) and using Maxwell equation $\nabla \times \vec{E} = -\frac{\partial \vec{B}}{\partial t}$, we obtain

$$\nabla \times \left(\frac{d\vec{J}_s}{dt} \right) = \frac{n_s e^2}{m} \nabla \times \vec{E} \quad (2.7)$$

$$\nabla \times \left(\frac{d\vec{J}_s}{dt} \right) = -\frac{n_s e^2}{m} \frac{\partial \vec{B}}{\partial t} \quad (2.8)$$

$$\frac{\partial}{\partial t} \left[\nabla \times \vec{J}_s + \frac{n_s e^2}{m} \vec{B} \right] = 0 \quad (2.9)$$

$$\nabla \times \vec{J}_s = -\frac{n_s e^2}{m} \vec{B} \quad (2.10)$$

This is London Second Equation.

Consider the differential form of Ampere's circuital Law:

$$\nabla \times \vec{B} = \mu_0 \vec{J}_s \quad (2.11)$$

where B is magnetic flux density and J_s is current density.

Taking the curl on both sides of eqn(2.11)

$$\nabla \times (\nabla \times \vec{B}) = \mu_0 (\nabla \times \vec{J}_s) \quad (2.12)$$

$$\nabla \times (\nabla \times \vec{B}) = \nabla(\nabla \cdot \vec{B}) - \nabla^2 \vec{B} \quad (2.13)$$

Plugging eqn(2.13) and London eqn(2.10) into eqn(2.12), we get

$$\nabla(\nabla \cdot \vec{B}) - \nabla^2 \vec{B} = -\left[\frac{\mu_0 n_s e^2 \vec{B}}{m}\right] \quad (2.14)$$

But

$$\nabla \cdot \vec{B} = 0$$

(Maxwell's Second equation or Gauss law for magnetism).

Therefore, eqn(2.14) becomes

$$\nabla^2 \vec{B} = \left[\frac{\mu_0 n_s e^2 \vec{B}}{m}\right] \quad (2.15)$$

$$\nabla^2 B = \frac{B}{\lambda_L^2} \quad (2.16)$$

Where λ_L is known as London's penetration depth and it has a unit of length.

$$\lambda_L = \left(\frac{m}{\mu_0 n_s e^2}\right)^{\frac{1}{2}} \quad (2.17)$$

The solution of differential equation(2.16)is

$$B = B(0)e^{\frac{-x}{\lambda_L}} \quad (2.18)$$

where $B(0)$ is the field at the surface and x is the depth inside the superconductor

Suppose $x = \lambda_L$, eqn (2.18) becomes $\frac{B(0)}{e}$.

London penetration depth

The London penetration depth is the distance inside the surface of a superconductor at which the magnetic field reduces $\frac{1}{e}$ times its value at the surface. The London penetration depth depends strongly on temperature and becomes much larger as temperature (T) approaches critical temperature T_c

$$\lambda = \sqrt{\frac{m}{4n_s e^2}} \quad (2.19)$$

where m -mass of electron , n_s -density of superconducting electron and e -charge of an electron

A small value of penetration depth implies that the magnetic field is effectively expelled from the interior of a sample. The number density of superconducting electrons is dependent on temperature as well as the penetration depth.

According to London model, the penetration depth rises asymptotically as the temperature approaches to the critical temperature T_c . Thus the field penetrates further and further as the temperature approaches the critical temperature T_c and does so completely above the critical temperature T_c [16]

Coherence length

Coherence length is a measure of the distance over which two electrons combine to form a Cooper pair. It is determined by energy gap.

$$\xi = \frac{2\hbar v_f}{\pi E_g}$$

It is also governed by the Landau-Ginzburg equations

$$\kappa = \frac{\lambda_L}{\xi}$$

When $\frac{\lambda_L}{\xi} > 1$ It is type II superconductor and When $\frac{\lambda_L}{\xi} < 1$ It is type I superconductor.

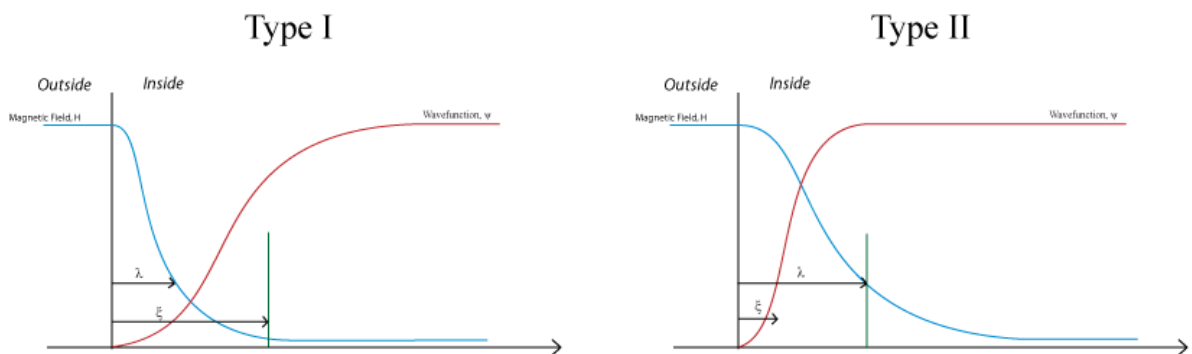


Figure 2.3: a) Type-I superconductor where the penetration depth is shorter than the coherence length. b) Type II superconductor where the coherence length is shorter than the penetration depth [16]

Types of superconductors

Superconductors could be classified into different types of superconductors based on different criteria, The most common classifications are,

1. By their response to a magnetic field: Superconductors can be Type-I, if they have a single critical magnetic field, above which all superconductivity is lost, In this Type-I superconductors, the penetration depth is shorter than coherence length.

Superconductors can also be Type-II, if they have two critical magnetic fields between which they allow partial penetration of the magnetic field. In addition to this, in Type-II superconductors, the coherence length is shorter than the penetration depth.

2. By the theory to explain them:

Superconductors can be conventional if they are explained by BCS theory. Superconductors can be Unconventional if they are not explained by BCS theory.

3. By their superconducting transition temperature:

Superconductors can be high temperature superconductors if the superconducting transition temperature is greater than 30 K Or Low temperature superconductors if the superconducting transition temperature is smaller than 30 K.

2.2 The BCS Theory

The microscopic theory of superconductivity was first proposed by John Bardeen and his graduate assistants Leon cooper, and Robert Schrieffer in 1957 [5]. They proposed a microscopic explanation that would later be their namesake: the BCS theory. This theoretical explanation later earned them the Nobel Prize in 1972, making John Bardeen the only man in history to be awarded this honor twice for the same subject. The two principal features of BCS theory are:-

1. Electrons form pairs called Cooper pairs, which propagate through out the lattice and
2. Such propagation is without resistance because the electrons move in resonance with phonons, therefore, the interaction described by BCS theory is known as the electron-phonon interaction.

BCS theory could successfully explain the existence of an energy gap between the ground state (superconducting state) and first excited state.

Consider a pair of electrons excited above the Fermi surface ε_F . Assume that the ground state of this pair will have zero net momentum and zero net spin (singlet spin state).

Let \vec{r}_1 and \vec{r}_2 be the positions of two electrons, assume that the two-particle wave function has the form:

$$\Psi(r_1, r_2) = \frac{1}{V} \sum_k D(k) e^{i\vec{k} \cdot \vec{r}_1} e^{i\vec{k} \cdot \vec{r}_2} \quad (2.20)$$

where V is volume

$$\vec{k}_1 = -\vec{k}_2$$

so the total momentum of the pair is zero.

Since the electrons are above a filled Fermi sphere, we must have

$$D(k) = 0, \text{ for all } |\vec{k}| < k_F$$

since these states are already occupied. If $V(\vec{r}_1, \vec{r}_2)$ is the interaction between two electrons, the Schrodinger equation is

$$-\frac{\hbar^2}{2m}[\nabla_1^2 + \nabla_2^2]\Psi + V(\vec{r}_1, \vec{r}_2)\Psi = E\Psi \quad (2.21)$$

Using the fourier transform

$$V(\vec{r}_1, \vec{r}_2) = \frac{1}{V} \sum_q V_q e^{i\vec{q} \cdot (\vec{r}_1 - \vec{r}_2)} \quad (2.22)$$

Plugging eqn(2.18) into Schrodinger eqn(2.17), we get

$$\frac{1}{V} \sum_k \frac{\hbar^2}{2m} (k+k) D(k) e^{i\vec{k} \cdot (\vec{r}_1 - \vec{r}_2)} + \frac{1}{V^2} \sum_{k', q} V_q e^{i\vec{q} \cdot (\vec{r}_1 - \vec{r}_2)} D(k') e^{i\vec{k}' \cdot (\vec{r}_1 - \vec{r}_2)} = E \frac{1}{V} \sum_k D(k) e^{i\vec{k} \cdot (\vec{r}_1 - \vec{r}_2)} \quad (2.23)$$

Let us substitute $\vec{q} = \vec{k} - \vec{k}'$ in the potential term

$$\sum_k \left[\frac{\hbar^2 k^2}{m} D(k) + \frac{1}{V} \sum_{k'} V_{k-k'} D(k') - ED(k) \right] e^{i\vec{k} \cdot (\vec{r}_1 - \vec{r}_2)} = 0 \quad (2.24)$$

$$\frac{\hbar^2 k^2}{m} D(k) + \frac{1}{V} \sum_{k'} V_{k-k'} D(k') = ED(k) \quad (2.25)$$

$$D(k) = 0 \text{ for } |\vec{k}| < k_F \quad (2.26)$$

Using

$$\varepsilon_k = \frac{\hbar^2 k^2}{2m}$$

, we have

$$(E - 2\varepsilon_k) D(k) = \frac{1}{V} \sum_{k'} v_{k-k'} D(k') \quad (2.27)$$

To simplify this, we take a crude approximation

$$v_{k-k'} = \begin{cases} -v_0, & \text{if } \varepsilon_k, \varepsilon_{k'} \text{ within } \hbar\omega_D \text{ of } \varepsilon_F \\ 0, & \text{otherwise} \end{cases} \quad (2.28)$$

The density of state is

$$D(k) = -\frac{v_0 \left(\frac{1}{v} \sum_{k'}' D(k') \right)}{E - 2\varepsilon_k} \quad (2.29)$$

where \sum' means a sum over \vec{k}' such that $|\vec{k}'| < k_F$ and $\frac{\hbar^2 k'^2}{2m} < \varepsilon_F + \hbar\omega_D$

Now sum both sides over \vec{k}

$$\left(\sum_k' D(k) \right) = -v_0 \left(\frac{1}{v} \sum_{k'}' D(k') \right) \left(\sum_k' \frac{1}{E - 2\varepsilon_k} \right) \quad (2.30)$$

Canceling $\sum' D(k')$ from both sides, we obtain

$$1 = -v_0 \frac{1}{V} \sum_k' \left(\frac{1}{E - 2\varepsilon_k} \right) \quad (2.31)$$

$$1 = -v_0 \int_{\varepsilon_F}^{\varepsilon_F + \hbar\omega_D} \frac{D(\varepsilon)}{E - 2\varepsilon_k} d\varepsilon \quad (2.32)$$

$$1 = -v_0 D(\varepsilon_F) \int_{\varepsilon_F}^{\varepsilon_F + \hbar\omega_D} \frac{1}{E - 2\varepsilon_k} d\varepsilon \quad (2.33)$$

$$1 = \frac{v_0 D(\varepsilon_F)}{2} \ln \left(\frac{2\varepsilon_F - E + 2\hbar\omega_D}{2\varepsilon_F - E} \right) \quad (2.34)$$

Solving for E

$$E = 2\varepsilon_F - \frac{2\hbar\omega_D}{e^{\frac{2}{D(\varepsilon_F)v_0}} - 1} \quad (2.35)$$

For weak potential, $v_0 D(\varepsilon_F) \ll 1$, we have

$$E - 2\varepsilon_F = -2\hbar\omega_D e^{\frac{2}{D(\varepsilon_F)v_0}}$$

since the pair of electrons, in the absence of the attractive potential V , would

have a minimum energy of $2\varepsilon_F$, the binding energy of the pair is

$$E' = E - 2\varepsilon_F = -2\hbar\omega_D e^{\frac{-2}{D(\varepsilon_F)v_0}} \quad (2.36)$$

The energy gap represents the energy required to break a cooper pair, hence, larger energy gaps correspond to more stable superconductors according to the BCS theory. The energy gap at $T=0$ is given by

$$2\Delta(0) = 3.5K_B T_c \quad (2.37)$$

where K_B is the Boltzmann constant

BCS theory predicts that the transition temperature related to ω_D

$$T_c = \frac{1.14\omega_D}{K_B} e^{\frac{-1}{D(0)V}} \quad (2.38)$$

where $D(0)V = \lambda$, λ is coupling parameter which expresses the material dependent strength of the coupling of electrons to the bosonic mode that leads to cooper pair formation.

The regime where this parameter is small, $\lambda \ll 1$, is called the weak coupling limit, which is the limit where BCS theory is valid. On the other hand, the regime where this parameter is large, $\lambda \gg 1$, is called the strong coupling regime, where BCS theory is not valid.

The other important parameter associated with superconductivity, which follows from BCS theory, is the presence of coherence length. It is defined as the distance over which two electrons combine to form a Cooper pair. The BCS theory makes a crucial assumption at the beginning that an attractive force exists between electrons [17].

In Type I superconductors, this force is due to Coulomb attraction between the electron and the crystal lattice. An electron in the lattice will cause a slight increase in positive charges around it. This increase in positive charge will, in turn, attract another electron. These two electrons are known as a Cooper pair. If the energy required to bind these electrons together is less than the energy from the thermal vibrations of the lattice attempting to break them apart, the pair will remain bound. This explains (roughly) why superconductivity requires low temperatures- the thermal vibration of the lattice must be small enough to allow the forming of Cooper pairs. In a superconductor, the current is made up of these Cooper pairs, rather than individual electrons. So, Cooper pairs are formed by Coulomb interactions with the crystal lattice. This is also what overcomes resistance. An electron inside the lattice causes a slight increase of positive charge due to Coulomb attraction. As the Cooper pair flows, the leading electron causes this increase of charge, and the trailing electron is attracted by it.

This BCS theory prediction of Cooper pair interaction with the crystal lattice has been verified experimentally by the isotope effect, that is, the critical temperature of a material depends on the mass of the nucleus of the atoms.

If an isotope is used (neutrons are added to make it more massive), the critical temperature decreases. This effect is most evident in Type I, and appears only weakly in Type II. The Cooper pairs are somewhat related to Bose-Einstein Condensation. The Cooper pairs act somewhat like bosons, which condense into their lowest energy state below the critical temperature, and lose electrical resistance [18]. BCS theory could also successfully predict the observed phenomena of isotope effect. The critical temperature varies inversely proportional to the isotopic mass (M)

$$M^{1/2}T_c = \text{constant} \Rightarrow T_c = \frac{\text{const}}{M^{1/2}} \quad (2.39)$$

An electron with wave vector \vec{k} emits a virtual phonon with wave vector \vec{q} which is absorbed by an electron. This scatters an electron with \vec{k} into $\vec{k}-\vec{q}$ and into $\vec{k}+\vec{q}$ as shown in fig(2.4), where \vec{q} is phonon wave vector.

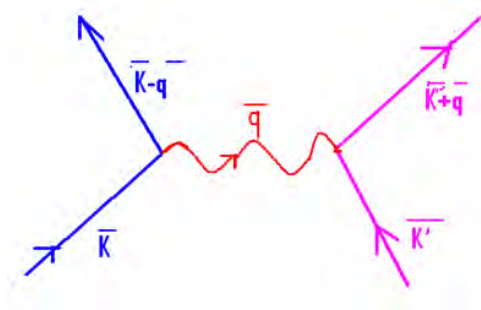


Figure 2.4: Electron-phonon interaction mediated by emission and absorption of a Virtual Phonon [19]

2.3 High Temperature Superconductivity

High temperature superconductivity (HTS) is the phenomena that is characterized by zero resistance and expulsion of magnetic field inside the superconductors, with a superconducting transition temperature T_c above 30 K. It was believed that the mixture of itinerant electrons (holes) together with some important antiferromagnetic correlations (or fluctuations) are important ingredient for the emergence of high temperature superconductivity [20].

In 1986 Bednorz and Muller discovered superconductivity in a lanthanum based cuprate perovskite material, which had a transition temperature of 35 K. Lanthanum strontium cuprate oxide ($\text{La}_{2-x}\text{Sr}_x\text{CuO}_4$) discovered in the same year [21]. In Jan, 1987, YBCuO was discovered with a superconducting transition temperature $T_c=92$ K [22].

In 1988, $\text{Bi}_2\text{Sr}_2\text{CaCu}_2\text{O}_{2+x}$ (bismuth Strontium calcium copper oxide) discovered with superconducting transition temperature $T=108$ K [23] and Thallium barium Calcium Copper Oxide (TBCCO) or $\text{TlBa}_2\text{Ca}_2\text{Cu}_4\text{O}_x$ also discovered with superconducting transition temperature $T_c=127$ K [24].

Recently, the highest temperature superconductor (at ambient pressure) is mercury barium calcium copper oxide ($\text{HgBa}_2\text{Ca}_2\text{Cu}_3\text{O}_x$), with T_c is 134 K [25] and reaches 164 K under high pressure [26]. Cuprates remained a high priority due to its high T_c until the discovery of superconductivity in iron-pnictide be led by Yoichi Kamihara who discovered that CuO plane is not a requirement for superconductivity.

In 2008, the highest T_c non cuprates superconductor is pnictide ($\text{Ca}_{1-x}\text{Nd}_x\text{FeAsF}$) with $T_c = 57$ K, currently reported [27].

The search for high temperature superconductors has been on going process since the discovery of the first high temperature superconductor.

The main goal of all this research is to get the High temperature superconductivity and room temperature superconductivity.

A graph of the high temperature superconductors and the year of their discovery is depicted in fig (2.5).

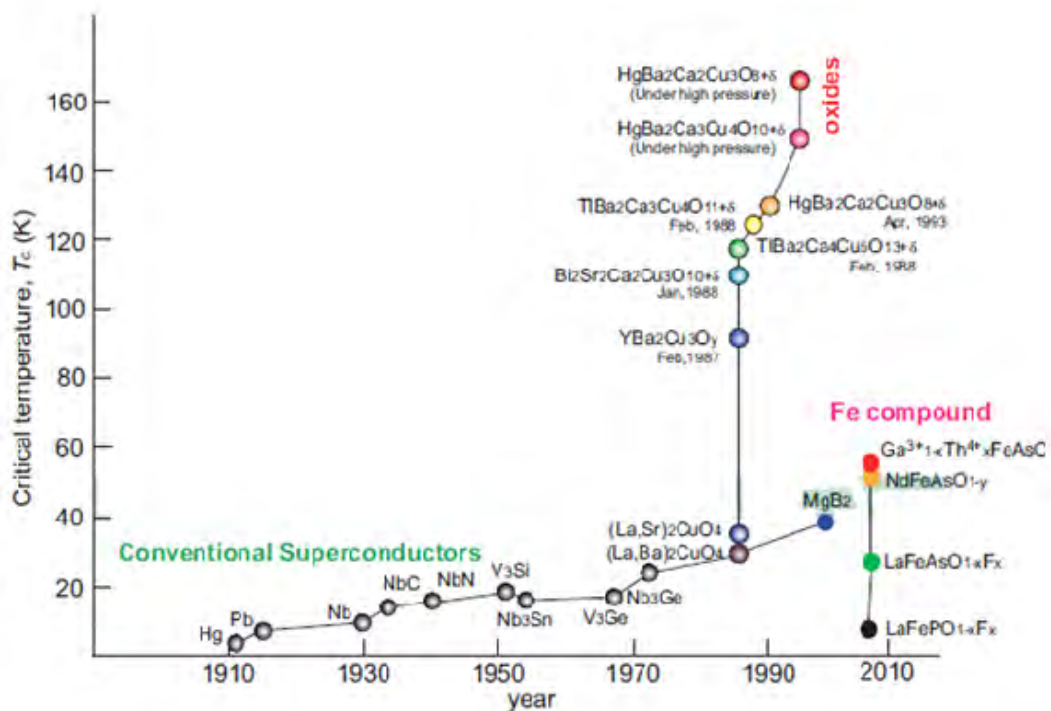


Figure 2.5: Graph represents the highest temperature superconductors and the year of discovery [28].

The application of high temperature superconductors, in general, could be classified into two categories:

Large scale and small scale: Large scale applications include: -high speed trains, magnetic energy storage, magnetic resonance imaging (MRI) for medical applications, and high energy Physics experiments, whereas small scale applications include: Josephson devices, superconducting quantum interference devices, microwave devices and so on [29].

2.3.1 Mechanisms of high temperature superconductivity

The mechanism of high temperature superconductivity is still highly controversial, this being due to mostly the lack of exact theoretical computations on such strongly interacting electron systems, however, there are different scenarios for mechanisms for high temperature superconductivity [93], namely, exciton, Bi-exciton, polaron, Bi-polaron and magnon.

1. Exciton: bound state of electron and hole which are attracted to each other by electrostatic force. It is an electrically neutral quasi particles, and has slightly less energy than the unbound electron and hole. The electron and hole may have either parallel or anti-parallel spins. The spins are coupled by the exchange interaction, giving rise to exciton fine structure. An exciton can move through the crystal and finally, the electron and hole recombine.
2. Bi-exciton: It is a bound state of two exciton.

3. Polaron: An electron in a material may cause a distortion in a lattice.

The combination of electron and distortion (which is a cloud of phonon) is a polaron. It is the interaction between electron and phonon via polarization. The physical properties of the polaron differ from the band electron, particularly it is characterized by its binding energy, effective mass, by its response to external electric and magnetic field.

4. Bipolarons: Bipolaron is a bound state of two polaron.

5. Magnon/spin fluctuation/: A magnon is a collective excitation of electron's spin structure in a crystal lattice. It is a quantized spin wave. A magnon carries a fixed amount of energy and momentum and it also possesses a spin of \hbar . Magnon as the name indicates are intimately related to magnetism. At low temperatures far below the temperature of magnetic ordering, magnon can be considered as weakly interacting bosons.

Despite these mechanisms, most solid state researchers have believed that magnon/magnetic spin fluctuation could be the possible mechanism for superconductivity in high temperature superconductors.

2.3.1.1 Explanation of the spin fluctuation mechanism

Even though the mechanism of high T_c superconductivity is not clearly understood, most rigorous theoretical calculations, including phenomenological and diagrammatic approaches, led to magnetic spin fluctuations as the pairing mechanism for these systems. The qualitative explanation is as follows:

In a normal conductor, a hole is created whenever an electron is moved. This causes a resistivity because charge neutrality must be conserved and as elec-

trons move under an electric field, they drag holes behind them through defects and thermal oscillations in the system. In contrast, in a superconductor, one gets an unlimited supply of electrons without creating holes behind. This is through the creation of so called Cooper pairs in a superconductor. Cooper pairs are pairs of electrons. In a normal conductor, creation of an electron leads to creation of a hole, which conserves the number of particles.

But in a superconductor, it is possible to create a Cooper pair without creating holes and therefore not to conserve the number of particles, hence leading to the unlimited supply of electrons [30]. In a conventional superconductor, Cooper pairs are created as follows.

When an electron moves through the system, it creates a depression in the atomic lattice through lattice vibrations known as phonons. If the depression of the lattice is strong enough, another electron can fall into the depression created by the first electron the so called water-bed effect and a Cooper pair is formed [31].

In a high T_c superconductor, the mechanism is extremely similar to a conventional superconductor, except, in this case, phonons virtually play no role and their role is replaced by spin-density waves. As all conventional superconductors are strong phonon systems, all high T_c superconductors are strong spin-density wave systems, within close vicinity of a magnetic transition to, for example, an antiferromagnet. When an electron moves in a high T_c superconductor, its spin creates a spin-density wave around it. This spin-density wave in turn causes a nearby electron to fall into the spin depression created by the first electron (water-bed effect again). Hence again, a Cooper pair is formed.

Eventually, when the system temperature is lowered , more spin density waves

and Cooper pairs are created and superconductivity begins when an unlimited supply of Cooper pairs, denoted as a phase transition happens. Note that in high T_c systems, as these systems are magnetic systems due to the Coulomb interaction, there is a strong Coulomb repulsion between electrons. This Coulomb repulsion prevents pairing of the Cooper pairs on the same lattice site, the pairing of the electrons occurs at near-neighbor lattice sites as a result.

This is the so called d-wave pairing, where the pairing state has a node (zero) at the origin [32]. Superconductivity in the cuprates has been a problem standing for more than two decades and there is still no agreement on the pairing mechanism.

2.3.2 Pairing symmetry

Pairing symmetry is a property of Cooper pairs, It is the bound electron pairs that is a distinctive characteristics of all superconductors, whether high temperature or conventional superconductor. The paired electrons act as if they were a single particle, and the energy required to break Cooper pairs is measured by the superconducting gap. The symmetry of the superconducting gap is known as the pairing symmetry. Pairing symmetry is an important characteristic of Cooper pairs that is intimately related to the mechanism of superconductivity. In conventional superconductors, the Cooper pairs have s-wave pairing symmetry, which takes the shape of a sphere. In contrast, Cooper pairs in the cuprate family of high-temperature superconductors exhibit d-wave pairing symmetry, which looks a bit like a four-leaf clover. The leaves, or lobes, are areas where the superconducting gap is finite. At the points where two leaves join, known as

nodes, the superconducting gap goes to zero.

What holds the Cooper pairs together?

In an ordinary superconductor, phonons provide the glue. A passing negatively charged electron draws the positively charged ions in the material slightly closer together in its wake, and that concentration of positive charge then pulls along the second electron. The subtle ripples in the crystal lattice are the phonons. But theorists say phonons do not pull hard enough to keep electrons paired at the sky high temperatures which are still far below the freezing point of water achieved in high temperature superconductors. Instead, many think the glue originates in interactions among the electrons themselves, such as waves of magnetism called spin fluctuations [33]

Symmetry of the gap can be s-wave, p-wave and d-wave, etc. the superconducting order parameter or gap function is a complex function with both amplitude and phase that describes the macroscopic quantum state of cooper pairs. Its amplitude can in general depend on momentum direction and can change sign through its phase component. It is isotropic (s-wave symmetry). Strong evidence has been deduced that the attractive electron pairing interaction in HTS cuprates is magnetic in origin [34].

In s-wave state, the energy gap $\Delta(T)$ is isotropic, i.e $\Delta(k)$ is constant over the Fermi surface.

For extended s-wave state, the energy gap $\Delta(T)$ is anisotropic, i.e $\Delta(k)$ exhibit a variation over the Fermi surface which has the same symmetry of crystal.

The *d*-wave state, the energy gap $\Delta(k)$ is anisotropic, but with a symmetry that is lower than the symmetry of the crystal.

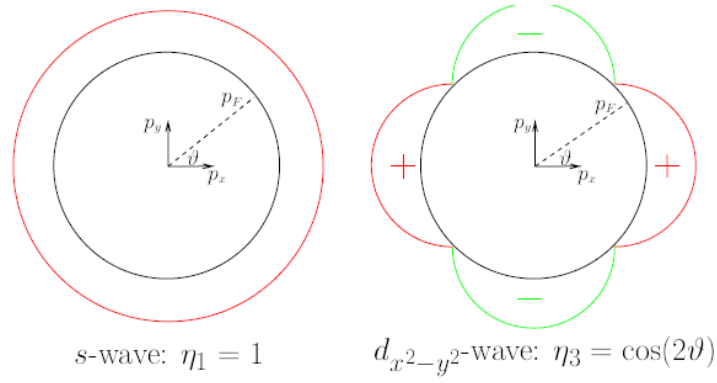


Figure 2.6: Pairing symmetry [35]

Conventional BCS theory assumes an S-wave symmetry of the superconducting gap function

$$\Delta(k) = \Delta_0$$

A pnictide superconductor possesses a spin-singlet extended s_{\pm} -wave symmetry, in which the superconducting order parameter changes its sign between the Fermi surfaces.

The cuprates superconductor on the other hand posses a d-wave gap function, leading to nodes and sign changes as a function of momentum

$$\Delta(k) = \Delta_0 \cos(2\phi) \quad (2.40)$$

where ϕ the angle of k -vector.

For S -wave (anisotropic) with basis function

$$\eta_1(k) = 1 \quad (2.41)$$

and For $d_{x^2-y^2}$ -wave with basis function

$$\eta_3(k) = \frac{1}{2} \quad (2.42)$$

The gap equation (the order parameter) can be expanded in the basis function

$$\Delta(k_F) = \sum \Delta_i \eta_i(K'_F) \quad (2.43)$$

2.4 Cuprates superconductivity

There are family of copper oxide compound collectively called cuprates. Cuprates superconductors are quasi two dimensional materials with their superconducting properties determined by electron moving within weakly coupled copper oxide CuO_2 layers. Neighboring layers containing ions such as lanthanum, barium, strontium, or other atoms act to stabilize the structure and dope electrons or holes onto the copper oxide layers. The undoped parents or mother compounds are Mott insulators with long range antiferromagnetic order at low temperature [36].

The cuprates superconductors take on a perovskite structure. The copper-oxide planes are checkerboard lattices with squares of O^{2-} ions with a Cu^{2+} ion at the center of each square. Chemical formula of superconducting materials generally contain fractional numbers to describe the doping required for superconductivity . The pairing symmetry for the cuprates materials have unconventional d-wave symmetry , meaning the wave function of cooper pairs has orbital angular momentum equals two [37]. The majority of superconducting cuprates are hole doped. The number of electron doped cuprate is very limited for example $\text{Nd}_{2-x}\text{Ce}_x\text{CuO}_4$ and $\text{Pr}_{2-x}\text{Ce}_x\text{CuO}_4$ [38].

2.4.1 Phase diagram for cuprates superconductivity

Phase diagram is a graphical representation of the states under different conditions of temperature and doping level. A typical phase diagram has temperature on y-axis and doping level on x-axis. The fundamental properties of cuprate materials is the existence of copper oxygen planes in their unit cell. The number of these planes changes between the different cuprates. The oxidation number of the atoms in the CuO_2 can be controlled by changing the molecular formula (this process is called doping) [39]. Doping changes the chemical and physical properties of the material. Most of the compounds are doped by adding holes (P type) , while some are doped by electrons (N type) . There are several critical doping levels in the phase diagram of the cuprates at which the ground state changes. The first critical doping level is when the long range antiferromagnetic order of the undoped parent compound is destroyed and replaced by a spin glass state, next superconductivity emerges then the spin glass is destroyed and finally, superconductivity is destroyed and replaced by a metallic state. These critical levels exist in the phase diagram of all cuprates which can be doped over a wide range such as $\text{YBa}_2\text{Cu}_3\text{O}_x$, but they vary between compounds [40]. The cuprates phase diagram is even more complicated and includes other phases, and it is still under investigation. Several attempts have been made to construct a universal phase diagram but thus far only partial diagrams, of only one or two phases, have been achieved. The doping process is very difficult to describe quantitatively because it involves many different electronic orbital and energies [41].

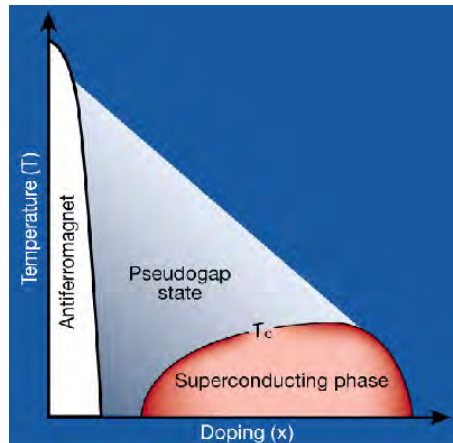


Figure 2.7: Typical cuprates phase diagram [42]

There are different phases of cuprates superconductor:-

1. Mott insulator: With no doping the cuprates are poor conductors. They are believed to be an example of the so called 'Mott insulator'. The Mott insulator is fundamentally different from a conventional (band) insulator. In the latter conductivity is blocked by the Pauli Exclusion Principle. In a Mott insulator conductivity is blocked instead by the electron-electron Coulomb repulsion [43].
2. Pseudo gap: The most mysterious part the phase diagram of cuprates comes after the loss of the antiferromagnetic ordering because of doping. Commonly known as the 'pseudogap' this phase it is a conductor but with properties much different from the properties of the usual conductors (generally Fermi liquids). Pseudogap state actually shares many common properties with the superconducting state for example the form (d-wave) of the gap in the electron spectrum is the same. The common view is that this is the region where the battle between two different types of order (

Mott insulator and superconductor) is fought. On the opposite side of the phase at a very high doping and temperature there is a cross-over to the 'normal' Fermi liquid behavior [44].

3. Superconductor: Increasing the doping in the pseudo gap state leads eventually to the Superconductive T_c becomes higher and higher until it reaches maximum (optimal doping) and then starts decreasing. Like conventional superconductor the current carriers are electron pairs (Cooper pairs). According to the conventional BCS theory after forming the condensate of Cooper pairs there is a uniform (hence the name s-wave) gap in the k-space electron spectrum. In High T_c superconductor there is still a gap but it is anisotropic with d-wave symmetry, However, the microscopic mechanism of the superconductor is still uncertain. It is clear that the electron-phonon interaction that is responsible for the conventional superconductor is too weak to do the same in the cuprates.

Superconductivity in the cuprates has been a puzzle for more than two decades and there is still no consensus on the pairing mechanism. Cuprates superconductors do not occur in nature, and have been synthesized in the laboratory. There are several hundred different cuprate materials.

The general formula of cuprate can be written as

$$(CuO_2)_n A_{n-1} X, \quad (2.44)$$

where n is a positive integer, A is an alkaline Earth or rare element or Y, X is an arbitrary collection of elements possibly including Cu and or O

Yttrium barium copper oxide ($\text{YBa}_2\text{Cu}_3\text{O}_{7-x}$)

Yttrium barium copper oxide, often abbreviated YBCO is a crystalline chemical compound with the formula $\text{YBa}_2\text{Cu}_3\text{O}_{7-x}$. Its nickname [YBCO-123, Y123] and it has a fully ordered orthorhombic crystal lattices, the doping distribution is squared. This material, a famous high temperature superconductors because it was the first material to achieve superconductivity above boiling point of liquid Nitrogen.

The superconducting properties of $\text{YBa}_2\text{Cu}_3\text{O}_{7-x}$ are sensitive to the value of x , its oxygen content. only those materials with $0 \leq x \leq 0.65$ are superconducting below T_c and when $x \sim 0.07$ the material superconduct at highest temperature of 95 K [45].

2.4.2 Structure of cuprates superconductor

The crystal structure of cuprate superconductor is of a perovskite type and it is highly an isotropic. Superconductivity in cuprates occur in CuO_2 planes. The CuO_2 layers in Cuprates are always separated by layers of other atom such as Bi, O, Y, Ba, La, e.t.c which provides the charge carriers into the CuO_2 planes [38]. Cuprate superconductors like $\text{La}_{2-x}\text{Sr}_x\text{CuO}_4$ (LSCO), $\text{Tl}_2\text{Ba}_2\text{CaCu}_2\text{O}_8$ (Tl-2212), $\text{HgBa}_2\text{Cu}_2\text{O}_6$ (Hg-1212), and $\text{YBa}_2\text{Cu}_3\text{O}_7$ (YBCO) type compounds with significant cations substitution have a tetragonal crystal structure.

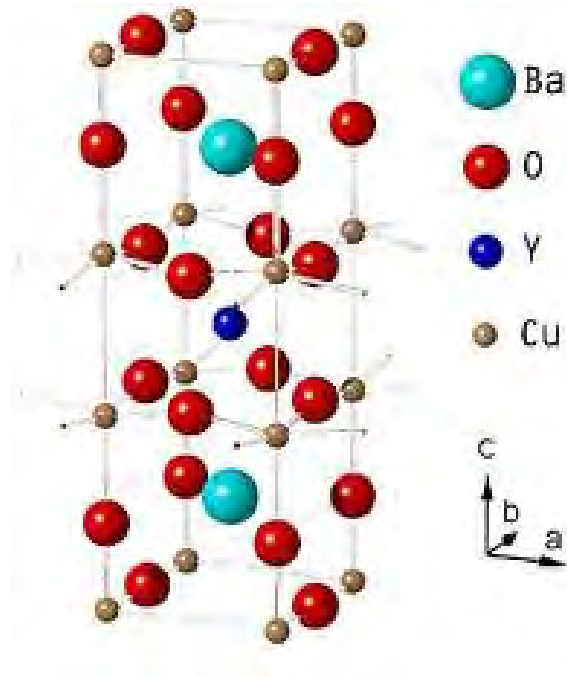
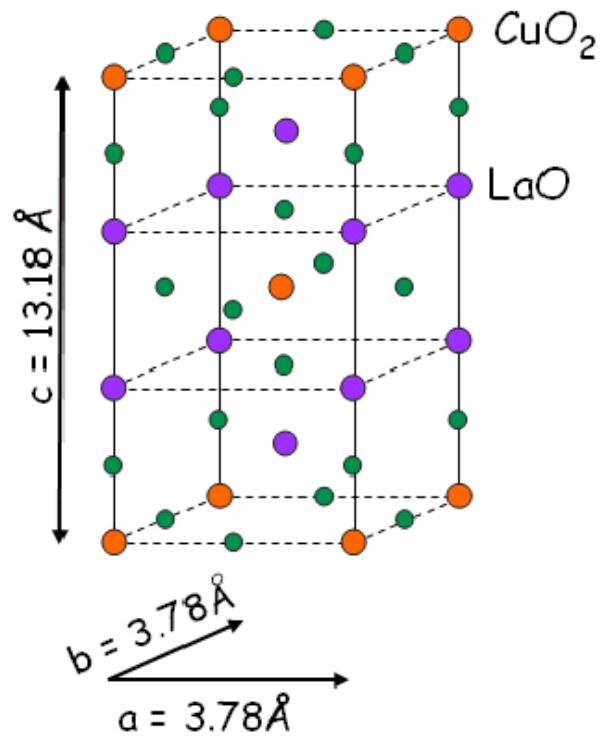
Figure 2.8: Structure of cuprates: YBa₂Cu₃O_{7-x} [46]

Figure 2.9: Structure of cuprates: LaCuO [46]

2.4.3 Layer of cuprates

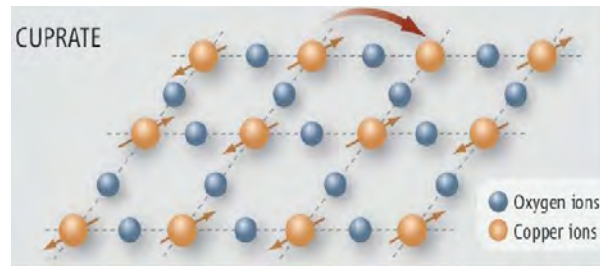


Figure 2.10: layer of cuprates [47]

2.4.4 Fermi surface of cuprates

The Cooper pairs in the cuprate family of high-temperature superconductors exhibit d-wave pairing symmetry, which looks a bit like a four-leaf clover. The leaves, or lobes, are areas where the superconducting gap is finite. At the points where two leaves join, known as nodes, the superconducting gap goes to zero

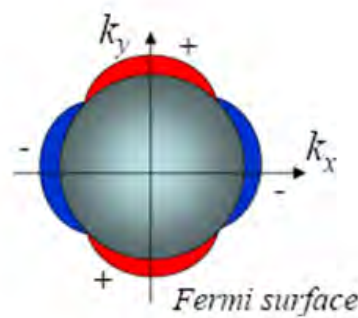


Figure 2.11: Fermi surface cuprates [48]

D wave nodes in K-space where gap vanishes and the gap is largest along the K_x and K_y -direction.

2.5 Pnictides superconductivity

Pnictides are any binary compound of Pnictogen and less electronegative element, Pnictogen: $Z=7$ nitrogen (N), $Z=15$ phosphorus (P), and $Z=33$ arsenic (As) etc.

Pnictogens have 5 electrons in the outer shell: 2 electrons in the s sub shell, 3 unpaired electrons in the p sub shell.

Pnictides are a relatively new class of superconductors discovered by group at the Tokyo Institute for Technology led by Yoichi Kamihara [49]. Pnictides are a type-II superconductor and thus produce vortices between H_{c1} and H_{c2} .

2.5.1 Discoveries of pnictides superconductors

The first pnictide superconductor, LaFePO, was discovered in 2006 with superconducting transition $T_c=4$ K [50], After this discovery, by doping some of the oxygen sites with fluorine, the critical temperature could be increased to ≈ 26 K for LaFeAsO $_{1-x}$ F $_x$ ($0.05 < x < 0.12$) [51], which was discovered by Kamihara et al in Feb, 2008. These crystals are formed by stacking LaOF and FeAs layers alternately. Each iron atom is surrounded tetrahedrally by four As atoms, and each FeAs layer is constructed by connecting the edges of the As tetrahedra. Moreover, subsequent studies clarified that replacement of La by other rare earth elements increases the transition temperature markedly.

41 K for Ce (CeF $_x$ O $_{1-x}$ FeAs) [52], 52 K for Pr (PrF $_x$ O $_{1-x}$ FeAs) [53],

52 K for Nd (NdF $_x$ O $_{1-x}$ FeAs) [54],

55 K for Sm (SmF $_x$ O $_{1-x}$ FeAs) [55] and 56 K for Gd $_{1-x}$ Th $_x$ FeAsO [56].

There are three groups of iron-arsenide (materials which contain layer of FeAs) [57].

The first group contains the materials of the type ReOFeAs where Re stands for rare earth element and AeFFeAs where Ae stands for Alkaline earth. Members of this group of materials are often referred to as the 1111 type compounds.

Second group contains compounds of the type AeFeAs and AFe_2A_2 with $A=Ba, Sr, Ca$ (alkaline). These material referred to as 122 type compounds. The third group consists of only material AFeAs and it is referred to as a 111 type compound. The recent discovery of high- T_c superconductivity in iron pnictides and related compounds has strongly intensified the research activity in solid-state physics. The highest transition temperature attained in iron pnictides is about 57 K to date, i.e ($Ca_{1-x}Nd_xFeAsF$ with $T_c=57$ K) [58]. It is the highest T_c non-cuprates superconductors.

2.5.2 Phase diagram for pnictides superconductivity

Experiments suggest that carrier doping is important method for controlling iron-pnictide superconductivity. It has effect on transition temperature and pairing symmetry. Carrier doping is the chemical substitution of atoms, only shifts the chemical potential and retains rigidly the band structure. They are distinct regions in the phase diagrams of iron pnictides, namely, antiferromagnetic, pseudogap, and superconducting region as depicted fig1.10. As the doping concentration increases, the superconducting transition temperature increases and reaches a maximum at some point, later on, superconducting transition temperature decreases monotonically, lastly, it vanishes.

The superconducting transition temperature T_c drops around high doping levels where the electron or hole pockets disappear. Pnictide superconductors exhibit antiferromagnetic order in the parent phases and superconductivity emerges by suppressing magnetism upon doping. The pnictides exhibit a property called magnetic frustration, a particular atomic arrangement that suppresses the natural tendency of iron atoms to magnetically order themselves in relation to each other. These frustration effects enhance magnetic quantum fluctuations, which may be responsible for the high temperature superconductivity [59].

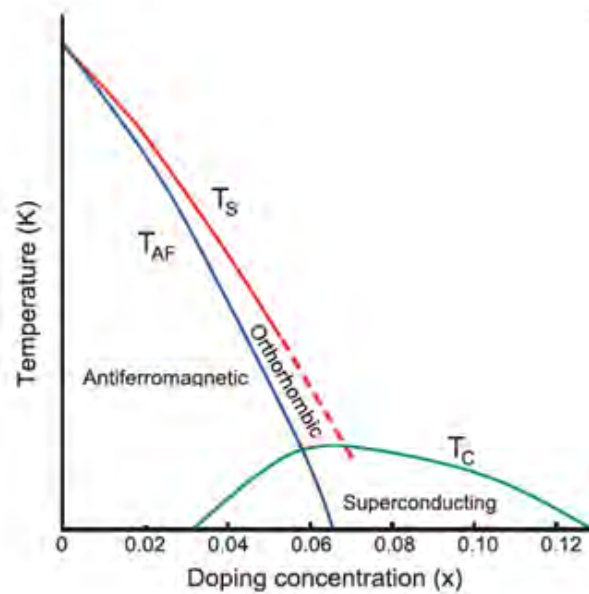


Figure 2.12: phase diagrams of pnictides [60]

2.5.3 Structure of pnictides superconductor

Pnictides are layered, similar to cuprates. The iron-arsenic plane is responsible for the superconductivity in pnictides. For example, the critical temperature of LaOFeAs was found to increase with a doping of fluorine. The doping was found

to increase the number of carriers in the conductive layer [61]. The iron, Fe^{2+} , forms tetrahedrons within the layers, and the pnictide's Fermi level is formed by $3d_{xy}$, $3d_{yz}$, or $3d_{zx}$ orbitals. This is markedly different from cuprates, which form a square, planar structure and where there is $3d_{x^2-y^2}$ symmetry [62]. The proposed pairing symmetry in pnictides is a spin-singlet extended s_{\pm} -wave symmetry, in which the superconducting order parameter changes its sign between the Fermi surfaces. Parent compound of pnictides is poor conductor or sometimes also semiconducting. Magnetism plays a key role in iron pnictide superconductors' crystal structure.

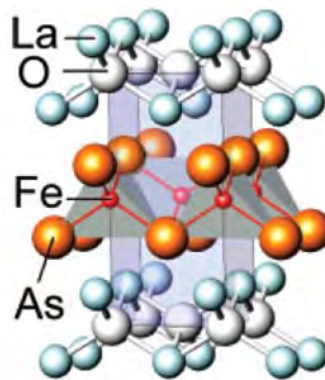


Figure 2.13: Structure of iron pnictides (1111), R0FeAs , R= rare earth [63]



Figure 2.14: Structure of iron pnictides (1111), $(\text{A,R})\text{FeAsF}$, A= Alkaline [63]

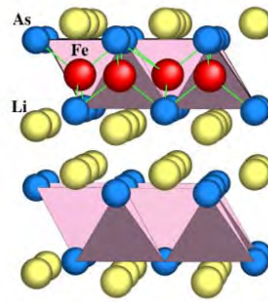


Figure 2.15: Structure of iron- pnictides (111), AFeAs [64]

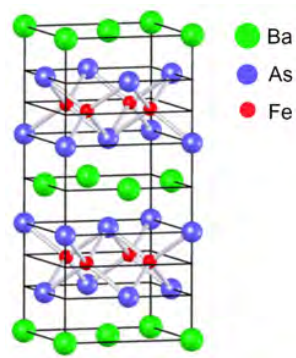


Figure 2.16: Structure of iron pnictide 122, BaFe₂As₂ [65]

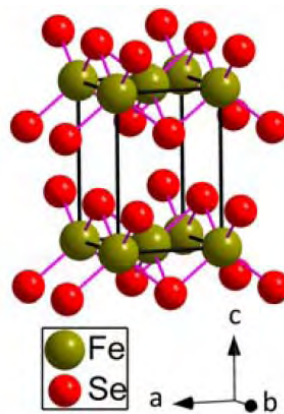


Figure 2.17: Structure of 11, Fe (S,Se,Te) [66]

2.5.4 Fermi surface of pnictides

The Fermi-surface topology is a key ingredient for high temperature superconductivity in iron-based layered pnictides. The so called s_{\pm} model predicts superconducting gaps of one sign on the Fermi surface.

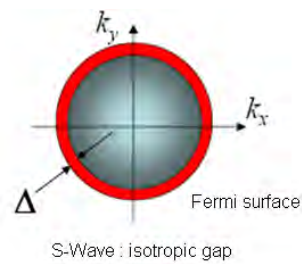


Figure 2.18: Fermi surface of pnictides [67]

2.5.5 Layer of pnictides

Layer of iron-Pnictides FeAs (Iron is purple and arsenic is yellow)

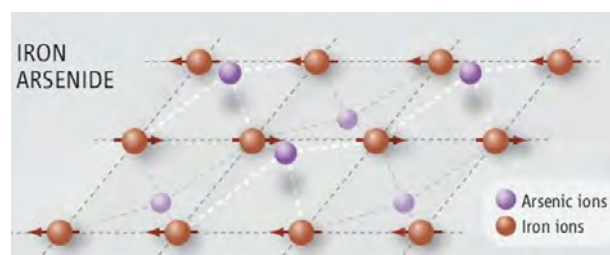


Figure 2.19: layer of pnictides [68].

Chalcogenides

Iron based superconductors are classified into two families iron pnictides and iron chalcogenides. Iron pnictides are compounds containing iron and pnictogen. Iron chalcogenides are compounds containing iron and chalcogen. The chalcogens are the chemical elements in group VI of the periodic table. This group is also known as oxygen family.

It consists of elements, oxygen (O), sulfur (S), selenium (Se) and tellurium (Te) and polonium (Po).

Eventhough, all the group VI elements are defined chalogens, the term chalcogenides more commonly used for sulphides (FeS), selenides (FeSe) and tellurides (FeTe).

Many metal ores exist as chalcogenides. It is denoted by Ch.

Iron Chalcogenides show low an isotropes, high critical fields and high critical current densities. Superconductivity in layered Fe chalcogenide was initially found in FeSe by Hsu et al. with T_c of 8 K at ambient pressure [69,91]. Reported value of superconducting transition temperature (T_c) in iron chalognides include 14 K in $\text{FeT}_{0.5}\text{S}_{0.5}$ [70,91], 2 K in $\text{Fe}_{1.13}\text{T}_{0.85}\text{S}_{0.1}$ [71,91], 10 K in $\text{FeT}_{0.8}\text{S}_{0.2}$ [72,91]

The high superconducting transition temperature has been achieved in layered materials such as cuprate, iron (Fe) based and MgB_2 superconductors. One of the notable groups of layered superconductors is the chalcognides.

Iron selenides (FeSe) shows a superconducting transition temperature around 10K and shows a marked increase of superconducting transition temperature upto 65 K under pressure [73,92]. On the other hand, FeTe undergoes an anti-ferromagnetic transition at 70 K.

However, a partial substitution of Te by S or Se suppresses the antiferromagnetic ordering and induces superconductivity. This family is very interesting because the physical properties markedly change upon the covalent substitutions of S, Se and Te [74].

Krizton Maziopa reported a new synthesizing method to intercalate alkaline metal to *FeSe* with general formula $Ax(C_5H_5N)_yFe_{2-z}Se_2$, ($A=Li, Na, K, Rb$) that shows superconducting onset $T_c \sim 45$ K [75].

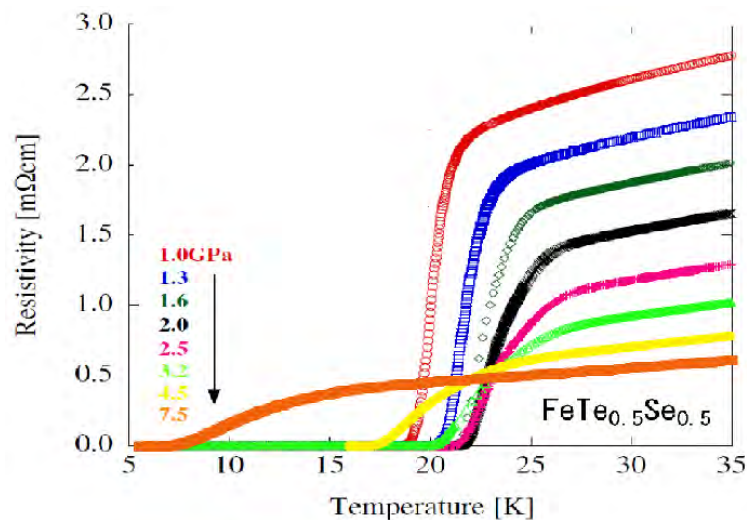


Figure 2.20: Temperature versus resistivity for $FeTe_{0.5}Se_{0.5}$ under pressure [76]

Fig2.20 displays that the superconducting transition temperatures depend on the pressure and doping concentration. As the pressure increases, the superconducting transition temperature for $FeTe_{0.5}Se_{0.5}$ decreases.

Structure of iron chalcogenides

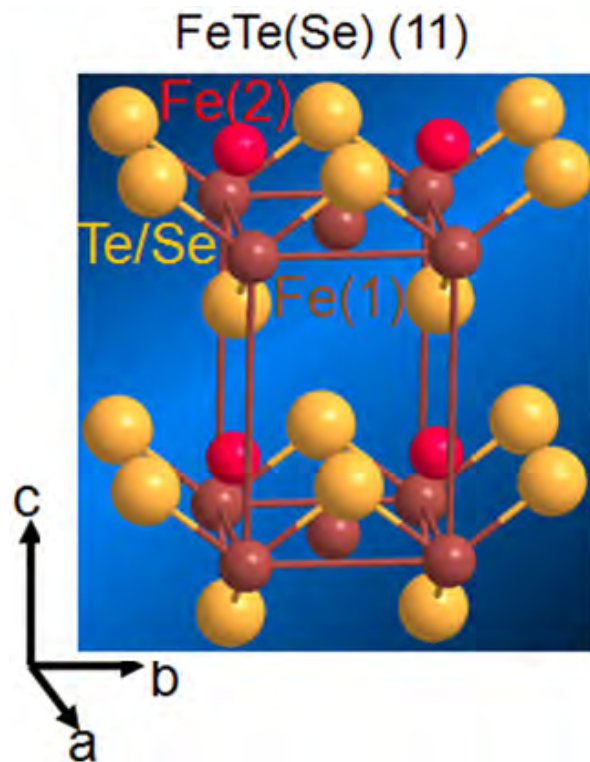


Figure 2.21: Structure of iron chalcogenides [77,66,83]

Iron Chalcogenides have low carrier density, high density of state and they are non toxic.

There is a similarity in electronic state of Fe chalcogenides and Fe pnictides ,moreover, they share the same pairing mechanism and they have similar fermi surface and band structure [78].

2.6 Electronic specific heat

The electronic specific heat (C_{el}) is defined as the ratio of heat used by the electrons to rise in temperature of the system.

The electronic specific heat of the electrons in a superconductor varies with absolute temperature (T) in the superconducting state. The electronic specific heat in superconducting is smaller than in normal state at low enough temperature, but it becomes larger than in the normal state as the temperature approached to the critical temperature T_c where it drops abruptly to the electronic specific heat in normal state for superconductors.

At sufficiently low temperatures, the normal heat capacity C_n is expressed as the sum of an electronic and the lattice heat capacity [79]

$$C_n = \gamma T + \frac{12}{5} \pi^4 R \left(\frac{T}{\theta} \right)^3 \quad (2.45)$$

where R is the gas constant, θ -Debye tetemperature of the lattice vibration γ -constant which is proportional to the density of states at the Fermi surface and which may depend on electron correlations and the electron-phonon interaction.

The first and third powers of temperatures correspond to an electronic and a lattice heat capacity respectively.

The electronic heat capacity of superconductors below critical temperature [80] is given by

$$\frac{C_{es}}{\gamma T_c} = a e^{-\frac{bT_c}{T}} \quad (2.46)$$

where a and b are constants

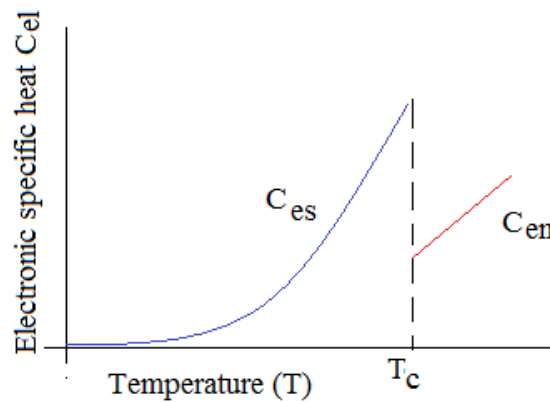


Figure 2.22: The electronic specific heat versus Temperature [81]

As we see from fig.2.22, specific heat is linearly proportional to the temperature which is in the normal state and exponential proportional to the temperature in superconducting state.

The electronic specific heat per atom of a superconductor is defined by

$$C_{el} = \frac{d}{dT} \left(\frac{1}{N} \sum_n 2\xi_k \langle n_k \rangle \right) = \frac{d}{dT} \left[\frac{1}{N} \sum_n 2\xi_k \langle \hat{a}_{k\uparrow}^\dagger \hat{a}_k \uparrow \rangle \right] \quad (2.47)$$

2.7 Application of Superconductivity

Superconductivities are widely used in various technologies, moreover, it is also ongoing research. One of the most successful applications of superconductors is in the production of very large magnetic fields, Here, let us explain some of the most important application of superconductor in generating very large magnetic fields, namely, Superconducting Magnetic Levitation, Magnetic Resonance Imaging (MRI) devices, High energy physics [82].

2.7.1 Magnetic Levitation Train



Figure 2.23: The Yamanashi MLX01MagLev Train [83]

The tracks are walls with a continuous series of vertical coils of wire mounted inside. The wire in these coils is not a superconductor. As the train passes each coil, the motion of the superconducting magnet on the train induces a current in these coils, making them electromagnets. The electromagnets on the train and outside produce forces that levitate the train and keep it centered above the track. In addition, a wave of electric current sweeps down these outside

coils and propels the train forward [84].

2.7.2 Magnetic Resonance Imaging (MRI)

Magnetic Resonance Imaging (MRI) scans produce detailed images of soft tissues. The superconducting magnet coils produce a large and uniform magnetic field inside the patient's body.



Figure 2.24: MRI (Magnetic Resonance Imaging) [85]

Magnetic resonance imaging machine

This technique uses the high field to split the degenerate spin state of hydrogen nucleus, which can then be investigated using electromagnetic radiation in the radio wave region. This allows the machine to image two dimensional cross-sections which have hydrogen atoms in different chemical environments. As the body contains many hydrogen atoms present in water, different tissues in the body give different signals. These two dimensional slices can be built up to form complete pictures of the area of the body being imaged [86].

Magnetic resonance imaging machine consists of five components [87]:-

- Radio frequency coil: this emits electromagnetic radiation of radio frequency, which excites hydrogen nuclei present within the patients.
- Patient table: Allows the patient to easily and safely be placed within the bore of the magnet
- Scanner: These detect the radio waves emitted by the hydrogen nuclei relaxing into their ground state
- Superconducting magnet: These are the superconducting magnets used to create a high enough field to split the usually degenerate ground state of hydrogen nuclei. The wires used are often of [NbTi] wires which must be maintained at cryogenic temperatures with liquid helium.
- Housing: This section of machine houses the electronics and cooling system which keeps the superconductors at low temperature.

High Energy Physics

High strength magnets are key components in particle colliders used to probe the most basic constituents of matter. They are used to deflect high velocity charged particles to keep them in a circle and allow them to be constantly accelerated [88].

Another application making use of superconductors to produce high strength magnetic fields are electric motor, generator, and magnetic energy storage.

Electronic application

Current micro electronics are beginning to be limited by the speed at which heat can be removed which is produced by the electronic circuits. In order to speed up computing power, interconnects between various components of the circuit can be shortened. However, this creates even more heating problems due to higher current densities which have to be used. Superconducting wires could eventually be used to remove resistive heating and help solve this problem [89]. Josephson devices, superconducting quantum interference devices (SQUID), microwave devices, RF and microwave filters (e.g.for mobile phone base stations, military ultra-sensitive/selective receivers) and resonators are some application superconductors in small scale.

The advantage of HTS:

- Significantly smaller computers and increased speed of computer chips.
- HTS generators and motors are substantially smaller and lighter than copper based machines.

The Disadvantage of HTS:

- Many HTS are made of toxic metals and disposal of them can affect the environment
- Powerful computers which are made from HTS can be used by the military to develop weapons and so on.

3

MATHEMATICAL TECHNIQUE

In this chapter, we will introduce the basic concept of Green functions method as mathematical techniques which are very essential to formulate the problem in the next chapter. In this technique, we have tried to derive the equation of motion of Heisenberg operators which is used to determine the superconducting order parameter, superconducting transition temperature and so on.

3.1 The Green Functions Method

The Green function methods for quantum many body systems were mainly developed in 1950's and early 60's. This concept was first introduced by British Mathematician Gorge Green in 1830 and that is why the function is named after him. The use of Green function method has become widespread in many body problems, particularly in problems of Solid state physics where a number of new results have been obtained.

The Green function method is an important part in the modern theory of superconductivity. This method permits a formulation of the theory in a very transparent and convenient form and provides a powerful tool to solve more complicated problems in high temperature superconductivity. A Green function is

used to solve inhomogeneous differential equation with boundary conditions.

There are various types of Green function. Some of these are:- Advanced Green function, Retarded Green function, casual, zero temperature, one particle, two particles and so on. To investigate the physics of high temperature superconductors based on many body theoretical models, the methods adopted for studying the microscopic Hamiltonian could be double time Green functions.

Green function or correlation function defined for two operators \hat{a} and \hat{b} which do not need to be hermitian, The operators \hat{a} and \hat{b} are:- fermions or bosons, creation or annihilation operators or displacement of an atoms in a lattices or current or charge densities.

For an arbitrary linear differential operator L in three dimension, the Green function $G(t, t')$ can be defined as

$$\hat{L}G(t, t') = \delta(t, t') \quad (3.1)$$

The Retarded Green function and the Advanced Green functions are defined as

$$G_r(t, t') = \ll a(\hat{t}), b(\hat{t}') \gg_r = -i\Theta(t - t') < [a(\hat{t}), b(\hat{t}')] >_r \quad (3.2)$$

$$G_a(t, t') = \ll a(\hat{t}), b(\hat{t}') \gg_a = i\Theta(t - t') < [a(\hat{t}), b(\hat{t}')] >_a \quad (3.3)$$

respectively.

In addition to this, the causal Green function is also defined as

$$G_c(t, t') = \ll a(\hat{t}), b(\hat{t}') \gg_c = -i < T_c(a(\hat{t})b(\hat{t}')) >_c$$

where $\ll \dots \gg$ represents the Green function, $\Theta(t - t')$ is called Heaviside step function. It is also called unit step function.

Heaviside function is a discontinuous function whose value is zero for negative

argument and one for positive argument. It was named after the English polymath Oliver Heaviside.

$$\theta(t, t') = \begin{cases} 1, & t > t' \\ 0, & t < t' \end{cases} \quad (3.4)$$

$\langle \dots \rangle$ denotes averaging over a grand canonical ensemble which can be defined as $\langle \dots \rangle = Z^{-1} \text{Tr}(e^{-i\beta\hbar})$

where Z is the grand partition function,

The Heaviside function is the integral of the Dirac delta function.

$$\theta(t, t') = \int_{-\infty}^t \delta(t - t') \quad (3.5)$$

$\hat{a}(t)$ and $\hat{b}(t')$ are annihilation and creation operators respectively.

$$[\hat{a}(t), \hat{b}(t)] = \hat{a}(t)\hat{b}(t) - \eta\hat{b}(t)\hat{a}(t)$$

The sign η is chosen depending on the operator, η is negative sign if $\hat{a}(t)$ and $\hat{b}(t)$ are fermions operators, and η is positive sign if they are boson operators.

T_ϵ is a time ordering operators in chronological order.

Again, we have for the operators in Heisenberg representation.

$$\hat{a}(t) = e^{\frac{iHt}{\hbar}} a(0) e^{-\frac{iHt}{\hbar}} \quad (3.6)$$

$$\hat{a}^+(t) = e^{-\frac{iHt}{\hbar}} a^+(0) e^{\frac{iHt}{\hbar}} \quad (3.7)$$

In Heisenberg picture(Heisenberg representation), the state vectors are time independent and the operators (observable) incorporate a dependence on time [97].

To drive the equation of motion for Heisenberg picture, we can proceed as follow:-

$$\frac{d\hat{a}(t)}{dt} = \frac{i}{\hbar} H e^{\frac{iHt}{\hbar}} \hat{a} e^{-\frac{iHt}{\hbar}} + e^{\frac{iHt}{\hbar}} \left(\frac{\partial \hat{a}}{\partial t} \right) e^{\frac{iHt}{\hbar}} + \frac{i}{H} e^{\frac{iHt}{\hbar}} \hat{a} \cdot (-H) e^{-\frac{iHt}{\hbar}} \quad (3.8)$$

$$\frac{d\hat{a}(t)}{dt} = \frac{i}{\hbar} (\hat{H}\hat{a} - \hat{a}\hat{H}) + e^{\frac{iHt}{\hbar}} \left(\frac{\partial \hat{a}}{\partial t} \right) e^{-\frac{iHt}{\hbar}} \quad (3.9)$$

$$\frac{d\hat{a}(t)}{dt} = \frac{i}{\hbar} [\hat{H}, \hat{a}(t)] + \frac{\partial \hat{a}(t)}{\partial t} \quad (3.10)$$

similarly

$$\frac{d\hat{a}^+(t)}{dt} = \frac{i}{\hbar} H e^{\frac{iHt}{\hbar}} \hat{a}^+ e^{-\frac{iHt}{\hbar}} + e^{\frac{iHt}{\hbar}} \left(\frac{\partial \hat{a}^+}{\partial t} \right) e^{\frac{iHt}{\hbar}} + \frac{i}{H} e^{\frac{iHt}{\hbar}} \hat{a}^+ \cdot (-H) e^{-\frac{iHt}{\hbar}} \quad (3.11)$$

$$\frac{d\hat{a}^+(t)}{dt} = \frac{i}{\hbar} (\hat{H}\hat{a}^+ - \hat{a}^+\hat{H}) + e^{\frac{iHt}{\hbar}} \left(\frac{\partial \hat{a}^+}{\partial t} \right) e^{\frac{iHt}{\hbar}} \quad (3.12)$$

$$\frac{d\hat{a}^+(t)}{dt} = \frac{i}{\hbar} [\hat{H}, \hat{a}^+(t)] + \frac{\partial \hat{a}^+(t)}{\partial t} \quad (3.13)$$

$$\frac{d\hat{a}^+(t)}{dt} = \frac{i}{\hbar} [\hat{H}, \hat{a}^+] \quad (3.14)$$

Letting $\hbar=1$, We got

$$\frac{d\hat{a}}{dt} = -i[\hat{a}, \hat{H}] \quad (3.15)$$

and

$$\frac{d\hat{a}^+(t)}{dt} = -i[\hat{a}^+, \hat{H}] \quad (3.16)$$

$[\hat{a}(t), \hat{b}(t')]$ denotes for commutation or anti-commutation.

The Green function

$$G_{k,\sigma}(t, t') = \ll \psi_{k,\sigma}(t) | \psi_{k,\sigma'}^+(t') \gg = \int_{-\infty}^{\infty} \frac{d\omega}{2\pi} G_{k,\sigma}(\omega) e^{-i\omega(t-t')} \quad (3.17)$$

For Nambu operators

$$\psi_{k,\sigma} = \begin{pmatrix} \hat{a}_{k,\sigma} \\ \hat{a}_{-k,\bar{\sigma}}^+ \end{pmatrix} \quad (3.18)$$

$$\psi_{k,\sigma}^+ = \begin{pmatrix} \hat{a}_{k,\sigma}^+ & \hat{a}_{k,-\sigma} \end{pmatrix} \quad (3.19)$$

where $\bar{\sigma} = -\sigma$

The fourier transform of the matrix Green function

$$G_{k,\sigma}(\omega) = \begin{pmatrix} G^{11}(\omega) & G^{12}(\omega) \\ G^{21}(\omega) & G^{22}(\omega) \end{pmatrix} \quad (3.20)$$

$$G_{k,\sigma}(\omega) = \begin{pmatrix} G_{k\sigma}(\omega) & F_{k,\sigma}(\omega) \\ F_{k,\sigma}^+(\omega) & -G_{-k\sigma}(-\omega) \end{pmatrix} \quad (3.21)$$

where

$$G_{\omega}^{11} = G_{k\sigma}(\omega) = \ll a_{k,\sigma} | a_{k,\sigma}^+ \gg$$

is normal component of the Green function,

$$G_{\omega}^{12} = F_{k,\sigma}(\omega) = \ll a_{k,\sigma} | a_{-k,\bar{\sigma}} \gg$$

anomalous component of the Green function

In explicit way

$$G_{k,\sigma}(\omega) = \begin{pmatrix} \ll \hat{a}_{k,\sigma} | \hat{a}_{k,\sigma}^+ \gg & \ll \hat{a}_{k,\sigma} | \hat{a}_{-k,\bar{\sigma}} \gg \\ \ll \hat{a}_{-k,\bar{\sigma}}^+ | \hat{a}_{k,\sigma}^+ \gg & \ll \hat{a}_{-k,\bar{\sigma}}^+ | \hat{a}_{-k,\bar{\sigma}} \gg \end{pmatrix} \quad (3.22)$$

The Decoupling Green function $G_{k\sigma}^0$ is

$$G_{k\sigma}^0(\omega) = \frac{1}{\omega - \epsilon(k) + \mu} \quad (3.23)$$

where $G_{k\sigma}^0(\omega)$ is the Green function of non-interacting electrons

The coupling Green function

$$G_{k\sigma}^\alpha(\omega) = \frac{1}{\omega - \epsilon(k) + \mu - \sum_\sigma^\alpha(k, \omega)} \quad (3.24)$$

$\sum_\sigma^\alpha(k, \omega)$ is the self energy describing the effects of electron-electron interaction

$$G_{k\sigma}^\alpha(\omega) = [\omega - \epsilon(k) + \mu - \sum_\sigma^\alpha(k, \omega)]^{-1} \quad (3.25)$$

Replacing

$$G_{k\sigma}^0(\omega) = [\omega - \epsilon(k) + \mu]^{-1}$$

We obtain

$$G_{k\sigma}^\alpha(\omega) = [[G_{k\sigma}^0(\omega)]^{-1} - \sum_\sigma^\alpha(k, \omega)]^{-1} \quad (3.26)$$

$$[[G_{k\sigma}^0(\omega)]^{-1} - \sum_\sigma^\alpha(k, \omega)]G_{k\sigma}^\alpha(\omega) = 1 \quad (3.27)$$

$$G_{k\sigma}^\alpha(\omega) = G_{k\sigma}^0(\omega) + \sum_\sigma^\alpha(k, \omega)G_{k\sigma}^\alpha(\omega)G_{k\sigma}^0(\omega) \quad (3.28)$$

$$G_{k\sigma}^\alpha(\omega) = G_{k\sigma}^0(\omega) + G_{k\sigma}^0(\omega) \sum_\sigma^\alpha(k, \omega)G_{k\sigma}^\alpha(\omega) \quad (3.29)$$

The Wick time ordering operator T_ϵ sorts operators in a product according to their time arguments:

$$T_\epsilon(a(\hat{t})b(\hat{t}')) = \theta(t - t')a(\hat{t})b(\hat{t}') + \epsilon\theta(t - t')b(\hat{t}')a(\hat{t}) \quad (3.30)$$

The ϵ makes it distinct from the Dirac time ordering operator. The spectral density is another very important function of many body theory [101].

$$S_{ab}(t, t') = \frac{1}{2\pi} \langle [a(\hat{t}), b(\hat{t}')]_\epsilon \rangle \quad (3.31)$$

The spectral density contains the same information as the Greens function.

We now prove the fact that Greens function and spectral density are homogeneous in time if the Hamiltonian is not explicitly time dependent.

$$\begin{aligned} \frac{\partial H}{\partial t} = 0 \rightarrow G_{ab}^{\alpha}(t, t') &= G_{ab}^{\alpha}(t - t'), [\alpha = r, a, c] \\ S_{ab}(t, t') &= S_{ab}(t - t') \end{aligned} \quad (3.32)$$

We only need to prove that for the so called correlation functions

$$\langle a(\hat{t})b(\hat{t}') \rangle, \langle b(\hat{t}')a(\hat{t}) \rangle \quad (3.33)$$

The proof is based on cyclic invariance of the trace

$$\begin{aligned} \langle a(\hat{t})b(\hat{t}') \rangle &= Tr\{e^{-\beta H} a(t), b(t')\} = Tr\{e^{-\beta H} e^{\frac{iHt}{\hbar}} a(0) e^{-\frac{iH(t-t')}{\hbar}} b(0) e^{-\frac{iHt'}{\hbar}}\} \\ &= Tr\{e^{-\beta H} e^{\frac{iH(t-t')}{\hbar}} a(0) e^{-\frac{iH(t-t')}{\hbar}} b(0)\} \\ \langle a(\hat{t})b(\hat{t}') \rangle &= Tr\{e^{-\beta H} a(t - t') b(0)\} \end{aligned} \quad (3.34)$$

Thus

$$\langle a(t), b(t') \rangle = \langle a(t - t') b(0) \rangle \quad (3.35)$$

Similarly

$$\begin{aligned} \langle b(\hat{t}')a(\hat{t}) \rangle &= Tr\{e^{-\beta H} b(t'), a(t)\} \\ &= Tr\{e^{-\beta H} e^{\frac{iHt'}{\hbar}} b(0) e^{\frac{iH(t-t')}{\hbar}} a(0) e^{-\frac{iHt}{\hbar}}\} \\ &= Tr\{e^{-\beta H} b(0) e^{\frac{iH(t-t')}{\hbar}} a(0) e^{-\frac{iH(t-t')}{\hbar}}\} \\ &= Tr\{e^{-\beta H} b(0) a(t - t')\} \\ \langle b(t'), a(t) \rangle &= \langle b(0), a(t - t') \rangle \end{aligned} \quad (3.36)$$

3.2 Equation of motion for Heisenberg operators

Let us now derive the equation of motion for Heisenberg operators

$$G(t, t') = \ll a(\hat{t}), b(\hat{t}') \gg = -i\Theta(t - t') \langle [a(\hat{t}), b(\hat{t}')] \rangle \quad (3.37)$$

Differentiating both side with respect to t

$$\frac{dG(t, t')}{dt} = -i \frac{d\theta(t - t')}{dt} \langle [a(\hat{t}), b(\hat{t}')] \rangle - i\Theta(t - t') \langle [\frac{da(t)}{dt}, b(t')] \rangle$$

multiplying both side by i

$$\begin{aligned} i \frac{dG(t, t')}{dt} &= \frac{d\theta(t - t')}{dt} \langle [a(\hat{t}), b(\hat{t}')] \rangle + \Theta(t - t') \langle [\frac{da(t)}{dt}, b(t')] \rangle \\ i \frac{dG(t, t')}{dt} &= \frac{d\theta(t - t')}{dt} \langle [a(\hat{t}), b(\hat{t}')] \rangle - i\Theta(t - t') \langle [\frac{ida(t)}{dt}, b(t')] \rangle \end{aligned} \quad (3.38)$$

From section 3.1, we have equations

$$\theta(t - t') = \int \delta(t - t') \quad (3.39)$$

$$\frac{d\theta(t - t')}{dt} = \frac{\delta(t - t')}{2\pi} \quad (3.40)$$

$$i \frac{d\hat{a}(t)}{dt} = [\hat{a}(t), \hat{H}] \quad (3.41)$$

Now plugging eqn(3.39), eqn(3.40) and eqn(3.41) into eqn(3.38), we obtain

$$i \frac{dG(t, t')}{dt} = \frac{\delta(t - t')}{2\pi} \langle [a(\hat{t}), b(\hat{t}')] \rangle - i\Theta(t - t') \langle [a(\hat{t}), b(\hat{t}')] \rangle \quad (3.42)$$

$$G(t, t') = \int G(\omega) e^{-i\omega(t-t')} dt$$

Differentiating with respect to time,t

$$\frac{dG(t, t')}{dt} = -i\omega \int G(\omega) e^{-i\omega(t-t')} dt$$

Replacing

$$G(t, t') = \int G(\omega) e^{-i\omega(t-t')} dt$$

we obtain

$$\frac{dG(t, t')}{dt} = -i\omega G(t, t') \quad (3.43)$$

Plugging eqn(3.3) into eqn(3.2), we get

$$\omega G(t, t') = \frac{\delta(t-t')}{2\pi} \langle [a(\hat{t}), b(\hat{t}')] \rangle + \ll [a(t), H], b(t') \gg \quad (3.44)$$

$$\omega \ll a(\hat{t})b(\hat{t}') \gg = \langle [a(\hat{t}), b(\hat{t}')] \rangle + \ll [a(t), H], b(t') \gg \quad (3.45)$$

This the equation of motion for Retarded Green function (correlation function) which is indispensable for formulation of the problems.

Generally, for all three Greens functions formally have the same equation of motion

$$i\hbar \frac{\partial G_{ab}^{\alpha}(t, t')}{\partial t} = \hbar \delta(t-t') \langle [a(\hat{t}), b(\hat{t}')] \rangle_{\epsilon} + \ll [\hat{a}, H], b(\hat{t}') \gg^{\alpha}$$

$$\omega \ll a(\hat{t}), b(\hat{t}') \gg_{\omega}^{\alpha} = \langle [a(\hat{t}), b(\hat{t}')]_{\epsilon} \rangle + \ll [\hat{a}, H], b(\hat{t}') \gg_{\omega}^{\alpha} \quad (3.46)$$

where $\alpha = (r, a, c)$, r stands for retarded Green function, a stands for advanced Green function, c stands for causal Green function

The Transverse spin susceptibility is defined by

$$\chi^{+-}(q, \tau) = - \langle T_\tau S^+(q, \tau) S^-(-q, 0) \rangle \quad (3.47)$$

Where τ is the imaginary time, T_τ is time ordering directive.

$$S^\alpha(q, \tau) = \frac{1}{\sqrt{N}} \sum_{k\sigma\sigma'} C_{k+q,\sigma}^+ \frac{\sigma_{\sigma\sigma'}^\alpha}{2} C_{k,\sigma'}$$

S is electron spin operator

$$\chi^{+-}(q, \tau) = -\frac{1}{N} \sum_k \langle T_\tau C_{k+q,\uparrow}^+ C_{k,\downarrow}(\tau) C_{k'-q,\downarrow}^+ C_{k',\uparrow}(0) \rangle \quad (3.48)$$

$$\chi^{+-}(q, \tau) = -\frac{1}{N} \sum_k \langle T_\tau C_{k+q,\uparrow}^+(\tau) C_{k+q,\uparrow}(0) \rangle_0 \langle T_\tau C_{k,\downarrow}(\tau) C_{k,\downarrow}^+(0) \rangle_0$$

$$\chi^{+-}(q, \tau) = \frac{1}{N} \sum_k \langle T_\tau C_{k+q,\uparrow}(0) C_{k+q,\uparrow}^+(\tau) \rangle_0 \langle T_\tau C_{k,\downarrow}(\tau) C_{k,\downarrow}^+(0) \rangle_0$$

$$\chi^{+-}(q, \tau) = \frac{1}{N} \sum_k G_{k+q,\uparrow}^0(\tau) G_{k,\downarrow}^0(\tau) \quad (3.49)$$

The fourier transform as a function of the bosonic Matsubara frequency $i\nu$ is

$$\chi_0^{+-}(q, i\nu) = \int_0^\beta d\tau e^{i\nu\tau} \chi_0^{+-}(q, \tau) \quad (3.50)$$

$$\chi_0^{+-}(q, i\nu) = \frac{1}{N} \sum_k \frac{1}{\beta} \frac{1}{i\omega_n - i\nu_n - \xi_{k+q}} \frac{1}{i\omega_n - \xi_k} \quad (3.51)$$

4

FORMULATION OF THE PROBLEM

In this chapter, we have tried to solve and determine the superconducting order parameter and the superconducting transition temperature (T_C) using a model Hamiltonian with Green function formalism.

4.1 Cuprate superconductivity

Cuprate superconductor could be either a hole doped or electron doped superconductor. For optimal (hole) doped superconductor (YBaCu₃O_{6.93}), the Hamiltonian for the system is given by

$$\hat{H} = \hat{H}_0 + \hat{H}_{sf} = \hat{H}_c + \hat{H}_l + \hat{H}_{sf} \quad (4.1)$$

where $\hat{H}_c = \sum_{k\sigma} \xi_{k\sigma} \hat{a}_{k\sigma}^+ \hat{a}_{k\sigma}$ describes the itinerant electrons.

$$\hat{H}_l = J_1 \sum S_i \cdot S_j + J_2 \sum S_i \cdot S_j \approx \sum_{k\sigma} \hbar\omega \hat{b}_{k\sigma}^+ \hat{b}_{k\sigma}$$

the localized electrons which yield the magnetism

$$\hat{H}_0 = \sum_{k\sigma} \xi_{k\sigma} \hat{a}_{k\sigma}^+ \hat{a}_{k\sigma} + \sum_{\alpha\beta} \hbar\omega \hat{b}_{k\sigma}^+ \hat{b}_{k\sigma} \quad (4.2)$$

where $\xi_k = \epsilon_k - \mu$

$$\hat{H}_{sf} = \sum_{k,k',\alpha,\sigma} JS_k^\alpha \cdot \sigma_{\sigma,\sigma'}^\alpha \hat{a}_{k\sigma}^+ \hat{a}_{k'\sigma} \quad (4.3)$$

is the spin-fermion interaction between two sets of electrons.

$$\hat{H}_{sf} = J \sum_{k,\sigma,\alpha} S_k^\alpha \cdot \sigma_{\sigma,\sigma'}^\alpha (\hat{a}_{k\sigma}^+ \hat{a}_{k'\sigma}) \quad (4.4)$$

where

σ Pauli matrix, S Spin operator

Employing the above expression

$$\sum_{\alpha} S_k^\alpha \cdot \sigma^\alpha = S_k^z \sigma^z + S_k^x \sigma^x + S_k^y \sigma^y \quad (4.5)$$

we know that

$$S_k^\pm = S_k^x \pm iS_k^y$$

explicitly

$$S_k^+ = S_k^x + iS_k^y \quad (4.6)$$

$$S_k^- = S_k^x - iS_k^y \quad (4.7)$$

rearranging this,we obtain

$$S_k^x = \frac{1}{2}[S_k^+ + S_k^-] \quad (4.8)$$

$$S_k^y = \frac{1}{2i}[S_k^+ - iS_k^-] \quad (4.9)$$

Similarly, for Pauli matrix is expressed as

$$\sigma^\pm = \frac{1}{2}[\sigma^x \pm i\sigma^y]$$

$$\sigma^+ = \frac{1}{2}[\sigma^x + i\sigma^y]$$

$$\sigma^- = \frac{1}{2}[\sigma^x - i\sigma^y]$$

$$\sigma^- = \frac{1}{2}[\sigma^x - i\sigma^y]$$

Again rearranging this, we obtain

$$\sigma^x = [\sigma^+ + \sigma^-] \quad (4.10)$$

$$\sigma^y = \frac{1}{i}[\sigma^+ - \sigma^-] \quad (4.11)$$

Now, plugging eqn(4.8), eqn(4.9), eqn(4.10) and eqn(4.11) into eqn(4.5) we get

$$\sum_{\alpha} S_k^{\alpha} \cdot \sigma^{\alpha} = S_k^z \sigma^z + \frac{1}{2}[S_k^+ - S_k^-][\sigma^+ + \sigma^-] + \frac{1}{2i}[S_k^+ - S_k^-] \frac{i}{2}[\sigma^+ - \sigma^-] \quad (4.12)$$

This reduced to

$$\sum_{\alpha} S_k^{\alpha} \cdot \sigma^{\alpha} = S_k^z \sigma^z + S_k^+ \sigma^- + S_k^- \sigma^+ \quad (4.13)$$

Plugging eqn(4.13) into eqn(4.3), we get

$$\hat{H}_{sf} = J \sum_{k,k'} [S_k^z \sigma^z + S_k^+ \sigma^- + S_k^- \sigma^+] \hat{a}_{k\sigma}^+ \hat{a}_{k'\sigma} \quad (4.14)$$

$$S_k^z = \frac{1}{2} \sum_{k,k'} [\hat{a}_{k\uparrow}^+ \hat{a}_{k'\uparrow} - \hat{a}_{k\downarrow}^+ \hat{a}_{k'\downarrow}] \quad (4.15)$$

$$S_k^+ = \sum_{k,k'} \hat{a}_{k\uparrow}^+ \hat{a}_{k'\downarrow} \quad (4.16)$$

$$S_k^- = \sum_{k,k'} \hat{a}_{k\downarrow}^+ \hat{a}_{k'\uparrow} \quad (4.17)$$

where the spin operator S_k^+ destroyed a down spin and created an up spin, while in S_k^- , it is the other way around. We also see that S_k^z counts the number of up spins minus the number of down spins.

The spin-electron interaction Hamiltonian will be

$$\begin{aligned} \hat{H}_{sf} = & \frac{1}{2} \sum_{k,k'} J [\hat{a}_{k\uparrow}^+ \hat{a}_{k'\uparrow} - \hat{a}_{k\downarrow}^+ \hat{a}_{k'\downarrow}] [\hat{a}_{k\uparrow}^+ \hat{a}_{k'\uparrow} - \hat{a}_{k\downarrow}^+ \hat{a}_{k'\downarrow}] + \\ & \sum_{k,k'} J [\hat{a}_{k\uparrow}^+ \hat{a}_{k'\downarrow} \hat{a}_{k\downarrow}^+ \hat{a}_{k'\uparrow} + \hat{a}_{k\downarrow}^+ \hat{a}_{k'\uparrow} \hat{a}_{k\uparrow}^+ \hat{a}_{k'\downarrow}] \end{aligned} \quad (4.18)$$

$$\begin{aligned} \hat{H}_{sf} = & \frac{1}{2} J \sum_{k,k'} [\hat{a}_{k\uparrow}^+ \hat{a}_{k'\uparrow} \hat{a}_{k\uparrow}^+ \hat{a}_{k'\uparrow} - \hat{a}_{k\uparrow}^+ \hat{a}_{k'\uparrow} \hat{a}_{k\downarrow}^+ \hat{a}_{k'\downarrow} - \hat{a}_{k\downarrow}^+ \hat{a}_{k'\downarrow} \hat{a}_{k\uparrow}^+ \hat{a}_{k'\uparrow} + \hat{a}_{k\downarrow}^+ \hat{a}_{k'\downarrow} \hat{a}_{k\downarrow}^+ \hat{a}_{k'\downarrow}] + \\ & \sum_{k,k'} J [\hat{a}_{k\uparrow}^+ \hat{a}_{k'\downarrow} \hat{a}_{k\downarrow}^+ \hat{a}_{k'\uparrow} + \hat{a}_{k\downarrow}^+ \hat{a}_{k'\uparrow} \hat{a}_{k\uparrow}^+ \hat{a}_{k'\downarrow}] \end{aligned} \quad (4.19)$$

The total Hamiltonian of the system is

Employing mean field approximation

The superconducting order parameter can be defined as

$$\Delta^{+\uparrow\uparrow} = J \sum_{k,k'} \langle \hat{a}_{k\uparrow}^+ \hat{a}_{k'\uparrow}^+ \rangle \quad (4.20)$$

$$\Delta^{\uparrow\uparrow} = J \sum_{k,k'} \langle \hat{a}_{k'\uparrow} \hat{a}_{k\uparrow} \rangle \quad (4.21)$$

$$\Delta^{+\uparrow\downarrow} = J \sum_{k,k'} \langle \hat{a}_{k\uparrow}^+ \hat{a}_{k'\downarrow}^+ \rangle \quad (4.22)$$

$$\Delta^{\uparrow\downarrow} = J \sum_{k,k'} \langle \hat{a}_{k\uparrow} \hat{a}_{k'\downarrow} \rangle \quad (4.23)$$

plugging eqn(4.23), eqn(4.24), eqn(4.25), and eqn(4.26) into eqn(4.22), we obtain

From chapter 3, we have the equation of motion

$$\omega G(t, t') = \frac{\delta(t - t')}{2\pi} \langle [a(t), b(t')] \rangle + \ll [a(t), H], b(t') \gg$$

$$\omega \ll \hat{a}_{k\sigma}, \hat{a}_{k\sigma}^+ \gg = \langle [\hat{a}_{k\sigma}, \hat{a}_{k\sigma}^+] \rangle + \ll [\hat{a}_{k\sigma}, \hat{H}], \hat{a}_{k\sigma}^+ \gg \quad (4.24)$$

$$\omega \ll \hat{a}_{k\uparrow}, \hat{a}_{k\uparrow}^+ \gg = \langle [\hat{a}_{k\uparrow}, \hat{a}_{k\uparrow}^+] \rangle + \ll [\hat{a}_{k\uparrow}, \hat{H}], \hat{a}_{k\uparrow}^+ \gg \quad (4.25)$$

$$\omega \ll \hat{a}_{k\uparrow}, \hat{a}_{k\uparrow}^+ \gg = 1 + \ll [\hat{a}_{k\uparrow}, \hat{H}], \hat{a}_{k\uparrow}^+ \gg \quad (4.26)$$

Now let us evaluate $[\hat{a}_{k\uparrow}, \hat{H}]$

$$[\hat{a}_{K\uparrow}, \hat{H}] = [\hat{a}_{k\uparrow}, \hat{H}_0] + [\hat{a}_{k\uparrow}, \hat{H}_{sf}] \quad (4.27)$$

$$[\hat{a}_{k\uparrow}, \hat{H}_0] = [\hat{a}_{\kappa\uparrow}, \sum_{\kappa\sigma} \xi_{\kappa\sigma} \hat{a}_{\kappa\uparrow}^+ \hat{a}_{\kappa\uparrow}] + [\hat{a}_{\kappa\uparrow}, \sum_{\kappa\sigma} \hbar\omega \hat{b}_{\kappa\uparrow}^+ \hat{b}_{\kappa\uparrow}]$$

$$[\hat{a}_{k\uparrow}, \hat{H}_0] = \sum_{\kappa\sigma} \xi_{\kappa\sigma} \hat{a}_{\kappa\uparrow} [a_{\kappa\uparrow}, \hat{a}_{\kappa\uparrow}^+]$$

$$[\hat{a}_{k\uparrow}, \hat{H}_0] = \xi_{\kappa} \hat{a}_{\kappa\uparrow} \quad (4.28)$$

$$[\hat{a}_{k\uparrow}, \hat{H}_{sf}] = [\hat{a}_{k\uparrow}, \frac{1}{2} \sum_{\kappa\kappa'} [\Delta^{+\uparrow\uparrow} \hat{a}_{k'\uparrow} \hat{a}_{k'\uparrow} + \Delta^{\uparrow\uparrow} \hat{a}_{k\uparrow}^+ \hat{a}_{k\uparrow}^+ + \Delta^{+\uparrow\downarrow} \hat{a}_{k'\downarrow} \hat{a}_{k'\downarrow} + \Delta^{\uparrow\downarrow} \hat{a}_{k\downarrow}^+ \hat{a}_{k\downarrow}^+]$$

$$\Delta^{+\uparrow\downarrow} \hat{a}_{k'\uparrow} \hat{a}_{k'\downarrow} + \Delta^{\uparrow\downarrow} \hat{a}_{k\uparrow}^+ \hat{a}_{k\downarrow}^+]$$

$$[\hat{a}_{k\uparrow}, \hat{H}_{sf}] = \frac{1}{2} \Delta^{\uparrow\uparrow} \hat{a}_{\kappa\uparrow}^+ + \Delta^{\uparrow\downarrow} \hat{a}_{\kappa\downarrow}^+ \quad (4.29)$$

Plugging eqn(4.34) and eqn(4.35) into eqn(4.36), we obtain

$$\omega \ll \hat{a}_{k\uparrow}, \hat{a}_{k\uparrow}^+ \gg = 1 + \xi_k \ll \hat{a}_{k\uparrow}, \hat{a}_{k\uparrow}^+ \gg + \frac{1}{2} \Delta^{\uparrow\uparrow} \ll \hat{a}_{k\uparrow}^+, \hat{a}_{k\uparrow}^+ \gg + \Delta^{\uparrow\downarrow} \ll \hat{a}_{k\downarrow}^+, \hat{a}_{k\downarrow}^+ \gg \quad (4.30)$$

$$(\omega - \xi_k) \ll \hat{a}_{k\uparrow}, \hat{a}_{k\uparrow}^+ \gg - \frac{1}{2} \Delta^{\uparrow\uparrow} \ll \hat{a}_{k\uparrow}^+, \hat{a}_{k\uparrow}^+ \gg - \Delta^{\uparrow\downarrow} \ll \hat{a}_{k\downarrow}^+, \hat{a}_{k\downarrow}^+ \gg = 1 \quad (4.31)$$

Similarly,

$$\omega \ll \hat{a}_{k\uparrow}^+, \hat{a}_{k\uparrow}^+ \gg = \ll [\hat{a}_{k\uparrow}^+, \hat{H}], \hat{a}_{k\uparrow}^+ \gg$$

Again, let us evaluate $[\hat{a}_{k\uparrow}^+, \hat{H}]$

$$[\hat{a}_{K\uparrow}^+, \hat{H}] = [\hat{a}_{k\uparrow}^+, \hat{H}_0] + [\hat{a}_{k\uparrow}^+, \hat{H}_{sf}] \quad (4.32)$$

$$\begin{aligned}
[\hat{a}_{k\uparrow}^+, \hat{H}_0] &= [\hat{a}_{k\uparrow}^+, \sum_{\kappa\sigma} \xi_{\kappa\sigma} \hat{a}_{\kappa\uparrow}^+ \hat{a}_{\kappa\uparrow}] + [\hat{a}_{k\uparrow}^+, \sum_{\kappa\sigma} \hbar\omega \hat{b}_{\kappa\uparrow}^+ \hat{b}_{\kappa\uparrow}] \\
[\hat{a}_{k\uparrow}^+, \hat{H}_0] &= \sum_{\kappa\sigma} \xi_{\kappa\sigma} \hat{a}_{\kappa\uparrow}^+ [a_{\kappa\uparrow}^+, \hat{a}_{\kappa\uparrow}] \\
[\hat{a}_{k\uparrow}^+, \hat{H}_0] &= -\xi_{\kappa} \hat{a}_{\kappa\uparrow}^+
\end{aligned} \tag{4.33}$$

$$\begin{aligned}
[\hat{a}_{k\uparrow}^+, \hat{H}_{sf}] &= [\hat{a}_{k\uparrow}^+, \frac{1}{2} \sum_{\kappa\kappa'} [\Delta^{+\uparrow\uparrow} \hat{a}_{k'\uparrow} \hat{a}_{k'\uparrow} + \Delta^{\uparrow\uparrow} \hat{a}_{k\uparrow}^+ \hat{a}_{k\uparrow}^+ + \Delta^{+\downarrow\downarrow} \hat{a}_{k'\downarrow} \hat{a}_{k'\downarrow} + \Delta^{\downarrow\downarrow} \hat{a}_{k\downarrow}^+ \hat{a}_{k\downarrow}^+ + \\
&\quad \Delta^{+\uparrow\downarrow} \hat{a}_{k'\uparrow} \hat{a}_{k'\downarrow} + \Delta^{\uparrow\downarrow} \hat{a}_{k\uparrow}^+ \hat{a}_{k\downarrow}^+]] \\
[\hat{a}_{k\uparrow}^+, \hat{H}_{sf}] &= -\frac{1}{2} \Delta^{+\uparrow\uparrow} \hat{a}_{k'\uparrow} - \Delta^{+\uparrow\downarrow} \hat{a}_{k'\downarrow}
\end{aligned} \tag{4.34}$$

Inserting eqn(4.39), eqn (4.40) into eqn(4.38), we obtain

$$\omega \ll \hat{a}_{k\uparrow}^+ \hat{a}_{k\uparrow}^+ \gg = -\xi_k \ll \hat{a}_{k\uparrow}^+ \hat{a}_{k\uparrow}^+ \gg - \frac{1}{2} \Delta^{+\uparrow\uparrow} \ll \hat{a}_{k'\uparrow} \hat{a}_{k\uparrow}^+ \gg - \Delta^{+\uparrow\downarrow} \ll \hat{a}_{k'\downarrow} \hat{a}_{k\uparrow}^+ \gg \tag{4.35}$$

$$(\omega + \xi_k) \ll \hat{a}_{k\uparrow}^+ \hat{a}_{k\uparrow}^+ \gg = -\frac{1}{2} \Delta^{+\uparrow\uparrow} \ll \hat{a}_{k'\uparrow} \hat{a}_{k\uparrow}^+ \gg - \Delta^{+\uparrow\downarrow} \ll \hat{a}_{k'\downarrow} \hat{a}_{k\uparrow}^+ \gg \tag{4.36}$$

Similarly,

$$\omega \ll \hat{a}_{k\downarrow}^+, \hat{a}_{k\uparrow}^+ \gg = \ll [\hat{a}_{k\downarrow}^+, \hat{H}], \hat{a}_{k\uparrow}^+ \gg \tag{4.37}$$

when we evaluate $[\hat{a}_{k\downarrow}^+, \hat{H}]$

$$[\hat{a}_{k\downarrow}^+, \hat{H}] = [\hat{a}_{k\downarrow}^+, \hat{H}_0] + [\hat{a}_{k\downarrow}^+, \hat{H}_{sf}] \tag{4.38}$$

$$\begin{aligned}
[\hat{a}_{k\downarrow}^+, \hat{H}_0] &= [\hat{a}_{k\downarrow}^+, \sum_{\kappa\sigma} \xi_{\kappa\sigma} \hat{a}_{\kappa\uparrow}^+ \hat{a}_{\kappa\uparrow}] + [\hat{a}_{k\downarrow}^+, \sum_{\kappa\sigma} \hbar\omega \hat{b}_{\kappa\uparrow}^+ \hat{b}_{\kappa\uparrow}] \\
[\hat{a}_{k\downarrow}^+, \hat{H}_0] &= \sum_{\kappa\sigma} \xi_{\kappa\sigma} \hat{a}_{\kappa\uparrow}^+ [a_{\kappa\downarrow}^+, \hat{a}_{\kappa\uparrow}] \\
[\hat{a}_{k\downarrow}^+, \hat{H}_0] &= -\xi_{\kappa} \hat{a}_{\kappa\downarrow}^+
\end{aligned} \tag{4.39}$$

$$\begin{aligned}
[\hat{a}_{k\downarrow}^+, \hat{H}_{sf}] &= [\hat{a}_{k\downarrow}^+, \frac{1}{2} \sum_{\kappa\kappa'} [\Delta^{+\uparrow\uparrow} \hat{a}_{k'\uparrow} \hat{a}_{k'\uparrow} + \Delta^{\uparrow\uparrow} \hat{a}_{k\uparrow}^+ \hat{a}_{k\uparrow}^+ + \Delta^{+\downarrow\downarrow} \hat{a}_{k'\downarrow} \hat{a}_{k'\downarrow} + \Delta^{\downarrow\downarrow} \hat{a}_{k\downarrow}^+ \hat{a}_{k\downarrow}^+ + \\
&\quad \Delta^{+\uparrow\downarrow} \hat{a}_{k'\uparrow} \hat{a}_{k'\downarrow} + \Delta^{\uparrow\downarrow} \hat{a}_{k\uparrow}^+ \hat{a}_{k\downarrow}^+]]
\end{aligned}$$

$$[\hat{a}_{k\downarrow}^+, \hat{H}_{sf}] = -\frac{1}{2}\Delta^{+\downarrow\downarrow}\hat{a}_{k'\downarrow} - \Delta^{+\uparrow\downarrow}\hat{a}_{k\uparrow} \quad (4.40)$$

Inserting eqn(4.45), and eqn(4.46) into eqn(4.43), we obtain

$$\omega \ll \hat{a}_{k\downarrow}^+ \hat{a}_{k\uparrow}^+ \gg = -\xi_k \ll \hat{a}_{k\downarrow}^+ \hat{a}_{k\uparrow}^+ \gg - \frac{1}{2}\Delta^{+\uparrow\uparrow} \ll \hat{a}_{k'\downarrow}^+ \hat{a}_{k\uparrow}^+ \gg - \Delta^{+\uparrow\downarrow} \ll \hat{a}_{k\uparrow}^+ \hat{a}_{k\uparrow}^+ \gg \quad (4.41)$$

$$(\omega + \xi_k) \ll \hat{a}_{k\downarrow}^+ \hat{a}_{k\uparrow}^+ \gg = -\frac{1}{2}\Delta^{+\downarrow\downarrow} \ll \hat{a}_{k'\downarrow}^+ \hat{a}_{k\uparrow}^+ \gg - \Delta^{+\uparrow\downarrow} \ll \hat{a}_{k\uparrow}^+ \hat{a}_{k\uparrow}^+ \gg \quad (4.42)$$

$$\omega \ll \hat{a}_{k\downarrow}, \hat{a}_{k\uparrow}^+ \gg = \ll [\hat{a}_{k\downarrow}, \hat{H}], \hat{a}_{k\uparrow}^+ \gg \quad (4.43)$$

When we evaluate $[\hat{a}_{k\downarrow}, \hat{H}]$

$$[\hat{a}_{k\downarrow}, \hat{H}] = [\hat{a}_{k\downarrow}, \hat{H}_0] + [\hat{a}_{k\downarrow}, \hat{H}_{sf}] \quad (4.44)$$

$$[\hat{a}_{k\downarrow}, \hat{H}_0] = [\hat{a}_{k\downarrow}, \sum_{k\sigma} \xi_{k\sigma} \hat{a}_{k\uparrow}^+ \hat{a}_{k\uparrow}] + [\hat{a}_{k\downarrow}, \sum_{k\sigma} \xi_{k\sigma} \hat{a}_{k\downarrow}^+ \hat{a}_{k\downarrow}] + [\hat{a}_{k\downarrow}, \sum_{k\sigma} \hbar\omega \hat{b}_{k\uparrow}^+ \hat{b}_{k\uparrow}]$$

$$[\hat{a}_{k\downarrow}, \hat{H}_0] = \sum_{k\sigma} \xi_{k\sigma} \hat{a}_{k\downarrow} [\hat{a}_{k\downarrow}, \hat{a}_{k\downarrow}^+]$$

$$[\hat{a}_{k\downarrow}, \hat{H}_0] = \xi_k \hat{a}_{k\downarrow} \quad (4.45)$$

$$[\hat{a}_{k\downarrow}, \hat{H}_{sf}] = [\hat{a}_{k\downarrow}, \frac{1}{2} \sum_{k,k'} [\Delta^{+\uparrow\uparrow} \hat{a}_{k'\uparrow}^+ \hat{a}_{k'\uparrow} + \Delta^{+\uparrow\downarrow} \hat{a}_{k\uparrow}^+ \hat{a}_{k\uparrow} + \Delta^{+\downarrow\downarrow} \hat{a}_{k'\downarrow}^+ \hat{a}_{k'\downarrow} + \Delta^{+\downarrow\downarrow} \hat{a}_{k\downarrow}^+ \hat{a}_{k\downarrow}]] +$$

$$\Delta^{+\uparrow\downarrow} \hat{a}_{k'\uparrow}^+ \hat{a}_{k'\downarrow} + \Delta^{+\downarrow\downarrow} \hat{a}_{k\uparrow}^+ \hat{a}_{k\downarrow}]$$

$$[\hat{a}_{k\downarrow}, \hat{H}_{sf}] = \frac{1}{2}\Delta^{+\downarrow\downarrow}\hat{a}_{k\downarrow}^+ + \Delta^{+\uparrow\downarrow}\hat{a}_{k\uparrow}^+ \quad (4.46)$$

Inserting eqn(4.51) and, eqn(4.52)into eqn(4.50) and then in eqn(4.49), we obtain

$$\omega \ll \hat{a}_{k\downarrow} \hat{a}_{k\uparrow}^+ \gg = \xi_k \ll \hat{a}_{k\downarrow} \hat{a}_{k\uparrow}^+ \gg + \frac{1}{2}\Delta^{+\downarrow\downarrow} \ll \hat{a}_{k\downarrow}^+ \hat{a}_{k\uparrow}^+ \gg + \Delta^{+\uparrow\downarrow} \ll \hat{a}_{k\uparrow}^+ \hat{a}_{k\uparrow}^+ \gg \quad (4.47)$$

$$(\omega - \xi_k) \ll \hat{a}_{k\downarrow} \hat{a}_{k\uparrow}^+ \gg - \frac{1}{2}\Delta^{+\downarrow\downarrow} \ll \hat{a}_{k\downarrow}^+ \hat{a}_{k\uparrow}^+ \gg - \Delta^{+\uparrow\downarrow} \ll \hat{a}_{k\uparrow}^+ \hat{a}_{k\uparrow}^+ \gg = 0 \quad (4.48)$$

We can write eqn(4.37), eqn(4.42), eqn(4.48),and eqn(4.54)in matrix terms

as

$$\begin{pmatrix} \omega - \xi_k & -\frac{\Delta^{\uparrow\uparrow}}{2} & -\Delta^{\uparrow\downarrow} & 0 \\ \frac{\Delta^{\uparrow\uparrow}}{2} & \omega + \xi_k & 0 & \Delta^{\uparrow\downarrow} \\ \Delta^{\uparrow\downarrow} & 0 & \omega + \xi_k & \frac{\Delta^{\downarrow\downarrow}}{2} \\ 0 & -\Delta^{\uparrow\downarrow} & -\frac{\Delta^{\downarrow\downarrow}}{2} & \omega - \xi_k \end{pmatrix} \begin{pmatrix} \langle\langle \hat{a}_{k\uparrow}, \hat{a}_{k\uparrow}^+ \rangle\rangle \\ \langle\langle \hat{a}_{k\uparrow}^+, \hat{a}_{k\uparrow}^+ \rangle\rangle \\ \langle\langle \hat{a}_{k\downarrow}, \hat{a}_{k\uparrow}^+ \rangle\rangle \\ \langle\langle \hat{a}_{k\downarrow}, \hat{a}_{k\uparrow}^+ \rangle\rangle \end{pmatrix} = \begin{pmatrix} 1 \\ 0 \\ 0 \\ 0 \end{pmatrix} \quad (4.49)$$

Now, let us find the determinant D

$$D = \begin{vmatrix} \omega - \xi_k & -\frac{\Delta^{\uparrow\uparrow}}{2} & -\Delta^{\uparrow\downarrow} & 0 \\ \frac{\Delta^{\uparrow\uparrow}}{2} & \omega + \xi_k & 0 & \Delta^{\uparrow\downarrow} \\ \Delta^{\uparrow\downarrow} & 0 & \omega + \xi_k & \frac{\Delta^{\downarrow\downarrow}}{2} \\ 0 & -\Delta^{\uparrow\downarrow} & -\frac{\Delta^{\downarrow\downarrow}}{2} & \omega - \xi_k \end{vmatrix}$$

To find the solution for $\langle\langle \hat{a}_{k\uparrow}^+, \hat{a}_{k\uparrow}^+ \rangle\rangle$

$$D_1 = \begin{vmatrix} \omega - \xi_k & 1 & -\Delta^{\uparrow\downarrow} & 0 \\ \frac{\Delta^{\uparrow\uparrow}}{2} & 0 & 0 & \Delta^{\uparrow\downarrow} \\ \Delta^{\uparrow\downarrow} & 0 & \omega + \xi_k & \frac{\Delta^{\downarrow\downarrow}}{2} \\ 0 & 0 & -\frac{\Delta^{\downarrow\downarrow}}{2} & \omega - \xi_k \end{vmatrix}$$

Neglecting the last two terms, we have

$$D_1 = \frac{-\Delta^{\uparrow\uparrow}}{2} [\omega^2 - \xi_k^2]$$

Therefore

$$\langle\langle \hat{a}_{k\uparrow}^+, \hat{a}_{k\uparrow}^+ \rangle\rangle = \frac{\frac{-\Delta^{\uparrow\uparrow}}{2} (\omega^2 - \xi_k^2)}{(\omega^2 - \xi_k^2)(\omega^2 - \xi_k^2 - \frac{1}{4}(\Delta^{\uparrow\uparrow})^2)} \quad (4.50)$$

$$\langle\langle \hat{a}_{k\uparrow}^+, \hat{a}_{k\uparrow}^+ \rangle\rangle = -\frac{\frac{-(\Delta^{\uparrow\uparrow})}{2}}{(\omega^2 - \xi_k^2 - \frac{1}{4}(\Delta^{\uparrow\uparrow})^2)} \quad (4.51)$$

Similarly, for $\downarrow\uparrow$

To find the solution for $\ll \hat{a}_{k\downarrow}^+ \hat{a}_{k\uparrow}^+ \gg$

$$D_3 = \begin{vmatrix} \omega - \xi_k & -\frac{\Delta^{\uparrow\uparrow}}{2} & 1 & 0 \\ \frac{\Delta^{\uparrow\uparrow}}{2} & \omega + \xi_k & 0 & \Delta^{\uparrow\downarrow} \\ \Delta^{\uparrow\downarrow} & 0 & 0 & \frac{\Delta^{\downarrow\downarrow}}{2} \\ 0 & -\Delta^{\uparrow\downarrow} & 0 & \omega - \xi_k \end{vmatrix}$$

$$D_3 = -\Delta^{\uparrow\downarrow}[\omega^2 - \xi_k^2 + (\Delta^{\uparrow\downarrow})^2]$$

Therefore

$$\begin{aligned} \ll \hat{a}_{k\downarrow}^+, \hat{a}_{k\uparrow}^+ \gg &= \frac{-\Delta^{\uparrow\downarrow}[\omega^2 - \xi_k^2 + (\Delta^{\uparrow\downarrow})^2]}{(\omega^2 - \xi_k^2)(\omega^2 - \xi_k^2 - \frac{1}{4}(\Delta^{\uparrow\downarrow})^2)} \\ \ll \hat{a}_{k\downarrow}^+, \hat{a}_{k\uparrow}^+ \gg &= \frac{-\Delta^{\uparrow\downarrow}}{\omega^2 - \xi_k^2 - \frac{1}{4}(\Delta^{\uparrow\downarrow})^2} + \frac{4\Delta^{\uparrow\downarrow}}{\omega^2 - \xi_k^2} - \frac{4\Delta^{\uparrow\downarrow}}{\omega^2 - \xi_k^2 - \frac{1}{4}(\Delta^{\uparrow\downarrow})^2} \\ \ll \hat{a}_{k\downarrow}^+, \hat{a}_{k\uparrow}^+ \gg &= \frac{-5\Delta^{\uparrow\downarrow}}{\omega^2 - \xi_k^2 - \frac{1}{4}(\Delta^{\uparrow\downarrow})^2} + \frac{4\Delta^{\uparrow\downarrow}}{\omega^2 - \xi_k^2} \end{aligned} \quad (4.52)$$

Case I

The superconducting order parameter for singlet($\downarrow\uparrow$) is given by

$$\Delta^{\uparrow\downarrow} = -\frac{1}{\beta} \sum_{n,k} J \ll \hat{a}_{k\downarrow}^+, \hat{a}_{k\uparrow}^+ \gg \quad (4.53)$$

Using

$$\frac{1}{v} \sum \Rightarrow \frac{1}{(2\pi)^3} \int dk^3 = \int_{\xi_F}^{\infty} d\xi D(\xi)$$

$$\Delta^{\uparrow\downarrow} = \frac{-1}{\beta} \sum_n \int_0^{\infty} d\xi D(\xi) J \left(-5 \frac{\Delta^{\uparrow\downarrow}}{\omega^2 - \xi_k^2 - \frac{1}{4}(\Delta^{\uparrow\downarrow})^2} + 4 \frac{\Delta^{\uparrow\downarrow}}{\omega^2 - \xi_k^2} \right) \quad (4.54)$$

Since

$$\Delta = \sum_{k,k'} \eta \Delta_i$$

$$D(\xi) = \eta D(0)$$

$$\Delta^{+\downarrow\uparrow} = \frac{1}{\beta} \sum_n \int_0^\infty d\xi \eta D(0) J \left[5 \frac{\eta \Delta^{+\downarrow\uparrow}}{\omega^2 - \xi_k^2 - \frac{1}{4}(\eta \Delta^{+\downarrow\uparrow})^2} - 4 \frac{\eta \Delta^{+\downarrow\uparrow}}{\omega^2 - \xi_k^2} \right]$$

For S-wave pairing $\eta = 1$, where η - basis function

$$\Delta^{+\downarrow\uparrow} = D(0) J \frac{1}{\beta} \sum_n \int_{-\xi_d}^\infty d\xi \left[5 \frac{\Delta^{+\downarrow\uparrow}}{\omega_n^2 + \xi_k^2 + (\frac{\Delta^{+\downarrow\uparrow}}{2})^2} - 4 \frac{\Delta^{+\downarrow\uparrow}}{\omega_n^2 + \xi_k^2} \right] \quad (4.55)$$

Replacing

$$\zeta^2 = \xi_k^2 + (\Delta/2)^2$$

and

$$\omega_n = \frac{(2n+1)\pi}{\beta}, \omega = i\omega_n$$

for Matsubara frequency of fermions

$$1 = D(0) J \frac{1}{\beta} \sum_n \int_0^{\hbar\omega_m} d\xi \left(5 \frac{1}{(2n+1)^2\pi^2 + \beta^2\zeta^2} - 4 \frac{1}{\frac{(2n+1)^2\pi^2}{\beta} + \xi_k^2} \right) \quad (4.56)$$

Let

$$\lambda_{sf} = JD(0)$$

$$1 = \frac{\lambda_{sf}}{\beta} \sum_n \int_0^{\hbar\omega_m} d\xi \left(5 \frac{1}{(2n+1)^2\pi^2 + \beta^2\zeta^2} - 4 \frac{1}{\frac{(2n+1)^2\pi^2}{\beta} + \xi_k^2} \right) \quad (4.57)$$

Again let $z = \beta\zeta, x = \beta\xi_k$

$$\frac{1}{\lambda_{sf}} = \beta \sum_n \int_0^{\hbar\omega_m} d\xi \left(5 \frac{1}{(2n+1)^2\pi^2 + z^2} - 4 \frac{1}{(2n+1)^2\pi^2 + x^2} \right) \quad (4.58)$$

$$\sum_n \frac{1}{(2n+1)^2\pi^2 + z^2} = \frac{\tanh(\frac{z}{2})}{2z} \quad (4.59)$$

$$\frac{1}{\lambda_{sf}} = \beta \int_0^{\hbar\omega_m} d\xi \left(5 \frac{\tanh(\frac{z}{2})}{2z} - 4 \frac{\tanh(\frac{x}{2})}{2x} \right) \quad (4.60)$$

Taking $\Delta^{\uparrow\downarrow} = \Delta$

$$\frac{1}{\lambda_{sf}} = 5 \int_0^{\hbar\omega_m} d\xi \frac{\tanh(\frac{\beta}{2} \sqrt{\xi_k^2 + (\Delta/2)^2})}{2\sqrt{\xi_k^2 + (\Delta/2)^2}} - 4 \int_0^{\hbar\omega_m} d\xi \frac{\tanh(\frac{\beta}{2} \xi_k)}{\xi_k} \quad (4.61)$$

(i) When $T = T_c \Rightarrow \Delta = 0$, then eqn(4.67) becomes

$$\frac{1}{\lambda_{sf}} = 5 \int_0^{\hbar\omega_m} d\xi \frac{\tanh(\frac{\beta}{2} \xi)}{\xi} - 4 \int_0^{\hbar\omega_m} d\xi \frac{\tanh(\frac{\beta}{2} \xi)}{\xi} = \int_0^{\hbar\omega_m} d\xi \frac{\tanh(\frac{\beta}{2} \xi)}{\xi} \quad (4.62)$$

Let $z = \frac{\beta}{2} \xi$

$$\frac{1}{\lambda_{sf}} = \int_0^{\frac{\beta}{2} \hbar\omega_m} dz \frac{\tanh(z)}{z} \quad (4.63)$$

Integration by parts

$$\begin{aligned} \frac{1}{\lambda_{sf}} &= \ln(\beta_c \hbar\omega/2) \tanh\left(\frac{\hbar\omega\beta_c}{2}\right) - \int_0^\infty \frac{\ln(z)}{\cosh(z)^2} dz \\ &= \log(\beta_c \hbar\omega/2) - [-\text{eulergamma} + \log(\frac{\pi}{4})] \end{aligned} \quad (4.64)$$

$$\frac{1}{\lambda_{sf}} = \log(\beta_c \hbar\omega/2) + \gamma - \log\left(\frac{\pi}{4}\right)$$

$$\frac{1}{\lambda_{sf}} = \log\left[\frac{2\beta_c \hbar\omega e^\gamma}{\pi}\right]$$

$$T_c = \frac{1.134 \hbar\omega_m}{K_B} e^{\frac{-1}{\lambda_{sf}}} \quad (4.65)$$

ii) Near superconducting transition temperature T_c

$$\frac{1}{\lambda_{sf}} = 5 \int_0^{\hbar\omega_n} d\xi \frac{\tanh(\beta/2\sqrt{\xi_k^2 + (\Delta/2)^2})}{2\sqrt{\xi_k^2 + (\Delta/2)^2}} - 4 \int_0^{\hbar\omega_n} d\xi \frac{\tanh(\beta/2\xi_k)}{\xi_k} \quad (4.66)$$

Using Taylor expansion

$$\begin{aligned} \frac{\tanh\frac{\beta}{2}\sqrt{\xi_k^2 + (\Delta/2)^2}}{\sqrt{\xi_k^2 + (\Delta/2)^2}} &= \frac{\tanh\frac{\beta}{2}\xi}{\xi} + \frac{(\Delta/2)^2}{2|\xi|} \frac{d}{dz} \frac{\tanh\frac{\beta}{2}z}{z} \Big|_{z=\xi} \\ &= \frac{\tanh\frac{\beta}{2}\xi}{\xi} + \frac{(\Delta)^2}{8|\xi|} \frac{d}{dz} \frac{\tanh\frac{\beta}{2}z}{z} \Big|_{z=\xi} \end{aligned} \quad (4.67)$$

Let us simplify

$$\begin{aligned} &\frac{d}{dz} \frac{\tanh\frac{\beta}{2}z}{z} \Big|_{z=\xi} \\ \frac{d}{dz} \frac{\tanh\frac{\beta}{2}z}{z} \Big|_{z=\xi} &= \frac{z\frac{\beta}{2}\operatorname{sech}^2(\frac{\beta}{2}z) - \tanh(\frac{\beta}{2}z)}{z^2} \Big|_{z=\xi} \\ &= \frac{\beta\operatorname{sech}^2(\frac{\beta}{2}z)}{z} - \frac{\tanh(\frac{\beta}{2}z)}{z^2} \\ \frac{d}{dz} \frac{\tanh\frac{\beta}{2}z}{z} \Big|_{z=\xi} &= \frac{\beta z - \sinh(\beta z)}{2z^2 \cosh^2(\frac{\beta}{2}z)} \end{aligned} \quad (4.68)$$

Plugging eqn(4.74) into eqn(4.73)

$$\frac{\tanh\frac{\beta}{2}\sqrt{\xi_k^2 + (\Delta/2)^2}}{\sqrt{\xi_k^2 + (\Delta/2)^2}} = \frac{\tanh\frac{\beta}{2}\xi}{\xi} + \frac{\Delta^2}{8} \left[\frac{\beta z - \sinh(\beta z)}{2z^2 \cosh^2(\frac{\beta}{2}z)} \right] \quad (4.69)$$

$$\frac{1}{\lambda_{sf}} = \int_0^{\omega_m} d\xi \frac{\tanh\frac{\beta}{2}\xi}{\xi} + 5\frac{\Delta^2}{8} \int_0^{\beta/2\omega_m} dz \frac{\beta z - \sinh(\beta z)}{2z^2 \cosh^2(\frac{\beta}{2}z)}$$

$$\frac{1}{\lambda_{sf}} = \int_0^{\omega_m} d\xi \frac{\tanh\frac{\beta}{2}\xi}{\xi} + 5\frac{\Delta^2}{8} \int_0^{\infty} dz \frac{\beta z - \sinh(\beta z)}{2z^2 \cosh^2(\frac{\beta}{2}z)} \quad (4.70)$$

Let us integrate the right hand side of eqn(4.76)

$$\text{let } y = (\beta/2)z \Rightarrow z = 2y/\beta, dy = \beta/2 dz$$

$$\int_0^{\infty} \frac{\beta z - \sinh(\beta z)}{2z^2 \cosh^2(\frac{\beta}{2}z)} dz = \int_0^{\infty} \frac{2y - \sinh(2y)\frac{2}{\beta}}{(2)^4 \frac{y^3}{\beta^3} \cosh^2(y)} dy$$

$$\int_0^\infty \frac{\beta z - \sinh(\beta z)}{2z^2 \cosh^2(\frac{\beta}{2}z)} dz = \frac{\beta^2}{8} \int_0^\infty \frac{2y - \sinh(2y)}{y^3 \cosh^2(y)} dy \quad (4.71)$$

when we integrate

$$\int_0^\infty \frac{2y - \sinh(2y)}{y^3 \cosh^2(y)} dy$$

we will get

$$\int_0^\infty \frac{2y - \sinh(2y)}{y^3 \cosh^2(y)} dy = \frac{-14\zeta(3)}{\pi^2} \quad (4.72)$$

where ζ zeta function

Employing this equation into eqn(4.77) and then into eqn(4.76), we obtain

$$\frac{1}{\lambda_{sf}} = \int_0^{\omega_m} d\xi \frac{\tanh(\frac{\beta}{2}\xi)}{\xi} + 5 \frac{\Delta^2}{8} \left(\frac{\beta_c^2}{8}\right) \left[-\frac{14}{\pi^2} \zeta(3)\right] \quad (4.73)$$

$$\ln\left(\frac{2\beta_c \omega e^\gamma}{\pi}\right) = \ln\left(\frac{2\beta \omega e^\gamma}{\pi}\right) - \frac{70\Delta^2 \zeta(3)}{64\pi^2 K_B^2 T_c^2}$$

$$\ln\left[\frac{T}{T_c}\right] = -\frac{70\Delta^2 \zeta(3)}{64\pi^2 K_B^2 T_c^2} \quad (4.74)$$

Now, we can approximate $e^x \simeq 1 + x$, $x = -\frac{70\Delta^2 \zeta(3)}{64\pi^2 K_B^2 T_c^2}$ and $\zeta(3) = 1.2025$

Employing this equation into eqn(4.80)

$$\Delta^2 = \frac{64\pi^2 K_B^2 T_c^2}{70(1.2025)} \left[1 - \frac{T}{T_c}\right]$$

$$\Delta = 6.63 K_B T_c \left[1 - \frac{T}{T_c}\right]^{1/2} \quad (4.75)$$

This is the superconducting order parameter as a function of temperature

Let $\Delta_0 = K_B T_c$

$$\Delta = 6.63 \Delta_0 \sqrt{1 - \frac{T}{T_c}} \quad (4.76)$$

Case II

The superconducting order parameter for triplet ($\uparrow\uparrow$) is given by

$$\Delta^{+\uparrow\uparrow} = -\frac{1}{\beta} \sum_{n,k} J \ll \hat{a}_{k\uparrow}^+, \hat{a}_{k\uparrow}^+ \gg \quad (4.77)$$

Using

$$\frac{1}{v} \sum \Rightarrow \frac{1}{(2\pi)^3} \int dk^3 = \int_{\xi_F}^{\infty} d\xi D(\xi)$$

$$\Delta^{+\uparrow\uparrow} = \frac{-1}{\beta} \sum_n \int_0^{\infty} d\xi D(\xi) J \frac{\eta \Delta^{+\uparrow\uparrow}/2}{\omega^2 - \xi_k^2 - \frac{1}{4}(\eta \Delta^{+\uparrow\uparrow})^2} \quad (4.78)$$

Since

$$\Delta = \sum_{k,k'} \eta \Delta_i$$

$$D(\xi) = \eta D(0)$$

$$\Delta^{+\uparrow\uparrow} = \frac{1}{\beta} \sum_n \int_0^{\infty} d\xi \eta D(0) J \frac{\eta \Delta^{+\uparrow\uparrow}/2}{\omega^2 - \xi_k^2 - \frac{1}{4}(\eta \Delta^{+\uparrow\uparrow})^2}$$

For D-wave pairing $\eta = \frac{1}{2}$, where η - basis function

$$\Delta^{+\uparrow\uparrow} = -2\eta D(0) J \frac{1}{\beta} \sum_n \int_{-\xi_d}^{\infty} d\xi \frac{\Delta^{+\uparrow\uparrow}/4}{\omega_n^2 + \xi_k^2 + (\frac{\Delta^{+\uparrow\uparrow}}{4})^2} \quad (4.79)$$

Replacing

$$\zeta^2 = \xi_k^2 + (\Delta/4)^2$$

$$1 = D(0) J \frac{1}{\beta} \sum_n \int_0^{\hbar\omega_m} d\xi \frac{1}{(2n+1)^2 \pi^2 + \beta^2 \zeta^2} \quad (4.80)$$

$$\frac{1}{\lambda_{sf}} = \int_0^{\hbar\omega_m} d\xi \frac{\tanh(\beta/2 \sqrt{\xi_k^2 + (\Delta/2)^2})}{2\sqrt{\xi_k^2 + (\Delta/2)^2}} \quad (4.81)$$

(1) When $T \rightarrow 0 \Rightarrow \beta \Rightarrow \infty$

$$\tanh\left(\frac{\beta\xi}{2}\right) \approx 1$$

$$\frac{1}{\lambda_{sf}} = \int_0^{\hbar\omega_m} d\xi \frac{1}{\sqrt{\xi^2 + \left(\frac{\Delta}{4}\right)^2}} \quad (4.82)$$

Let

$$\begin{aligned} \xi &= \frac{\Delta}{4} \tan(u) \Rightarrow d\xi = \frac{\Delta}{4} \sec^2(u) du \\ \int \frac{d\xi}{\sqrt{\xi^2 + \left(\frac{\Delta}{4}\right)^2}} &= \int \frac{\frac{\Delta}{4} \sec^2(u) du}{\sqrt{(\Delta/4)^2 \tan^2 u + (\Delta/4)^2}} \\ &= \int \frac{\frac{\Delta}{4} \sec^2(u) du}{(\Delta/4) \sqrt{\tan^2 u + 1}} \end{aligned}$$

$$\int \frac{d\xi}{\sqrt{\xi^2 + \left(\frac{\Delta}{4}\right)^2}} = \int \sec(u) du$$

Now, multiplying $\sec(u)$ by $[\tan(u) + \sec(u)]$

$$\int \sec(u) du = \int \sec(u) \frac{(\tan(u) + \sec(u))}{\tan(u) + \sec(u)} du = \int \frac{\sec(u)\tan(u) + \sec^2(u)}{\tan(u) + \sec(u)} du$$

Again, let $s = \tan(u) + \sec(u) \Rightarrow du = (\sec^2(u) + \tan(u)\sec(u)) du$

$$\int \sec(u) du = \int \frac{1}{s} ds = \ln(\tan(u) + \sec(u)) + \text{constant}$$

$$\int d\xi \frac{1}{\sqrt{\xi^2 + \left(\frac{\Delta}{4}\right)^2}} = \ln\left[\frac{\xi}{\frac{\Delta}{4}} + \frac{\sqrt{\xi^2 + \left(\frac{\Delta}{4}\right)^2}}{\frac{\Delta}{4}}\right] \quad (4.83)$$

$$\int_0^{\hbar\omega} d\xi \frac{1}{\sqrt{\xi^2 + \left(\frac{\Delta}{4}\right)^2}} = \ln\left[\frac{\sqrt{(\hbar\omega)^2 + \left(\frac{\Delta}{4}\right)^2}}{\frac{\Delta}{4}} + \frac{\hbar\omega}{\frac{\Delta}{4}}\right]$$

$$= \ln\left[\frac{4\hbar\omega}{\Delta} + \frac{4\hbar\omega}{\Delta}\right]$$

$$\int_0^{\hbar\omega} d\xi \frac{1}{\sqrt{\xi^2 + \left(\frac{\Delta}{4}\right)^2}} = \ln\left[\frac{8\hbar\omega}{\Delta}\right] \quad (4.84)$$

Plugging eqn(4.90) into eqn(4.88), we obtain

$$\Delta = 8\hbar\omega e^{\frac{-1}{\lambda_{sf}}} \quad (4.85)$$

(2) When $T = T_c \Rightarrow \Delta = 0$, then eqn(4.87) becomes

$$\frac{1}{\lambda_{sf}} = \int_0^{\hbar\omega_m} d\xi \frac{\tanh(\frac{\beta}{2}\xi)}{\xi} \quad (4.86)$$

Let $z = \frac{\beta}{2}\xi$

$$\frac{1}{\lambda_{sf}} = \int_0^{\frac{\beta}{2}\hbar\omega_m} dz \frac{\tanh(z)}{z} \quad (4.87)$$

Integration by parts

$$\begin{aligned} \frac{1}{\lambda_{sf}} &= \ln(\beta_c \hbar\omega/2) \tanh\left(\frac{\hbar\omega\beta_c}{2}\right) - \int_0^\infty \frac{\ln(z)}{\cosh(z)^2} dz \\ &= \log(\beta_c \hbar\omega/2) - [-\text{eulergamma} + \log\left(\frac{\pi}{4}\right)] \end{aligned} \quad (4.88)$$

$$\frac{1}{\lambda_{sf}} = \log(\beta_c \hbar\omega/2) + \gamma - \log\left(\frac{\pi}{4}\right) \quad (4.89)$$

$$\frac{1}{\lambda_{sf}} = \log\left[\frac{2\beta_c \hbar\omega e^\gamma}{\pi}\right]$$

$$\frac{1}{\lambda_{sf}} = \log\left[\frac{2\hbar\omega e^\gamma}{K_B T_c \pi}\right]$$

$$T_c = \frac{1.134 \hbar\omega_m}{K_B} e^{\frac{-1}{\lambda_{sf}}} \quad (4.90)$$

Eventhough there is no experimental evidence for superconductivity of $YBa_2Cu_3O_7$ to be triplet, there is a situation where superconductivity of $YBa_2Cu_3O_7$ could be triplet.

The superconducting transition temperature for triplet superconductors are very small, but, with appropriate parameters the superconducting temperature could be enhanced.

(3) Near critical temperature T_c

$$\frac{1}{\lambda_{sf}} = \int_0^{\hbar\omega_n} d\xi \frac{\tanh(\beta/2\sqrt{\xi_k^2 + (\Delta/4)^2})}{2\sqrt{\xi_k^2 + (\Delta/4)^2}}$$

Using Taylor expansion

$$\begin{aligned} \frac{\tanh\frac{\beta}{2}\sqrt{\xi_k^2 + (\Delta/4)^2}}{\sqrt{\xi_k^2 + (\Delta/4)^2}} &= \frac{\tanh\frac{\beta}{2}\xi}{\xi} + \frac{(\Delta/4)^2}{2|\xi|} \frac{d}{dz} \frac{\tanh\frac{\beta}{2}z}{z} \Big|_{z=\xi} \\ &= \frac{\tanh\frac{\beta}{2}\xi}{\xi} + \frac{(\Delta)^2}{16|\xi|} \frac{d}{dz} \frac{\tanh\frac{\beta}{2}z}{z} \Big|_{z=\xi} \\ \frac{1}{\lambda_{sf}} &= \int_0^{\omega_m} d\xi \frac{\tanh\frac{\beta}{2}\xi}{\xi} + \frac{\Delta^2}{16} \int_0^{\infty} dz \frac{\beta z - \sinh(\beta z)}{2z^2 \cosh^2(\frac{\beta}{2}z)} \end{aligned} \quad (4.91)$$

since

$$\int_0^{\infty} dz \frac{\beta z - \sinh(\beta z)}{2z^2 \cosh^2(\frac{\beta}{2}z)} = \left(\frac{\beta_c^2}{8}\right) \left[-\frac{14}{\pi^2} \zeta(3)\right] \quad (4.92)$$

$$\frac{1}{\lambda_{sf}} = \int_0^{\omega_m} d\xi \frac{\tanh\frac{\beta}{2}\xi}{\xi} + \frac{\Delta^2}{16} \left(\frac{\beta_c^2}{8}\right) \left[-\frac{14}{\pi^2} \zeta(3)\right] \quad (4.93)$$

Further simplifying, we obtain

$$\ln\left(\frac{2\beta_c\omega e^\gamma}{\pi}\right) = \ln\left(\frac{2\beta\omega e^\gamma}{\pi}\right) - \frac{14\Delta^2\zeta(3)\beta_c}{128\pi^2}$$

$$\ln\left[\frac{T}{T_c}\right] = -\frac{14\Delta^2\zeta(3)\beta_c}{128\pi^2}$$

$$e^x \simeq 1 + x, \text{ where } x = \frac{14\Delta^2\zeta(3)}{128\pi^2 K_B^2 T_c^2}$$

and

$$\zeta(3) = 1.2025$$

\Rightarrow

$$\Delta = 9.38 K_B T_c \sqrt{1 - \frac{T}{T_c}} \quad (4.94)$$

4.2 Pnictides Superconductivity

For optimal doped iron pnictide, the Hamiltonian of the system is given by

$$\hat{H} = \sum_{k\sigma} \xi_{k\sigma} \hat{a}_{k\sigma}^+ \hat{a}_{k\sigma} + \sum_{k\sigma} \hbar\omega \hat{b}_{k\sigma}^+ \hat{b}_{k\sigma} + \sum_{k,k'} g(k, k') \hat{n}_{k\uparrow} \hat{n}_{k'\downarrow} \quad (4.95)$$

The interacting Hamiltonian is

$$\hat{H}_I = \sum_{k\sigma} g(k, k') \hat{a}_{k\uparrow}^+ \hat{a}_{k\uparrow} \hat{a}_{k'\downarrow}^+ \hat{a}_{k'\downarrow} \quad (4.96)$$

The mean field approximation The superconducting gap equation

$$\Delta = \sum_{k,k'} g(k, k') \langle \hat{a}_{k\uparrow} \hat{a}_{k'\downarrow} \rangle, \Delta^+ = \sum_{k,k'} g^*(k, k') \langle \hat{a}_{k'\downarrow}^+ \hat{a}_{k\uparrow}^+ \rangle \quad (4.97)$$

Plugging eqn(4.104) into eqn(4.103), we obtain

$$\hat{H}_I = \sum_{k,k'} \{ \Delta^+ \hat{a}_{k\uparrow} \hat{a}_{k'\downarrow} + \Delta \hat{a}_{k\uparrow}^+ \hat{a}_{k'\downarrow}^+ \} \quad (4.98)$$

From equation of motion, we have

$$\omega \ll \hat{a}_{k\sigma}, \hat{a}_{k\sigma}^+ \gg = \langle [\hat{a}_{k\sigma}, \hat{a}_{k\sigma}^+] \rangle + \ll [\hat{a}_{k\sigma}, \hat{H}], \hat{a}_{k\sigma}^+ \gg \quad (4.99)$$

$$\omega \ll \hat{a}_{k\uparrow}, \hat{a}_{k\uparrow}^+ \gg = \langle [\hat{a}_{k\uparrow}, \hat{a}_{k\uparrow}^+] \rangle + \ll [\hat{a}_{k\uparrow}, \hat{H}], \hat{a}_{k\uparrow}^+ \gg \quad (4.100)$$

$$\omega \ll \hat{a}_{k\uparrow}, \hat{a}_{k\uparrow}^+ \gg = 1 + \ll [\hat{a}_{k\uparrow}, \hat{H}], \hat{a}_{k\uparrow}^+ \gg \quad (4.101)$$

Now let us evaluate $[\hat{a}_{k\uparrow}, \hat{H}]$

$$[\hat{a}_{k\uparrow}, \hat{H}] = [\hat{a}_{k\uparrow}, \hat{H}_0] + [\hat{a}_{k\uparrow}, \hat{H}_I] \quad (4.102)$$

$$\begin{aligned} [\hat{a}_{k\uparrow}, \hat{H}_0] &= [\hat{a}_{k\uparrow}, \sum_{k\sigma} \xi_{k\sigma} \hat{a}_{k\uparrow}^+ \hat{a}_{k\uparrow}] + [\hat{a}_{k\uparrow}, \sum_{k\sigma} \hbar\omega \hat{b}_{k\uparrow}^+ \hat{b}_{k\uparrow}] \\ [\hat{a}_{k\uparrow}, \hat{H}_0] &= \xi_k \hat{a}_{k\uparrow} \end{aligned} \quad (4.103)$$

$$[\hat{a}_{k\uparrow}, \hat{H}_I] = [\hat{a}_{k\uparrow}, \sum_{k,k'} \Delta^+ \hat{a}_{k\uparrow} \hat{a}_{k'\downarrow}] + [\hat{a}_{k\uparrow}, \Delta \hat{a}_{k\uparrow}^+ \hat{a}_{k'\downarrow}^+]$$

$$[\hat{a}_{k\uparrow}, \hat{H}_I] = \Delta \hat{a}_{-k\downarrow}^+ \quad (4.104)$$

Plugging eqn(4.110) and eqn(4.111) into eqn(4.108)

$$\omega \ll \hat{a}_{k\uparrow}, \hat{a}_{k\uparrow}^+ \gg = 1 + \xi_k \ll [\hat{a}_{k\uparrow}, \hat{a}_{k\uparrow}^+] \gg + \Delta \ll [\hat{a}_{-k\downarrow}^+, \hat{a}_{k\uparrow}^+] \gg$$

$$(\omega - \xi_k) \ll \hat{a}_{k\uparrow}, \hat{a}_{k\uparrow}^+ \gg - \Delta \ll [\hat{a}_{-k\downarrow}^+, \hat{a}_{k\uparrow}^+] \gg = 1 \quad (4.105)$$

Similarly

$$\omega \ll \hat{a}_{-k\downarrow}^+, \hat{a}_{k\uparrow}^+ \gg = \langle [\hat{a}_{-k\downarrow}^+, \hat{a}_{k\uparrow}^+] \rangle + \ll [\hat{a}_{-k\downarrow}^+, \hat{H}], \hat{a}_{k\uparrow}^+ \gg \quad (4.106)$$

$$\omega \ll \hat{a}_{-k\downarrow}^+, \hat{a}_{k\uparrow}^+ \gg = \ll [\hat{a}_{-k\downarrow}^+, \hat{H}], \hat{a}_{k\uparrow}^+ \gg \quad (4.107)$$

Again, let us evaluate $[\hat{a}_{-k\downarrow}^+, \hat{H}]$

$$[\hat{a}_{-K\downarrow}^+, \hat{H}] = [\hat{a}_{-K\downarrow}^+, \hat{H}_0] + [\hat{a}_{-K\downarrow}^+, \hat{H}_I] \quad (4.108)$$

$$[\hat{a}_{-K\downarrow}^+, \hat{H}_0] = [\hat{a}_{-K\downarrow}^+, \sum_{k\sigma} \xi_{k\sigma} \hat{a}_{k\uparrow}^+ \hat{a}_{k\uparrow}] + [\hat{a}_{-K\downarrow}^+, \sum_{k\sigma} \hbar\omega \hat{b}_{k\uparrow}^+ \hat{b}_{k\uparrow}]$$

$$[\hat{a}_{-K\downarrow}^+, \hat{H}_0] = -\xi_k \hat{a}_{-k\downarrow}^+ \quad (4.109)$$

$$[\hat{a}_{-K\downarrow}^+, \hat{H}_I] = [\hat{a}_{k\uparrow}, \sum_{k,k'} \Delta^+ \hat{a}_{k\uparrow} \hat{a}_{k'\downarrow}] + [\hat{a}_{-K\downarrow}^+, \Delta \hat{a}_{k\uparrow}^+ \hat{a}_{k'\downarrow}^+]$$

$$[\hat{a}_{-K\downarrow}^+, \hat{H}_I] = -\Delta^+ \hat{a}_{k\uparrow} \quad (4.110)$$

Plugging eqn(4.116) and eqn(4.117) into eqn(4.114)

$$\omega \ll \hat{a}_{-K\downarrow}^+, \hat{a}_{k\uparrow}^+ \gg = -\xi_k \ll [\hat{a}_{-K\downarrow}^+, \hat{a}_{k\uparrow}^+] \gg - \Delta^+ \ll [\hat{a}_{k\uparrow}, \hat{a}_{k\uparrow}^+] \gg$$

$$(\omega + \xi_k) \ll \hat{a}_{-K\downarrow}^+, \hat{a}_{k\uparrow}^+ \gg + \Delta^+ \ll \hat{a}_{k\uparrow}, \hat{a}_{k\uparrow}^+ \gg = 0 \quad (4.111)$$

Using eqn(4.112) and eqn(4.118), we can write it in a matrix terms as

$$\begin{pmatrix} \omega - \xi_k & -\Delta \\ \Delta^+ & \omega + \xi_k \end{pmatrix} \begin{pmatrix} \ll \hat{a}_{k\uparrow}, \hat{a}_{k\uparrow}^+ \gg \\ \ll \hat{a}_{-K\downarrow}^+, \hat{a}_{k\uparrow}^+ \gg \end{pmatrix} = \begin{pmatrix} 1 \\ 0 \end{pmatrix} \quad (4.112)$$

The Determinate

$$D = \begin{vmatrix} \omega - \xi_k & -\Delta \\ \Delta^+ & \omega + \xi_k \end{vmatrix} \quad (4.113)$$

$$D = \omega^2 - \xi_k^2 + \Delta^2 \quad (4.114)$$

To determine the solution for

$$\langle\langle \hat{a}_{-K\downarrow}^+, \hat{a}_{k\uparrow}^+ \rangle\rangle$$

we use the determinant

$$D_2 = \begin{vmatrix} \omega - \xi_k & 1 \\ \Delta^+ & 0 \end{vmatrix} \quad (4.115)$$

$$D_2 = -\Delta^+ \quad (4.116)$$

Therefore,

$$\langle\langle \hat{a}_{-K\downarrow}^+, \hat{a}_{k\uparrow}^+ \rangle\rangle = \frac{D_2}{D} = \frac{-\Delta^+}{\omega^2 - \xi_k^2 + \Delta^2} \quad (4.117)$$

Similarly

To determine the solution for

$$\ll \hat{a}_{k\uparrow}, \hat{a}_{k\uparrow}^+ \gg$$

we use the determinant

$$D_1 = \begin{pmatrix} 1 & -\Delta \\ 0 & \omega + \xi_k \end{pmatrix} \quad (4.118)$$

$$D_1 = \omega + \xi_k \quad (4.119)$$

Therefore

$$\ll \hat{a}_{K\uparrow}, \hat{a}_{k\uparrow}^+ \gg = \frac{D_1}{D} = \frac{\omega + \xi_k}{\omega^2 - \xi_k^2 + \Delta^2} \quad (4.120)$$

For pnictide superconductors, the pairing symmetry is singlet ($S = 0, \downarrow\uparrow$)

The superconducting order parameter is

$$\Delta^{+\downarrow\uparrow} = -\frac{g}{\beta} \sum_{n,k} \ll \hat{a}_{-K\downarrow}^+, \hat{a}_{k\uparrow}^+ \gg \quad (4.121)$$

$$\Delta^{+\downarrow\uparrow} = \sum_{k,k'} g(k, k') \frac{1}{\beta} \sum_n \int_{-\infty}^{\infty} D(\xi) \frac{\eta \Delta^{+\downarrow\uparrow}}{\omega^2 - \xi_k^2 + (\eta \Delta)^2} d\xi \quad (4.122)$$

$$\Delta^{+\downarrow\uparrow} = -2 \sum_{k,k'} g(k, k') \frac{1}{\beta} \sum_n \int_0^{\infty} \eta D(0) \frac{\eta \Delta^{+\downarrow\uparrow}}{\omega^2 - \xi_k^2 + (\eta \Delta)^2} d\xi$$

$$\Delta(k) = \sum_{k,k'} \eta \Delta(k')$$

and $\eta = 1$ for singlet (s)

$$\Delta = -2 \sum_{k,k'} g(k, k') D(0) \Delta \frac{1}{\beta} \sum_n \int_0^{\hbar\omega_m} d\xi \frac{1}{\omega^2 - \xi_k^2 + \Delta^2}$$

$$1 = -2 \sum_{k,k'} g(k, k') D(0) \frac{1}{\beta} \sum_n \int_0^{\hbar\omega_m} d\xi \frac{1}{\omega^2 - \xi_k^2 + \Delta^2}$$

$$\lambda_{sf} = \sum_{k,k'} g(k, k') D(0)$$

$$\omega = i\omega_n$$

$$\frac{1}{\lambda_{sf}} = \frac{2}{\beta} \sum_n \int_0^{\hbar\omega_m} d\xi \frac{1}{\omega_n^2 + \xi^2 - \Delta^2} \quad (4.123)$$

$$\text{Let } x^2 = \xi^2 - \Delta^2$$

$$\frac{1}{\lambda_{sf}} = \frac{2}{\beta} \sum_n \int_0^{\hbar\omega_m} d\xi \frac{1}{\omega_n^2 + x^2} \quad (4.124)$$

We know that

$$\frac{1}{\beta} \sum_n \frac{1}{\omega_n^2 + x^2} = \frac{\tanh(\frac{\beta}{2}x)}{2x} \quad (4.125)$$

Plugging eqn(4.132) into eqn(4.131) and then eqn(4.130)

$$\frac{1}{\lambda_{sf}} = \int_0^{\hbar\omega_m} d\xi \frac{\tanh(\frac{\beta}{2}x)}{x} \quad (4.126)$$

$$\frac{1}{\lambda_{sf}} = \int_0^{\hbar\omega_m} d\xi \frac{\tanh(\frac{\beta}{2}\sqrt{\xi^2 - \Delta^2})}{\sqrt{\xi^2 - \Delta^2}} \quad (4.127)$$

1)

$$\text{When } T = 0, \beta \Rightarrow \infty$$

i.e

$$\tanh(\frac{\beta}{2}\sqrt{\xi^2 - \Delta^2}) \rightarrow 1$$

$$\frac{1}{\lambda_{sf}} = \int_0^{\hbar\omega_m} \frac{1}{\sqrt{\xi^2 - \Delta^2}} d\xi$$

$$\frac{1}{\lambda_{sf}} = \ln\left(\frac{2\hbar\omega_m}{\Delta}\right)$$

$$\Delta(0) = 2\hbar\omega_m e^{\frac{-1}{\lambda_{sf}}} \quad (4.128)$$

2)When

$$T \rightarrow T_C(\beta \rightarrow \beta_C), \Delta(\beta_C) \rightarrow 0$$

$$\frac{1}{\lambda_{sf}} = \int_0^{\hbar\omega_m} d\xi \frac{\tanh\frac{\beta}{2}\sqrt{\xi_k^2 - \Delta^2}}{\sqrt{\xi_k^2 - \Delta^2}} \quad (4.129)$$

$$\frac{1}{\lambda} = \int_0^{\hbar\omega_b} d\xi \frac{\tanh\frac{\beta}{2}\xi}{\xi}$$

let

$$x = \beta\xi$$

$$\frac{1}{\lambda_{sf}} = \int_0^{\hbar\omega_w} \frac{\tanh(\frac{x}{2})}{x} dx$$

Using integration by parts, We have

$$\frac{1}{\lambda_{sf}} = \log(\beta_c\omega_m/2)\tanh(\frac{\omega_m\beta_c}{2}) - \int_0^{\beta_c\omega_m/2} \frac{\log(x)}{\cosh(x)^2} dx \quad (4.130)$$

$$\frac{1}{\lambda_{sf}} = \log(\beta_c\omega_m/2)\tanh(\frac{\omega_m\beta_c}{2}) - \int_0^{\infty} \frac{\log(x)}{\cosh(x)^2} dx$$

$$\frac{1}{\lambda_{sf}} = \log(\beta_c\hbar\omega_m/2) - [-\gamma + \log(\frac{\pi}{4})] \quad (4.131)$$

$$\frac{1}{\lambda_{sf}} = \log\left[\frac{2\beta_c\hbar\omega_m e^\gamma}{\pi}\right] \quad (4.132)$$

$$T_c = \frac{2\hbar\omega_m}{K_B} e^\gamma \pi e^{\frac{-1}{\lambda_{sf}}} \quad (4.133)$$

$$\gamma = 0.577, \frac{e^\gamma}{\pi} = 0.567$$

$$T_c = 1.134 \frac{\hbar\omega_m}{K_B} e^{\frac{-1}{\lambda_{sf}}} \quad (4.134)$$

3) Near critical temperature T_c

$$\frac{1}{\lambda_{sf}} = 2T \sum_n \int_0^{\hbar\omega} d\xi \frac{1}{\omega_n^2 + \xi^2 - \Delta^2} \quad (4.135)$$

$$2T \sum_n \left[\frac{1}{\omega_n^2 + \xi^2 - \Delta^2} \right] = 2T \sum_n \left[\frac{1}{\omega_n^2 + \xi^2} + \frac{|\Delta|^2}{(\omega_n^2 + \xi^2)^2} \right] \quad (4.136)$$

$$2T \sum_n \int_0^{\hbar\omega} \frac{1}{(\omega_n^2 + \xi^2)^2} = 2T \sum_n \left(\frac{-\pi}{2\omega_n^3} \right)$$

$$2T \sum_n \int_0^{\hbar\omega} \frac{1}{(\omega_n^2 + \xi^2)^2} = -\pi(T) \sum_n \left[\frac{1}{(2n+1)^3 \pi^3 T^3} \right]$$

$$2T \sum_n \int_0^{\hbar\omega} \frac{1}{(\omega_n^2 + \xi^2)^2} = -\frac{1}{\pi^2 T^2} \sum_n \left[\frac{1}{(2n+1)^3} \right]$$

$$2T \sum_n \int_0^{\hbar\omega} \frac{1}{(\omega_n^2 + \xi^2)^2} = -\frac{1}{\pi^2 T^2} \sum_n \left[\frac{1}{(2n+1)^3} \right] \quad (4.137)$$

$$2T \sum_n \int_0^{\hbar\omega} \frac{1}{\omega_n^2 + \xi^2} = \int_0^{\omega} \frac{\tanh\left(\frac{\beta\xi_k}{2}\right)}{\xi_k} d\xi \quad (4.138)$$

Plugging eqn(4.144), and eqn(4.145) into eqn(4.143), and then into eqn(4.142),

we obtain

$$\frac{1}{\lambda_{sf}} = \int_0^{\hbar\omega} \frac{\tanh\left(\frac{\beta\xi_k}{2}\right)}{\xi_k} d\xi - \frac{\Delta^2}{\pi(T^2)} \sum_n \frac{1}{(2n+1)^3} \quad (4.139)$$

$$\ln\left(\frac{T}{T_c}\right) = -\frac{\Delta^2}{\pi(T^2)} \sum_n \frac{1}{(2n+1)^3} \quad (4.140)$$

$$\sum_n \frac{1}{(2n+1)^3} = \frac{7}{8}\zeta(3) \quad (4.141)$$

Now, we can approximate

$$e^x \approx 1 + x, \text{ where } x = -\frac{\Delta^2}{\pi(T^2)} \frac{7}{8} \zeta(3) \quad (4.142)$$

Plugging eqn(4.149), and eqn(4.148) into eqn(4.147), we obtain

$$\frac{T}{T_C} = 1 - \frac{\Delta^2}{\pi(T^2)} \frac{7}{8} \zeta(3)$$

$$\Delta^2 = \frac{8}{7\zeta(3)} \pi T_C \left(1 - \frac{T}{T_C}\right) \quad (4.143)$$

$$\zeta(3) = 1.2025$$

⇒

$$\Delta = 3.06 T_C \sqrt{1 - \frac{T}{T_C}} \quad (4.144)$$

This is the expression for the superconducting order parameter as function of temperature for pnictide superconductor.

where T_c is the superconducting transition temperature

4.3 Electronic specific heat

The electronic specific heat per atom of a superconductor is defined by

$$C_{el} = \frac{d}{dT} \left(\frac{1}{N} \sum_n 2\xi_k \langle n_k \rangle \right) \quad (4.145)$$

$$C_{el} = \frac{d}{dT} \left[\frac{1}{N} \sum_n 2\xi_k \langle \hat{a}_k^\dagger \hat{a}_k \rangle \right] \quad (4.146)$$

Now let us find $\langle \hat{a}_k^\dagger \hat{a}_k \rangle$

5

RESULTS AND DISCUSSION

This chapter concerns with theoretical results of high temperature superconductivity which are obtained using the equations derived in chapter 4. The main focus is on the superconductive transition temperature, the superconducting order parameter, coupling strength and the electronic heat capacity.

The first part is regarding the doped cuprate superconductor ($\text{YBa}_2\text{Cu}_3\text{O}_{6.93}$) and the second part is concerned on doped pnictide superconductor $\text{Ca}_{1-x}\text{Nd}_x\text{FeAsF}$, furthermore, we analysis the results briefly.

We have determined analytically the gap equation for superconductivity, and calculated the superconducting transition temperature. Moreover, the results of our work are best described by plotting figures.

- Superconducting order parameter (Δ) Versus Temperature (T),
- The temperature (T) versus coupling strength (λ)

5.1 The Superconducting Transition Temperature (T_C) for cuprate based superconductor

Here, we are going to calculate the superconducting transition temperature based on the equation derived in chapter three

From eqn(4.96), we have

$$T_{sc} = \frac{1.134\hbar\omega_m}{K_B} \exp\left(\frac{-1}{\lambda_{sf}}\right) \quad (5.1)$$

Now, taking

$$\begin{aligned} \frac{\hbar\omega_m}{K_B} &= 158.7K, \lambda \approx 1.5 \\ T_{sc} &= 180K \exp\left(\frac{-1}{1.5}\right) \approx 92.4K \\ T_{sc} &\approx 92.4K \end{aligned}$$

This is the superconducting transition temperature for $\text{YBa}_2\text{Cu}_3\text{O}_{6.93}$

Similarly, for $\text{HgBa}_2\text{Ca}_2\text{Cu}_3\text{O}_x$

$$T_{sc} = \frac{1.134\hbar\omega_m}{K_B} \exp\left(\frac{-1}{\lambda_{sf}}\right) \quad (5.2)$$

Now taking

$$\begin{aligned} \frac{\hbar\omega_m}{K_B} &= 225K, \lambda \approx 2.1 \\ T_{sc} &= 255K \exp\left(\frac{-1}{2.13}\right) \approx 158.42K \\ T_{sc} &\approx 158.42K \end{aligned}$$

which is the superconducting transition temperature for $\text{HgBa}_2\text{Ca}_2\text{Cu}_3\text{O}_x$

Compounds	Theoretical (calculated) value of T_c	Experimental value of T_c
$\text{YBa}_2\text{Cu}_3\text{O}_{6.93}$	92.4 K	95 K
$\text{HgBa}_2\text{Ca}_2\text{Cu}_3\text{O}_x$	158.42 K	160 K
$\text{Bi}_2\text{Ba}_2\text{Sr}_2\text{Ca}_2\text{Cu}_3\text{O}_6$	108.5 K	110 K
$\text{Tl}_2\text{Ba}_2\text{Ca}_2\text{Cu}_3\text{O}_{10}$	123K	125K

Table 5.1: Comparison between theoretical and experimental value of superconducting transition temperatures for cuprates

Using eqn(4.81), we can plot superconducting order parameter(Δ) versus temperature (T),

From the fig.5.1, we can observe that the superconducting order parameter

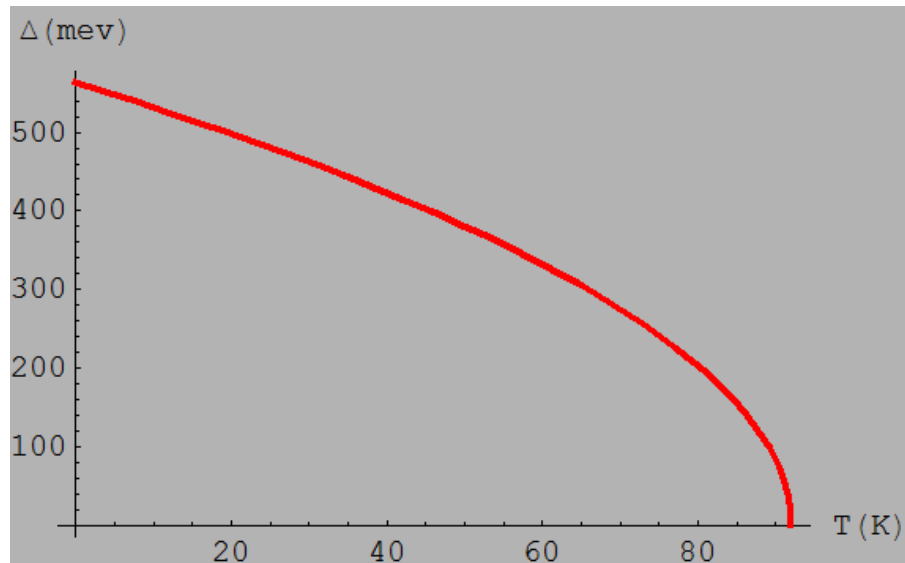


Figure 5.1: Superconducting order parameter (Δ) versus superconducting transition temperature(T_c) for $\text{YBa}_2\text{Cu}_3\text{O}_{6.93}$ [90]

decreases monotonically as the temperature increases and it vanishes at $T_c=92.4$ K. Below T_c , it is the region of superconducting state whereas above T_c , it is normal state.

Again, Using eqn(4.71), we can plot superconducting transition temperature versus coupling constant λ as depicted below.

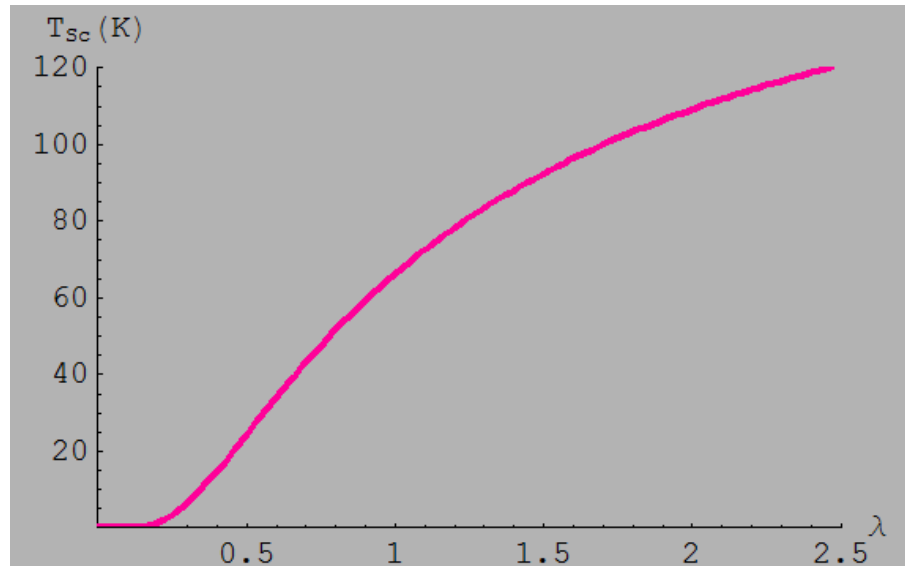


Figure 5.2: Superconducting transition temperature (T_c) versus coupling strength (λ) $\text{YBa}_2\text{Cu}_3\text{O}_{6.93}$ [90]

The superconducting transition temperature increases as the coupling strength parameter increases and slowly increases when the coupling strength parameter increases further.

5.2 The Transition Temperature(T_C)for Pnictides Superconductor

From eqn(4.141),we have

$$T_{sc} = \frac{1.134\hbar\omega_m}{K_B} \exp\left(\frac{-1}{\lambda_{sf}}\right) \quad (5.3)$$

Now,taking

$$\begin{aligned} \frac{\hbar\omega_m}{K_B} &= 102K, \lambda \approx 1.36 \\ T_{sc} &= 116K \exp\left(\frac{-1}{1.36}\right) \approx 55.62K \\ T_{sc} &\approx 55.62K \end{aligned}$$

which is the superconducting transition temperature for pnictides superconductor $Gd_{1-x}Th_xFeAs$.

$$T_{sc} = \frac{1.134\hbar\omega_m}{K_B} \exp\left(\frac{-1}{\lambda_{sf}}\right) \quad (5.4)$$

Now,taking

$$\begin{aligned} \frac{\hbar\omega_m}{K_B} &= 102K, \lambda \approx 1.4 \\ T_{sc} &= 116K \exp\left(\frac{-1}{1.4}\right) \approx 56.8K, \\ T_{sc} &\approx 56.8K \end{aligned}$$

which is the superconducting transition temperature for pnictides superconductor $Ca_{1-x}Nd_xFeAsF$.

Compounds	Theoretical(calculated) value of T_c	Experimental value of T_c
$\text{Ca}_{1-x}\text{Nd}_x\text{FeAsF}$	56 K	57 K
$\text{Gd}_{1-x}\text{Th}_x\text{FeAsO}$	55.6 K	55 K
$\text{SmO}_{1-x}\text{F}_x\text{FeAs}$	57.4 K	55 K

Table 5.2: Comparison between theoretical and experimental value of superconducting transition temperatures for iron pnictides

The following figure shows superconducting order parameter(Δ) versus temperature(T).

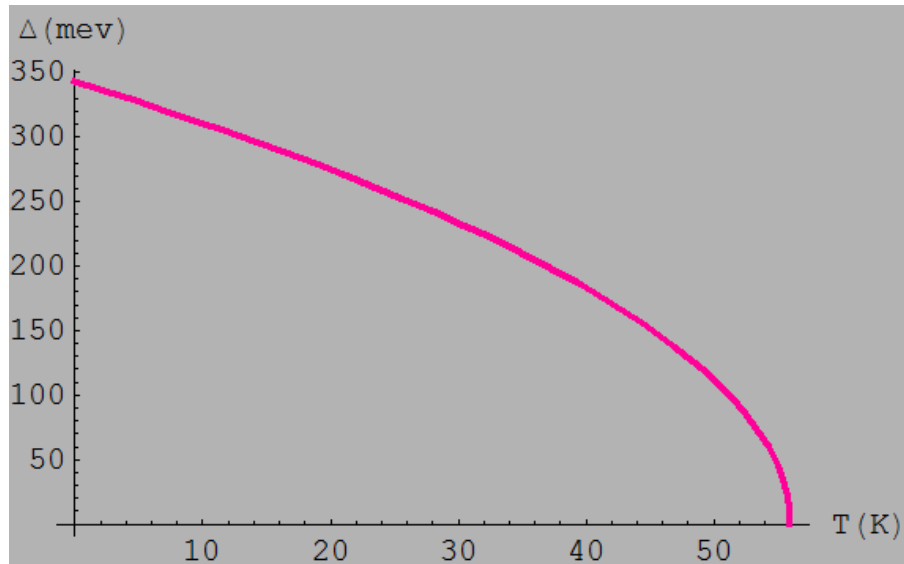


Figure 5.3: Superconducting order parameter (Δ) versus superconducting transition temperature (T_c) for $\text{Ca}_{1-x}\text{Nd}_x\text{FeAsF}$

From the fig.5.3, we can observe that the superconducting order parameter decreases monotonically as the temperature increases and it vanishes at $T_{sc}=57$ K. Below T_{sc} , it is the region of superconducting state whereas above T_{sc} , it is normal state.

Using eqn(4.141), we can plot superconducting transition temperature (T_c) versus coupling constant (λ) as depicted below.

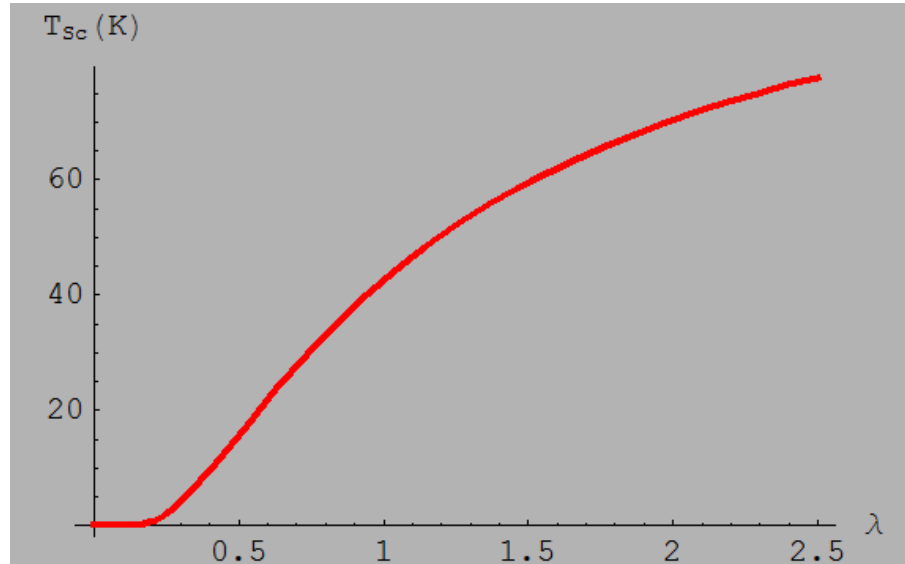


Figure 5.4: Superconducting transition temperature(T_c) versus coupling strength (λ) for $\text{Ca}_{1-x}\text{Nd}_x\text{FeAsF}$

The superconducting transition temperature depends on the coupling strength (λ) and frequency of magnon (spin fluctuation) ω_m .

Keeping the coupling strength constant, the superconducting transition temperature increases linearly as magnon frequency increases.

For Various magnon frequencies, We can plot superconducting transition temperature(T_c) versus coupling constant λ as shown below.

When $\omega_m=13.4\text{THz}$

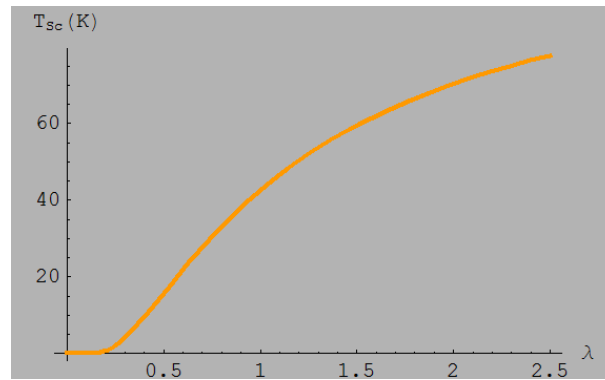


Figure 5.5: Superconducting transition temperature(T_c) versus coupling strength (λ)

When $\omega_m=18\text{THz}$

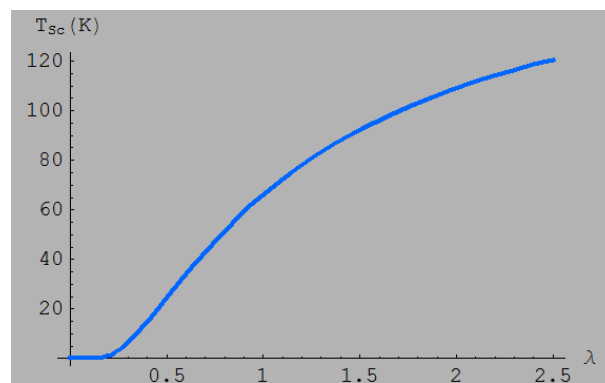


Figure 5.6: Superconducting transition temperature(T_c) versus coupling strength (λ)

When $\omega_m=11.5\text{THz}$

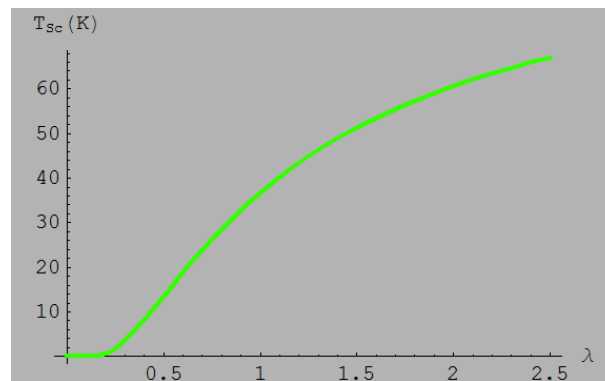


Figure 5.7: Superconducting transition temperature (T_c) versus coupling strength (λ)

When $\omega_m=10.4\text{THz}$.

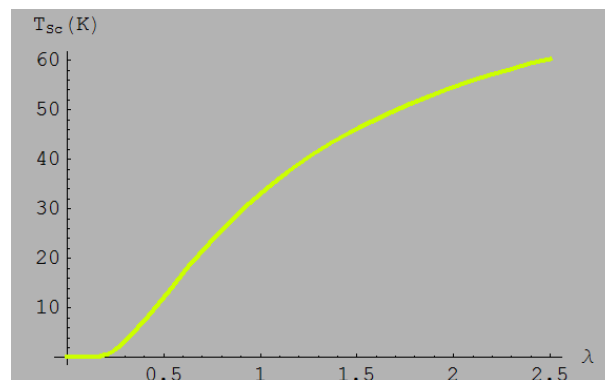


Figure 5.8: Superconducting transition temperature (T_c) versus coupling strength (λ)

The superconducting transition temperature increases as the coupling strength parameter increases and slowly increases when the coupling strength increases further.

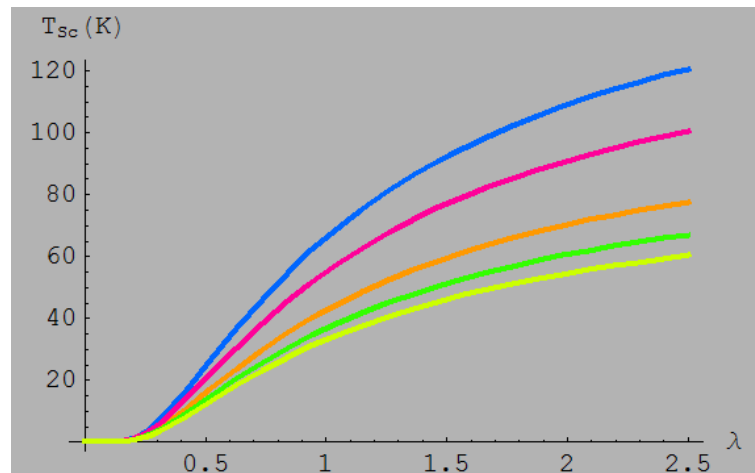


Figure 5.9: Superconducting transition temperature (T_c) versus coupling strength (λ) [90]

A superconductor whether conventional or high temperature superconductors, the superconducting order parameter monotonically decreases with temperature and vanishes at the superconducting transition temperature as depicted below.

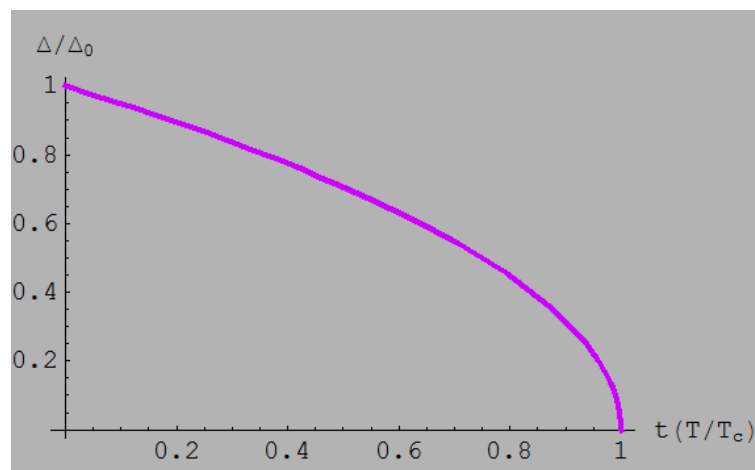


Figure 5.10: Superconducting order parameter ($\frac{\Delta}{\Delta_0}$) versus ($t = \frac{T}{T_c}$)

5.3 Electronic specific heat

The electronic specific heat for cuprate ($\text{YBa}_2\text{Cu}_3\text{O}_{6.93}$) superconductor is determined by equation(4.164)

$$C_{el} = \frac{2D(0)}{NK_B T^2} \pi^2 \xi^2 e^{\frac{-\delta}{k_B T}}$$

We have used, $\frac{\xi_k}{K_B} = 250K, K_B = 1.38 \times 10^{-23} \frac{J}{K}, D(0) = 0.362 \times 10^{19}$ per Joule

$\xi_k = 3.45 \times 10^{-21} J, N = \text{number of atoms per unit volume}$

$$C_{el} = \frac{8.55 \times 10^{-5}}{NT^2} e^{\frac{-250}{T}}$$

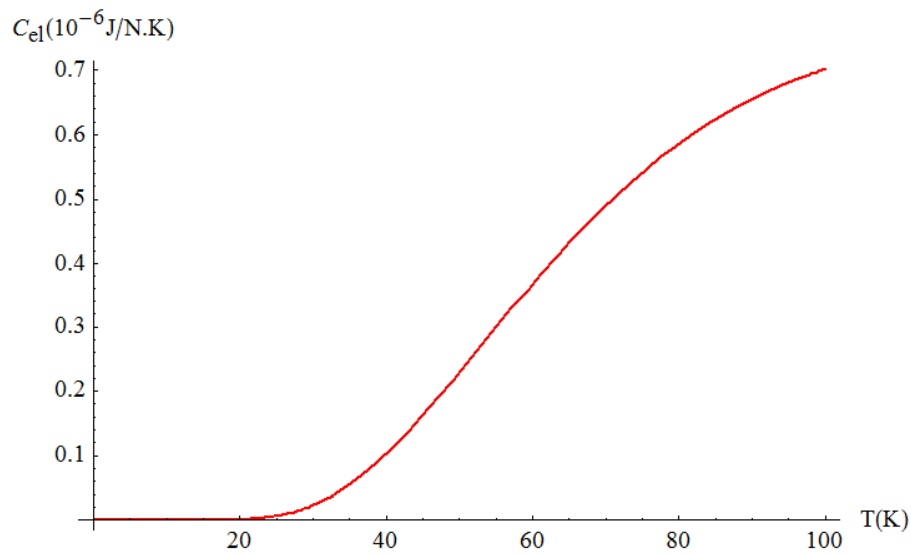


Figure 5.11: The electronic specific heat versus Temperature for $\text{YBa}_2\text{Cu}_3\text{O}_{6.93}$

As we noticed from fig.5.11, the electronic specific heat is very steady at low enough temperature, and increases rapidly as the temperature increases until it reaches the critical temperature.

The electronic specific heat for pnictide (CaNdFeAsF) superconductor could be computed by equation (4.164)

$$C_{el} = \frac{2D(0)}{NK_B T^2} \pi^2 \xi^2 e^{\frac{-\delta}{k_B T}}$$

We have used, $\frac{\xi}{K_B} = 160K, K_B = 1.38 \times 10^{-23} \frac{J}{K}, D(0) = 0.217 \times 10^{19}$ perJoule

$$C_{el} = \frac{4.57 \times 10^{-5}}{NT^2} e^{\frac{-160}{T}}$$

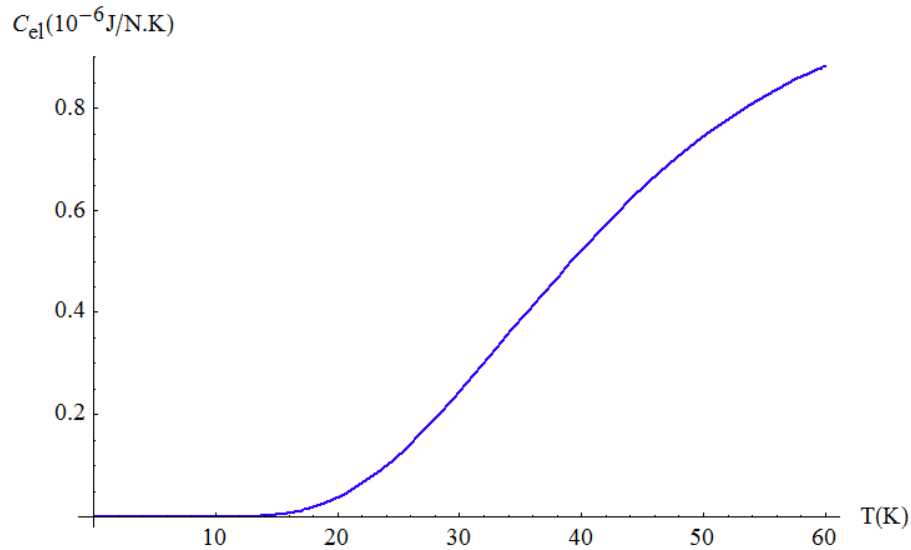


Figure 5.12: The electronic specific heat versus Temperature for CaNdFeAsF

As we noticed from fig.5.12, the electronic specific heat is very steady at low enough temperature, and increases rapidly as the temperature increases until it reaches the critical temperature.

6

CONCLUSION

In this work, starting with a model Hamiltonian consisting of the non-interaction and spin-fermion interaction, we have studied the high temperature superconductivity involving cuprate and pnictides theoretically with the help of retarded Green function technique.

We have determined analytically the superconducting transition temperature for $\text{YBa}_2\text{Cu}_3\text{O}_{6.93}$ and CaNdFeAsF and the results are very close to the experiment results.

We also noticed that the superconducting order parameter decreases monotonically with the increasing temperature and disappear at the superconducting transition temperature for $\text{YBa}_2\text{Cu}_3\text{O}_{6.93}$ and CaNdFeAsF .

Below superconducting transition temperature (T_{sc}), it is a region of superconducting state and beyond superconducting transition temperature, it is a normal state. Furthermore, the superconducting transition temperature is linearly proportional to the coupling strength and magnon/spin wave/ frequency.

We have also determined the electronic specific heat in superconducting state and plotted C_{el} versus temperature for $\text{YBa}_2\text{Cu}_3\text{O}_{6.93}$ and CaNdFeAsF . From the graphs, we have noticed that at low enough temperature, the electronic specific heat in superconducting state does not change noticeably, however, as temperature increases further, the electronic specific heat in superconducting state increases rapidly until it reaches the critical temperature.

Cuprates superconductors are materials with their superconducting properties determined by electrons moving with coupled copper oxide layers.

In pnictides, the iron-arsenic plane is responsible for superconductivity.

The possible mechanism for cuprates and pnictides superconductivity is antiferromagnetic spin fluctuation or spin density waves/ magnon/, and the proposed pairing symmetry for cuprates is $d_{x^2+y^2}$ -wave symmetry where as for pnictide is a spin singlet extended S_{\pm} -wave symmetry in which the superconducting order parameter changes its sign between the Fermi surfaces.

Iron-pnictides superconductors share many similarities with cuprates among them: layered structure, antiferromagnetic phases next to superconductivity and phase diagrams and may be a common mechanism of superconductivity in them as in both superconductivity appears as magnetism is destroyed since both are close proximity with each other.

Bibliography

- [1] Heike Kammerling Onnes, Commun.Phys.Lab.Univ.Leiden, **12**, 120 (1911).
- [2] Charles Kittel, Introduction to solidstate Physics, 8th edition (1986).
- [3] S.Saxena, R.C Gupta and P.N Saxena, solid state physics, Book, India(975).
- [4] Peierls R.E, Quantum theory of solids, Book, Oxford (2001).
- [5] J.Bardeen, L.N.Cooper, and J.R.Schrieffer, Phys.Rev.**108**, 1175 (1957).
- [6] J.R.Gavaler, Appl.phys.Lett, **23**, 480 (1973).
- [7] M.J.Rosseinsky etal, Phys.Rev.Lett.**66**, 2830 (1991)
- [8] K.Holczer *etal*, Science**252**, 1154 (1991)
- [9] Bednorz, J.G. and K.A.Muller, Z.Phys.B**64**, 189 (1986).
- [10] J.Nagmatsu *etal*, Nature, **410**, 63 (2001).
- [11] Schilling A., Cantoni M., Guo J.D., Ott H.R. Nature, **363**, 56-58 (1993).
- [12] Gao.L.*etal*, Phys.Rev.B.**50**, 4260-4263 (1994).
- [13] C.Wang, L.Li, S.Chi, Z.Zhu, Z.Ren, Y.Li, Y.Wang, X.Lin, Y.Luo, S.Jiang, X.Xu, G.Cao, and Z.Xu: Europhys.Lett.**83**, 67006 (2008).
- [14] Shigei Fujita and Salvador Godoy, Theory of high temperature superconductivity, Dordrecht (2001).

- [15] K.H.Bennemann and J.Kettersson, superconductivity: conventional and unconventional superconductors, springer, volume1, Berlin (2008).
- [16] University of Cambridge, Teaching and Learning Packages (2008).
- [17] S.Saxena, R.C Gupta and P.N Saxena, solid state physics, Book, India
- [18] Shigel Fujita and SalvadorGodey, Theory of high temperature superconductivity, Newyork (2001).
- [19] Philip L.Taylor and Olletteinonen, A Quantum approach to Condensed Matter Physics, Cambridge University Press, NewYork, (2002).
- [20] Thomas P.Sheahen, Introduction to High Temperature Superconductivity, NewYork (2002)
- [21] J.G.Bednorz and K.A.Muller, Z.Phys.B,**64**, 189,1989.
- [22] Wu.K.M:Ashburn.J.R., Torng , Phys.Rev.Lett.**58**. 908, 1987.
- [23] H.Maeda, Y.Tanka,M.Fukutumi, T.Asano, Japanese Journal of Applied Physics, **27**, L209-L210 (1988).
- [24] Z.Z.Shheng, A.M.Hermann, Nature **332** (6160):138-139,1988.
- [25] Schilling A., Cantoni M., Guo J.D., Ott H.R., Nature, **363**, 56-58 (1993).
- [26] Gao.L.*etal*, Phys.RevB.**50**, 4260-4263,1994.
- [27] C.Wang, L.Li, S.Chi, Z.Zhu, Z.Ren, Y.Li, Y.Wang, X.Lin, Y.Luo, S.Jiang, X.Xu, G.Cao and Z.Xu: Europhys.Lett.**83**, 67006 (2008).
- [28] University of Cambridge, Teaching and Learning Packages.12, Sep, (2008).

- [29] High temperature superconductivity, engineering application, springer, Berlin (2004).
- [30] Andrier Mourahkine, high temperature superconductivity in cuprate, springer, 2002
- [31] <http://www.high temperture superconductivity/>
- [32] Monhoux, P.; Balatsky, A.V.; Pines D., Phys.Rev.B, **42**, 22 (1992).
- [33] <http://www.springer.com/material/book/> (2002).
- [34] Nikollay Plakida, High temperature cuprate superconductors, Springer, book, London, New York (2010).
- [35] Monthoux, P.; Balatsky, A.V.; Pines, D. Physical Review B, **42**, 22 (1992).
- [36] J. Orenstein and A.J Millis, Advanced in Physics of high temperature superconductivity, Science, 288 (2000).
- [37] D.J. Scalapino, The case for d-wave pairing in cuprate superconductor, Phys.Rep., 329-365 (1995).
- [38] Barry P. Martins, Recent Developments in Superconductivity Research, Nova Science pulisher, Inc. New York (2007).
- [39] Akito Kobayashi, J.phys.Soc.Jpn, 711640-1642, 2002.
- [40] Chadra Varma, Phase diagram of cuprates, Nature **468**, 184-185 (2010).
- [41] Akito Kobayashi, Atsushi Tsuruta, Taamitusa Matsuura and Yoshihiro Kuroda, J.Phys.Soc.Jpn, **71**, 1640-1643 (2002).

- [42] AD.Drew, *etal*, Nature materials **8**, 310, 2009
- [43] J.Orenstein and A.J Millis, Advanced in Physics of high temperature superconductivity, Science, 288 (2000).
- [44] Chadra Varma, Phase diagram of cuprates, Nature,**468**, 184-185 (2010).
- [45] Rullier-Albnque F. *etal*, Europhys.lett. **50**, 81 (2008).
- [46] B.Buchner, Phase Diagram of Pnictide Superconductors.
- [47] Adrian Cho, Science **320**, 870 (2008).
- [48] B.Bchner, Phase Diagram of Pnictide Superconductors, IFW, Dresden.
- [49] Kamihara, *etal*, JACS, **128**, 10012 (2006).
- [50] Y.Kamihara,*etal*, Iron Based Layered Superconductors LaOFeP, J.Am.Chem.Soc.**128**, 100123 (2006).
- [51] Y.Kamihara, T.Watanabe, M.Hirano, H.Hosono, J.Am.Chem.Soc.**130**, 3296 (2008).
- [52] G.F.Chen, Z.Li, D.Wu, G.Li, W.Z.Hu, J.Dong, P.Zeng, J.L.Luo, and N.L.Wang: Phys.Rev.Lett. **100**, 105 (2008).
- [53] Z.A.Ren, J.Yang, W.Lu, W.Yi, G.C.Che, X.L.Dong, L.L.Sun, and Z.X.Zhao: Mater.Res.Innovation, **12**,105 (2008).
- [54] Z.A.Ren, J.Yang, W.Lu, W.Yi, X.L.Shen, Z.C.Li, G.Che, X.L.Dong, L.L.Sun, F.Zhou, and Z.X.Zhao: Europhys.Lett.**82**,57002 (2008).
- [55] X.H.Chen, T.Wu,G.Wu, R.H.Lu.Liu, H.C.Chen, D.F.Fang; Nature, 453, 761, 2008.

- [56] C.Wang, L.Li, S.Chi, Z.Zhu, Z.Ren, Y.Li, Y.Wang, X.Lin, Y.Luo, S.Jiang, X.Xu, G.Cao and Z.Xu: *Europhys.Lett.***83**, 67006 (2008).
- [57] Y.Izyumov, E.Kurmaev, (springer-Verlag, Berlin Heideberg, 2010)
- [58] C.Wang, L.Li, S.Chi, Z.Zhu, Z.Ren, Y.Li, Y.Wang, X.Lin, Y.Luo, S.Jiang, X.Xu, G.Cao and Z.Xu: *Europhys.Lett.***83**, 67006 (2008).
- [59] <http://www.pnictides superconductor.com/>
- [60] Johannes *etal*, *Physical Review B* , (2009).
- [61] <http://www.pnictides superconductor.com/>
- [62] Kamihara, Y.Hiramatsu, H.Hirano, M.Kawamura, R.Yanagi, H.Kamiya, and T.Hosono, *J.Am.Chem.Soc.***128**, 10012-10013 (2006).
- [63] Hiroki Takahashi, *etal*, *Nature* , 06972 (2008).
- [64] Z.Deng *etal*, *EPL*, **87**, 37004, 2009.
- [65] I.R.Shein and A.L.Ivanovskii, *JETP*,**89**, 41 (2009).
- [66] E. C.Hsu *etal*, *proc.Natt.Acad.Sci. , USA*, **105**, 1462 (2008).
- [67] University of Cambridge, *Teaching and Learning Packages* , (2008).
- [68] Adrian Cho, *Science* **320**, 870, (2008).
- [69] E.C.Hsu ,*etal*, *Proc.National Acad.Sci.***38**, 105, 14262 (2008).
- [70] B.C.Sales *etal*, *Bulk Superconductivity at 14 K in Single Crystals of $\text{Fe}_y\text{Te}_x\text{S}_{1-x}$* , *Phys.Rev.B* **79**, 094521 (2009).
- [71] R.Hu,E.S.Bozin *etal*, *Phys.Rev.B***80**, 214514 (2009).

- [72] Y.Mizuguchi *etal*, Appl.Phys.Lett.**94**, 012503 (2009).
- [73] S.Medvedev *etal*, Nature Mater,**8**, 630-633 (2009).
- [74] T.Mizuguchi, F.Tomioka, S.Tsuda, T.Yamaguchi, Y.Takano,Appl.Phy.Lett.
94, 012503 (2009).
- [75] C.C.Chang, T.K.Chen, W.C.Lee.Lin, M.J.Wang, Y.C.Wen, P.M.Wu, M.K.Wu,
Superconductivity in Fe-chalcogenides, Physics C,**524**, 423-234 (2015).
- [76] K.Horigane *etal*, J.Phys.Soc, Jpn**78**, 063705 (2009).
- [77] Jinsheng Wen, Guangy Ong, Genda Gu, JM Tranquada, and RJ Biregeneau,
Rp.Prog, **74**, 1234503, 2011.
- [78] A.Subedi, L.Zhang, D.J.Singh and M.H.Du, Phys.Rev.B**78**, 134514 (2008).
- [79] A.H.Wilson, Theory of metals, Cambridge University press, second edition,
Cambrige (1953).
- [80] Norman E.Phillips, Physical Reviews, **3**, 114 (1959).
- [81] S.L.Kakani and Amit Kakani, Material Science, Book, New Delhi (2004).
- [82] Narliker, A.V, High Temperature Superconductivity 2-Engineering applica-
tion, Springer, Berlin (2004).
- [83] www.physicscentral.com/explore/action/super.cfm
- [84] [Science.how stuff works.com/transport/engine.../Maglev-train](http://Science.howstuffworks.com/transport/engine.../Maglev-train)
- [85] <http://www.Magnetic resonance imaging>.
- [86] www.ccas-web.org/superconductivity/medicalimaging/

- [87] <http://www.Technological application of superconductivity/>
- [88] High Temperature superconductivity in Perspective, Book, Washington D.C, April(1990).
- [89] The new superconducting electronics, Harold Weinstock and Richard W.Ralstom, book, USA (1992).
- [90] Mequanint Assefa, P.Singh, International Journal of engineering and Scientific research (IJESR), **3**, 42-52 (2015).
- [91] Hyungju Oh, Jisoo Moon, Donghan Shin, Chang-Youn Moon, Hyoung Joon Choi*, Progress in superconductivity, **13**, 65-84 (2011).
- [92] Shaolong He, *etal*, Phases diagram and electronic indication of high temperature superconductivity at 64 K in single layer $FeSe$ film, Nature Mater,**12**, 3648 (2013).
- [93] Singh P., Sinha K.P, J.Solidstate Communication, **73**, 45 (1990).
- [94] Philip L.Taylor and Oli Heinonen, A quantum approach to Condensed Matter Physics, book, Cambridge University Press, NewYork, USA (2002).
- [95] Michele Cini, Topics and Methods in Condensed Matter Theory, book, Springer-verlag, Berlin-Heidelberg (2007).
- [96] Tedor M Mishonov and Evgeni S Penev, Theory of high temperature superconductivity, A Conventional approach, book, World Scientific publishing Co.Plc.Ltd, SA (2011).

- [97] A.A.Abrikosov, L.P.Gorkov and I.Ye.Dzyaloshinskii, Quantum Field Theoretical Methods in Statistical Physics, 2nd edition Pergamon press Ltd, Oxford (1965).
- [98] Takashi Yanagiawa, Mitake Miyazaki, Kunihiko Yamaji, Journal of modern Physics,4, 33-64 (2013).
- [99] Toru Morya, Spin Fluctuation in Itinerant Electron magnetism, Springer-verlag, Berlin Heidelberg, NewYork, Tokyou (1985).
- [100] Yuri M.Galperin, Introduction to Modern Solidstate Physics, Oslo (2011).
- [101] Double Time Green Functions in Statistical Physics, Usp.Fiz.Nauk71, 320-345 (1960).

DECLARATION

I hereby declare that this PhD dissertation is my original work and has not been presented for a degree in any other universities, and that all sources of material used for the dissertation have been duly acknowledged.

Name: Mequanint Assefa

Signature: _____

This PhD dissertation has been submitted to for examination with my approval as University advisor.

Name: Professor Pooran Singh

Signature: _____

Place and date of submission:

Department of Physics

Addis Ababa University

October 2015

PUBLICATIONS

1. Theoretical Study of High Temperature Superconductivity:

The case of Cuprate ($\text{YBa}_2\text{Cu}_3\text{O}_{6.93}$) by Mequanint Assefa, P. Singh, International Journal of Engineering and Scientific Research (IJESR), 3, 42-51, (2015)

2. Study of Spin Fluctuation Induced High Temperature Superconductivity involving pnictides (CaNdFeAsF) on process to be published.